

A BRUSHLESS, DIRECT-DRIVE, WIND-TURBINE ALTERNATOR

A Thesis

Presented To

The Faculty of Graduate Studies

The University of Manitoba

in partial fulfillment

of The Requirements For The Degree of

Master of Science

In

Electrical Engineering

By

Calvin Wai Chiu Cheung

September, 1979

A BRUSHLESS, DIRECT-DRIVE, WIND-TURBINE ALTERNATOR

BY

CALVIN WAI CHIU CHEUNG

A dissertation submitted to the Faculty of Graduate Studies of
the University of Manitoba in partial fulfillment of the requirements
of the degree of

MASTER OF SCIENCE

✓
© 1979

Permission has been granted to the LIBRARY OF THE UNIVERSITY OF MANITOBA to lend or sell copies of this dissertation, to the NATIONAL LIBRARY OF CANADA to microfilm this dissertation and to lend or sell copies of the film, and UNIVERSITY MICROFILMS to publish an abstract of this dissertation.

The author reserves other publication rights, and neither the dissertation nor extensive extracts from it may be printed or otherwise reproduced without the author's written permission.



ABSTRACT

A design concept for low-speed brushless wind turbine alternators is introduced. A prototype machine was built and tested to demonstrate the concept. Optimal designs were obtained by a Direct Search optimisation method. An alternate design is suggested and compared with the prototype design. A range of recommended rated power outputs is suggested for each design.

ACKNOWLEDGEMENTS

The author wishes to express his deepest gratitude to Dr. R. M. Mathur for suggesting the thesis topic, for his guidance in the preparation of this thesis and his financial support.

Special thanks go to Dr. R. W. Menzies for his assistance in the optimisation method and comments on the thesis.

Thanks are due to Dr. Murty, Dr. El-Marsafawy, and M. S. Chahal for their valuable suggestions and Bristol Aerospace Limited for supplying part of the material for the fabrication of the prototype machine.

The author also is indebt to his friends Shirley, Linda and Danny for their help in typing the manuscript.

TABLE OF CONTENTS

ABSTRACT	i
ACKNOWLEDGEMENTS	ii
TABLE OF CONTENTS	iii
LIST OF FIGURES	v
LIST OF TABLES	vii
LIST OF SYMBOLS	viii
 Chapter	page
I. INTRODUCTION	1
1.1 General	1
1.2 Factors Affecting The Performance of The Wind Power System	2
1.3 Types of Brushless Alternator	5
1.4 Scope of The Thesis	9
II. BRUSHLESS LUNDELL ALTERNATORS	10
2.1 General	10
2.2 Design Procedure	12
2.3 Poles and Frequency	13
2.4 Main Dimensions	14
2.5 Stator Winding Design	19
2.6 Leakage Reactance	26
2.6.1 Slot Leakage Reactance	26
2.6.2 Overhang Leakage Reactance	30
2.7 Magnetic Circuit	31
2.7.1 Total Ampere Turns Per Phase	32
2.8 Field Winding Design	33
2.9 Iron Loss	35
2.10 Eddy Loss	35
2.11 Temperature Rise	36
2.12 Efficiency	37
III. SAMPLE DESIGN	38
3.1 Specification For Design	38
3.2 Stator Winding	39
3.3 Magnetic Circuit	41
3.4 Field Winding	43
3.5 Performance	43
3.6 Measurment of Material Properties	44
IV. TESTS ON THE PROTOTYPE MACHINE	48
4.1 Introduction	48
4.2 Open-Circuit Test	48

4.3	Short-Circuit Test	53
4.4	Equivalent Circuit of The Machine	57
V.	OPTIMUM DESIGN OF BRUSHLESS ALTERNATORS	61
5.1	Effects of Some Parameters on Machine Performance	64
5.2	Optimisation	64
5.3	Specified Constraint Value And Scaling Factors	75
5.4	Operation of The Optimisation Program	76
5.5	Test Runs Results	78
VI.	ALTERNATE DESIGNS	81
6.1	Introduction	81
6.2	Sample Design on Type 1	84
VII.	CONCLUSIONS	87
	REFERENCES	88
	APPENDIX I	90
	APPENDIX II	93

LIST OF FIGURES

Figure		page
1.1.	The Electrical Power Output of The Windmill	3
1.2.	Stationary Field Brushless Machines	8
2.1.	Brushless Lundell Alternator	11
2.2.	The Shape of Armature Coils	25
2.3.	Slot Leakage Flux With Double-Layer Winding	27
3.1.	Stator Winding of The Machine	42
3.2.	Experimental Set-Up of Material Properties Measurment	45
3.3.	Magnetic Characteristic of The Stator Laminations .	46
3.4.	Magnetic Characteristic of The Frame	47
4.1.	Open-Circuit Test With 8 V Connection	49
4.2.	Open-Circuit Test With 16 V Connection	50
4.3.	Open-Circuit Test With 32 V Connection	51
4.4.	Short-Circuit Test With 8 V Connection	54
4.5.	Short-Circuit Test With 16 V Connection	55
4.6.	Short-Circuit Test With 32 V Connection	56
4.7.	Inductive Load Test With 32 V Connection	58
4.8.	Equivalent Circuit of The Machine With 32 V Connection	59
5.1.	Stator Winding of New Design	62
5.2.	Air Gap Flux Vs. Efficiency And Weight	65
5.3.	Stator Bore Diameter Vs. Efficiency And Weight . .	66
5.4.	Stator Core Length Vs. Efficiency And Weight . . .	67
5.5.	Stator Current Density Vs. Efficiency And Weight .	68
5.6.	Field Current Density Vs. Efficiency And Weight . .	69

5.7.	Stator Back Core Vs. Efficiency And Weight	70
5.8.	Flow diagram of the optimisation program	77
5.9.	Weight of First Design Vs. Rated Power Outputs . .	80
6.1.	Type 1 Brushless Alternator	82
6.2.	Type 2 Brushless Alternator	83
6.3.	Weight of Type 1 Vs. Rated Power Outputs	86

LIST OF TABLES

Table	page
3.1. Specifications of Design	38
3.2. Design Schedule	40
4.1. Discrepance Between Test And Calculated Results . .	52
5.1. New Design Parameters	63
5.2. Results From The Test Runs	79
6.1. Comparison of Two Designs	85

List of Symbols

act	Threshold electrical loading.
acf	Furling electrical loading.
a	number of circuit in stator.
af	number of circuit in field.
As	Area of the slot.
Asc	Conductor size of the field winding.
Ascs	Conductor size of the stator winding.
ATmg	Ampere turns per pole at the main gap.
ATar	Demagnetizing A.T. per pole for armature reaction.
ATfd	Total A.T. per pole pair for the field.
Bt	Average threshold air gap flux density.
Bf	Average furling air gap flux density.
Cpp	Number of coils per phase.
Cl _t	Stator I^2R loss at threshold.
Cl _f	Stator I^2R loss at furling.
Db	Stator bore diameter.
Dens	Density of laminations.
Ef	Exciter voltage.
f(x)	Function of x.
Ft	Threshold frequency.
Ff	Furling frequency.
g(x)	Constraint function.
Gt	Threshold output coefficient.
Gf	Furling output coefficient.
ht	Slot depth.

I _{ft}	Threshold full load current.
I _{ff}	Furling full load current.
I _{pp}	Stator current per path.
J _f	Field current density.
J _s	Stator current density.
K _d	Distribution factor.
K _e	Coil-span factor.
K _{ed}	Eddy current loss ratio.
K _s	Skewing factor.
K _w	Winding factor.
L	Stator core length.
L _m	Stator mean turn length.
L _f	Mean turn of field winding.
L _t	Mutual leakage inductance.
n _t	Threshold r.p.s.
n _f	Furling r.p.s.
N _t	Threshold r.p.m.
N _f	Furling r.p.m.
N _s	Number of slots.
N _c	Number of conductors per slot.
p	The p th power of a function.
P	Number of poles.
P _f	Power factor.
P _{lf}	Field I^2R loss.
P _e	Iron loss.
P _c	Power transfered by conduction.
P _r	Power transferred by radiation.

Pv	Power transferred by convection.
P(X,Fs)	Objective function.
Qt	Threshold KVA output.
Qf	Furling KVA output.
Rp	Stator resistance per path.
Rph	Stator resistance per phase.
Rf	Field resistance per circuit.
Sf	Space factor.
Sp _i	Slots per phase with in phase coils.
Sp _o	Slots per phase with out of phase coils.
Sp	Slots per pole.
T ₁	Final temperature of the machine.
T ₂	Ambient temperature of the air.
T _{pc}	Number of turns per coil.
T _{ph}	Number of turns per phase.
T _{pf}	Number of field turns per circuit.
V _p	E.M.F. per phase.
V _t	Rotor peripheral threshold speed.
V _f	Rotor peripheral furling speed.
w _t	Weight of iron.
W _t	Threshold rated output power.
W _f	Furling rated output power.
W _o	Slot width.
X _o	Slot mutual reactance.
X _{oh}	Overhang leakage reactance.
X _s	Slot self leakage reactance.
X _{st}	Total slot leakage reactance.

y_s	Slot pitch.
y_s'	Effective slot pitch.
ϵ	Short pitch angle.
ϵ_m	Emissivity of material.
δ	Angle between coils emf in electrical radian.
Φ	Average flux per pole.
β	Skew angle.
τ	Pole pitch.
ρ	Resistivity of copper at 75 ⁰ C.
ρ_s	Resistivity of iron at 75 ⁰ C.
λ_s	Slot leakage flux.
λ_{ab}	Slot mutual leakage flux.
μ_o	Permeability of air.

Chapter I

INTRODUCTION

1.1 General

The generation of electrical power from the wind has received attention in recent years in Canada. Both the National Research Council and the Bristol Aerospace Limited have developed the vertical axis windmill for power generation.¹ Due to the cold climate and the inaccessibility of large areas of Canada, the requirement of regular maintenance on the brushes and the slip rings limits the use of conventional alternators in windmill applications. Thus, the development of a maintenance-free alternator in remote, unmanned locations is desirable. The objective of this thesis is to develop an efficient, direct-drive, fully controllable brushless alternator for the vertical axis windmill application.

The average wind speed in Canada lies in the 7 to 13 m.p.h. range. For a 8.7 ft diameter vertical axis wind turbine, the shaft speed is about 100 to 150 r.p.m. The mechanical power that can be obtained is about 60 to 200 watts. Since only a small amount of power is extracted from the wind, a speed-up transmission is not desirable because the frictional loss in the gears constitutes a great portion

of the power generated. The ideal machine for this application should have the following characteristics :

- (1) Capability of low speed operation (40-200 r.p.m.) with reasonable efficiency (75% or above),
- (2) Controllable self excitation,
- (3) Capability of self starting,
- (4) No slip rings.

A direct-drive, fully controllable, brushless alternator will satisfy the above characteristics.

1.2 Factors Affecting The Performance of The Wind Power System

Theoretically, the mechanical power extracted from wind is proportional to the area intercepted by the turbine and the cube of wind speed. A large amount of mechanical power is expected from an efficient turbine situated in a strong wind location. However, due to the low power coefficient, about 0.35, of the wind turbines, only a small portion of the available power is obtained from the wind. Figure 1.1 shows the theoretical electrical power output of the vertical axis windmill with a 75% efficient generator coupled to it. Since the mechanical power output from the turbine is low, any additional of speed-up mechanism loss

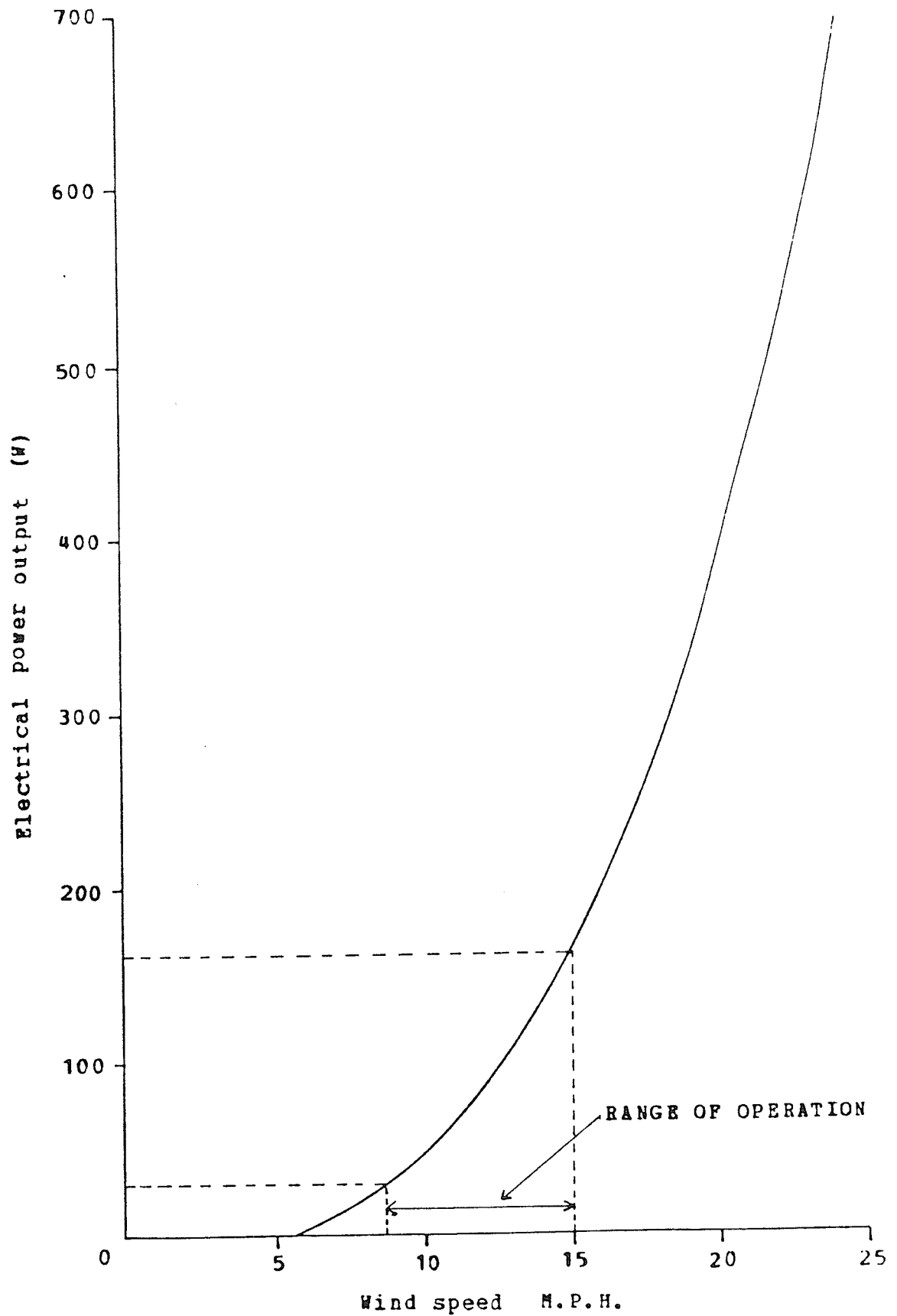


Figure 1.1: The Electrical Power Output of The Windmill

will further reduce the mechanical power input to the alternator. The brushes and the bearings also constitute some losses in mechanical power.

The vertical axis turbine has a low starting and accelerating torque. If a 10:1 ratio speed-up transmission is applied, the starting torque required is ten times the friction torque of the alternator plus the friction torque of the gearbox. For such a high torque, the wind turbine may not be able to start or to accelerate.

A direct-coupled machine can ease the starting and accelerating problems. However, due to the low shaft speed (100-150 r.p.m.) of the turbine, an alternator with larger diameter is required.

Due to the variation of the wind speed, a controllable field excitation can provide an easy way to match the machine to the load over a wide range of speed. The capabilities of self start and self excitation are also necessary for the application of the windmill in remote locations where an alternate electrical supply is not available.

The intermittent operating characteristic of the windmill may cause additional problems in a cold environment. The

cold weather in winter, and the all year round cold climate in the Arctic, creates a starting problem for the generator. When the windmill stops due to insufficient wind, there is a danger of frosting the brushes and the slip rings.

The brushes and the slip rings of a conventional synchronous alternator require regular maintenance such as :

- (1) Cleaning and machining of the slip rings,
- (2) Replacing the degraded slip rings due to corrosive environment, and
- (3) Adjusting, cleaning and replacing the brushes.

When the windmills are used in remote areas, the maintenance cost tends to be high. The maintenance cost can therefore be minimized if the brushless alternators are used instead.

In order to accomplish a high efficiency wind power system, a direct-drive, fully controllable brushless alternator is desired.

1.3 Types of Brushless Alternator

There are four main types of brushless machines :

- (1) Permanent magnet machine;
- (2) Rotating rectifier brushless machine;
- (3) Inductor alternator; and
- (3) Stationary field brushless machine.

(1) Permanent magnet machine

The permanent magnet machines have no control over the field excitation. To maintain a constant voltage for various wind speed, a regulator rated at full output power must be incorporated between the alternator and load. The cogging or detenting forces cause starting problems when coupled to a low torque wind turbine. In addition, the cost of the permanent magnets is comparatively expensive. Apart from these disadvantages, the permanent magnet machine is comparatively small and light weight and has an inherently high efficiency.

(2) Rotating rectifier brushless machine

This type of machine has a fully controllable field. It is essentially two machines on the same shaft. The stator of the exciter provides field to induce voltage in the rotor winding. The voltages are rectified and fed to the rotor field of the alternator. Thus, the field excitation of the alternator can be controlled by adjusting the stator current of the exciter.

This alternator requires the design of two machines and therefore is costly. Because of the probable inefficiency of two machines, the overall efficiency will be reduced, hence it is not economical for low rating alternators.

(3) Inductor alternator

Present designs are limited to high speed, high frequency, single-phase alternators. Currently a parallel study is underway to investigate the applicability of the Guy-type inductor alternator for wind turbines.

(4) Stationary field brushless machine

This type of alternator is similar to the Lundell machine, except there is no winding in its rotor. Fig 1.2 shows two configurations of this type of alternator. The field is provided by concentrated axial winding about the shaft or the inside of the frame. A magnetic field is produced across the auxiliary airgap on the rotor, hence voltage is induced on the stator phase winding. The main advantage of this machine is that no brushes are required, and yet the excitation is fully controllable. Since the rotor is simply of the claw-poles type, it is economical to manufacture.

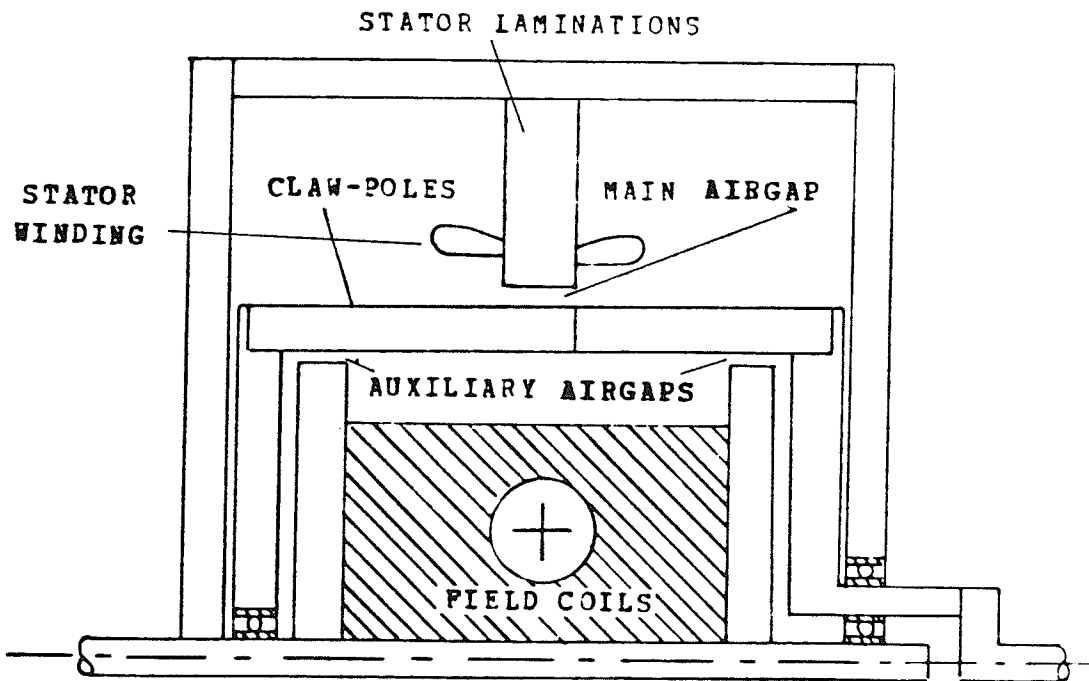
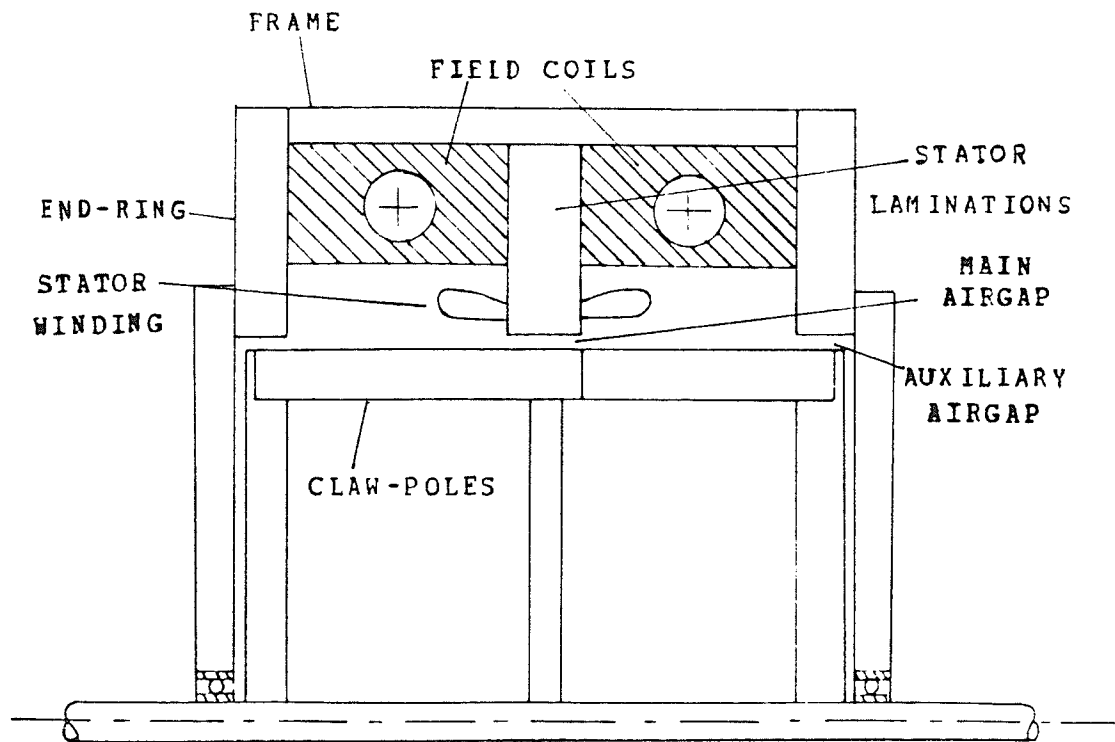


Figure 1.2: Stationary Field Brushless Machines

1.4 Scope of The Thesis

A reliable, simple and fully controllable brushless alternator for windmill applications is desirable for unmanned locations and the cold weather in Canada. The development of a stationary field, brushless alternator capable to operate at reasonable efficiency (75% or more) over a wide range of wind speeds is the main theme of this thesis.

The studies of the development are as follows :

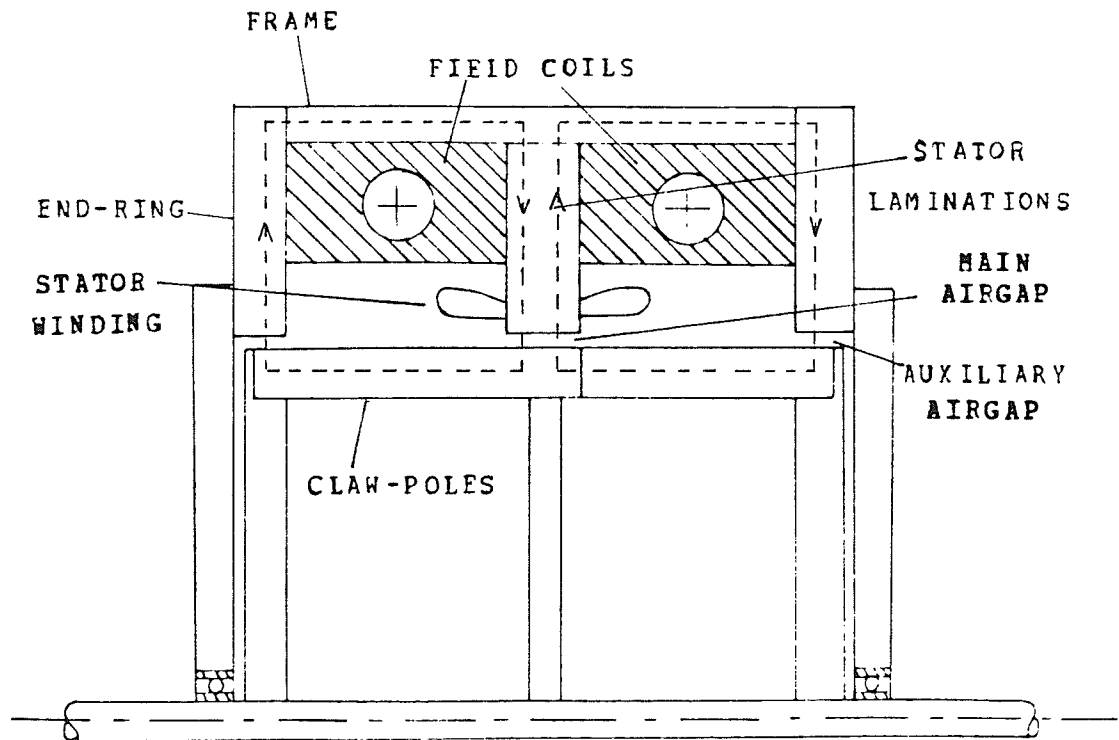
- (1) Concept and theory of the design,
- (2) Sample design of a prototype machine,
- (3) Tests on the prototype,
- (4) Final design,
- (5) Optimal design, and
- (6) Alternate designs.

Chapter II

BRUSHLESS LUNDELL ALTERNATORS

2.1 General

A brushless Lundell alternator is a modified conventional Lundell machine^{2 3}. Fig. 2.1 shows the main feature of a brushless Lundell alternator. The rotor is similar to the Lundell type with claw-poles, but the field winding is stationary instead of rotating. Thus, no brushes are required for feeding current to the field winding. The field winding is placed along the inside surface of the frame on both sides of the stator back core. The frame and the end-rings are made of magnetic materials to form part of the magnetic path for saving material. The stator winding is the conventional three-phase winding. The magnetic path is shown by broken lines. There are two auxiliary airgaps between the end-rings and the rotor pole-claws. The main magnetic flux, produced by the field coils at the frame, travels along the frame to the first end-ring. The magnetic flux passes through the first auxiliary airgap to the pole claws (say, North poles). Here the flux distributes among the poles and penetrates into the stator through the main airgap. The flux goes circumferentially along the stator back core and returns through the main airgap at one pole pitch apart to the South poles. Here the flux crosses the



CLAW-POLES

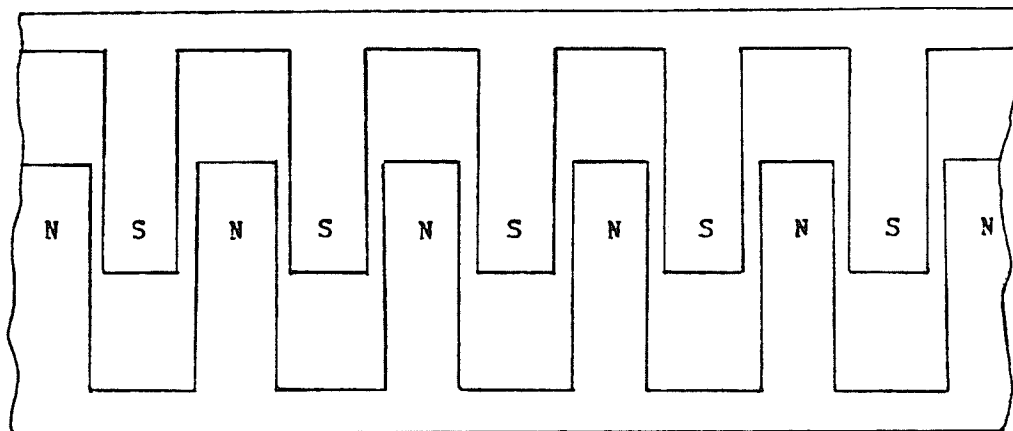


Figure 2.1: Brushless Lundell Alternator

second auxiliary airgap to the second end-ring and returns to the frame, thus completing the full magnetic circuit.

The stator has a three-phase double-layer lap winding. This machine has three different rated open circuit voltage outputs, as will be discussed later, and hence requires at least four identical winding sections. The teeth are tapered and the slots are rectangular in shape. The stator core laminations are skewed one slot pitch.

2.2 Design Procedure

A design must meet a set of specifications and constraints. The specifications are usually the following: rated power, rated voltage, power factor, efficiency, frequency and the r.p.m. of the machine. Generally, the constraints are efficiency, the cost and the weight of the machine. For this thesis the design specifications are described in Chapter Three. The design procedure is divided into seven major parts :

- (1) Poles and frequency,
- (2) Main dimensions,
- (3) Stator winding design,
- (4) Leakage reactance,
- (5) Magnetic circuit,
- (6) Field winding design,

(7) Losses and efficiency.

Each part of the design procedure will be discussed in the succeeding sections.

2.3 Poles and Frequency

A windmill is a variable speed prime mover so the alternator has to operate over a range of speed. The lowest operating speed of the alternator is designated as the threshold speed and the highest as the furling speed. The actual furling (or maximum) speed of the wind turbine may be considerably higher. The number of poles of the machine is first estimated by using the given frequency at furling, F_f , and the r.p.m. at furling, N_f , with the expression :

$$P = \frac{120.F_f}{N_f} \quad (2.1)$$

From Equation (2.1), the closest even number of poles, P , is used to compute the exact frequencies at furling and threshold. The frequency is expressed as :

$$F_f = \frac{P.N_f}{120} \quad \text{or} \quad F_t = \frac{P.N_t}{120} \quad (\text{Hz}) \quad (2.2)$$

where F_f and F_t are frequency at furling and threshold respectively.

2.4 Main Dimensions

After the number of poles and frequencies are computed, the main dimensions can be determined. First, an average airgap flux density, B , for the machine is assumed. The average flux per pole is therefore expressed as

$$\Phi = \frac{\pi \cdot D_b \cdot L \cdot B}{P} \quad (\text{Wb/Pole}) \quad (2.3)$$

where D_b is the stator bore diameter,
 L is the core length.

The angular speeds of the machine at threshold and furling are :

$$n_t = \frac{N_t}{60} \quad (\text{rev./sec.}) \quad (2.4)$$

$$n_f = \frac{N_f}{60} \quad (\text{rev./sec.}) \quad (2.5)$$

The e.m.f. per phase is given by

$$\begin{aligned} V_p &= 4.44 \Phi \cdot F \cdot T_{ph} \cdot K_w \\ &= 2.22 \pi \cdot D_b \cdot L \cdot T_{ph} \cdot K_w \cdot B \cdot n \quad (V) \end{aligned} \quad (2.6)$$

where F is the operating frequency,
 n is the angular speed,
 K_w is the winding factor,
and T_{ph} is the number of turns per phase.

If δ_b , L , T_{ph} , K_w are all fixed, V_p is directly proportional to B and n , i.e.,

$$V_p \propto B.n \quad (2.7)$$

For a constant voltage machine, V_p is almost constant between n_f and n_t , and therefore B has to be varied accordingly. The threshold flux density, B_t , is thus related to the furling flux density, B_f , by

$$B_t = \frac{n_f.B_f}{n_t} \quad (T) \quad (2.8)$$

Since $n_f > n_t$, therefore $B_t > B_f$. To prevent saturation at low speed operation, the threshold airgap flux density, B_t , is first chosen and then B_f is obtained from Equation 2.8.

The electrical loading, ampere conductor per meter of the airgap surface, at threshold and furling is defined as

$$a_{ct} = \frac{6.T_{ph}.I_{ft}}{\pi.\delta_b} \quad (a.c./m.) \quad (2.9)$$

where I_{ft} is the threshold full load current.

$$a_{cf} = \frac{6.T_{ph}.I_{ff}}{\pi.D_b} \quad (a.c./m) \quad (2.10)$$

where I_{ff} is the furling full load current.

From Equations 2.6, 2.8, 2.9, 2.10, the KVA output at threshold and furling of the machine can be expressed as

$$Q_t = 10.955 D_b^2 . L . n_t . a_{ct} . B_t . K_w \quad (KVA) \quad (2.11)$$

$$Q_f = 10.955 D_b^2 . L . n_f . a_{cf} . B_f . K_w \quad (KVA) \quad (2.12)$$

The output coefficient for threshold is defined as

$$\begin{aligned} G_t &= \frac{Q_t}{D_b^2 . L . n_t} \\ &= 10.955 a_{ct} . B_t . K_w \times 10^{-3} \end{aligned} \quad (2.13)$$

and for furling as:

$$\begin{aligned} G_f &= \frac{Q_f}{D_b^2 . L . n_f} \\ &= 10.955 a_{cf} . B_f . K_w \times 10^{-3} \end{aligned} \quad (2.14)$$

From Equations 2.13 and 2.14, the ratio of the output coefficient at threshold and furling is expressed as

$$\frac{G_f}{G_t} = \frac{Q_f . n_t}{Q_t . n_f} \quad (2.15)$$

The ratio between a_{ct} and a_{cf} is obtained from Equations 2.8, 2.11 and 2.12 as

$$\frac{a_{cf}}{a_{ct}} = \frac{Q_t}{Q_f} \quad (2.16)$$

Since Q_t and Q_f are specified outputs, the electrical loadings at threshold and furling have to be different and the difference depends on the ratio of Q_t and Q_f . By calculating the ratio Q_f/F_f , the estimated value of electrical loading at furling, a_{cf} , can be obtained⁴. The electrical loading at threshold, a_{ct} , is evaluated from Equation 2.16. The output coefficients at furling and threshold are calculated from Equations 2.13 and 2.14, with an estimated winding factor K_w between 0.8 to 1.0, usually 0.9.

From Equation 2.13, the bore diameter, D_b , of the machine is given by

$$D_b = \frac{(P \cdot Q_t \times 10^{-3})^{1/3}}{(K_r \cdot \pi \cdot n_t \cdot G_t)} \quad (m.) \quad (2.17)$$

where K_r is the ratio of armature length L to pole-pitch.

$$K_r = \frac{L}{\tau} = \frac{L}{\pi \cdot D_b / P} \quad (2.18)$$

Generally, K_r is chosen between 0.8 to 2.5.⁴ After the stator bore diameter is determined, the length of the stator core can be computed with the expression

$$L = \frac{Q_t \times 10^{-3}}{n_t \cdot G_t \cdot D_b^2} \quad (\text{m.}) \quad (2.19)$$

In Equations 2.17 and 2.19, the threshold value is used for calculation, because the airgap flux density at threshold is higher than that at furling. If B_f is used for calculation, saturation may occur in the iron when the machine is operating at low speed. The iron loss and leakage flux would also be high.

The rotor peripheral speed is used to check the mechanical safety of the machine. The rotor peripheral speed at threshold and furling are :

$$V_t = \pi \cdot D_b \cdot n_t \quad (\text{m./sec.}) \quad (2.20)$$

$$V_f = \pi \cdot D_b \cdot n_f \quad (\text{m./sec.}) \quad (2.21)$$

The rotor peripheral speed can reach up to about 30 to 60 m/s⁵, but for mechanical rigidity, it is preferable to limit it to less than 15 m/s. For the design procedure peripheral speed is used as a constraint. If it exceeds the mechanical

safety limits, a new ratio of armature length to pole pitch has to be chosen. The stator bore diameter and core length are recomputed again until the mechanical safety is satisfied.

2.5 Stator Winding Design

When a machine is designed for multiple output voltages, a number of parallel circuits are required. For a 'm' phase machine with 'a' number of parallel paths, the number of slots N_s must be a multiple of $m.a$, i.e.,

$$\frac{N_s}{m.a} = \text{integer} \quad (2.22)$$

The number of slots depends on the type of winding desired. In general, the integral slot winding has an integral number of slots per pole per phase, while for the fractional slot winding, the number of slots per pole per phase can be a fraction.

After the number of slots is determined, the slot pitch is calculated using the expression

$$y_s = \frac{\pi.D_b}{N_s} \quad (2.23)$$

Choosing the ratio between tooth width and slot pitch of about 0.3 to 0.7, the tooth pitch is calculated. If the flux density in the tooth is higher than 1.8T, saturation may occur. A ratio between tooth pitch and slot pitch must therefore be changed to a higher value.

There are many choices of armature windings. The most commonly used winding is a double layer lap winding with short-pitched coils. The advantages of double layer lap winding are :

- (a) ease of manufacturing
- (b) fractional slotting can be used
- (c) chorded spans are obtained

A double-layer lap winding is used in this design. A phase spread of 60° or 120° is chosen to fix the coil span. The electrical space phase angle between coil axes is then calculated. The distribution factor K_d of the winding is computed by the expression

$$K_d = \frac{\sin(k.\delta)/2}{k.\sin\delta/2} \quad (2.24)$$

where k is the number of coils per pole per phase.

δ is the angle between coils emf.

The coil-span factor k_e is obtained by the Equation

$$K_e = \cos \epsilon / 2 \quad (2.25)$$

where ϵ is the angle by which a coil is short pitched.

The stator laminations are skewed one slot pitch to prevent cogging. The skew factor is

$$K_s = \frac{\sin \beta / 2}{\beta / 2} \quad (2.26)$$

where $\beta = \tan^{-1} (y_s / L)$

where y_s is the slot pitch,
 L is the core length.

The winding factor is expressed as

$$K_w = K_d \cdot K_e \cdot K_s \quad (2.27)$$

After determining the winding factor K_w , the estimated K_w is replaced with the calculated value. The stator bore diameter, D_b , core length, L , electrical loading and output coefficient are computed from Equations 2.9, 2.10, 2.13, 2.14, 2.17, and 2.19. If the electrical loading and output coefficient are too large, the main dimensions have to be recalculated.

The number of turns required at furling and threshold is

calculated with the following expression

$$T_{ph} = \frac{V_p \times 1.05}{0.11624 \ n \cdot K_w \cdot B \cdot D_b \cdot L} \quad (2.28)$$

where n is the angular speed,
 B is the airgap flux density.

The factor 1.05 allows for a first estimate for the voltage drop in the winding under full load. The larger number of turns between furling and threshold is used.

The full load current at furling and threshold is obtained by the expressions

$$I_{ft} = \frac{W_t}{m \cdot P_f \cdot V_p} \quad (A) \quad (2.29)$$

where W_t is the rated output power at threshold,
 P_f is the power factor,
 m is the number of phase.

$$I_{ff} = \frac{W_f}{m \cdot P_f \cdot V_p} \quad (A) \quad (2.30)$$

where W_f is the rated output power at furling.

The furling current is used to calculate the conductor size.

For 'a' parallel paths, the current per path at furling is

$$I_{pp} = \frac{I_{ff}}{a} \quad (A) \quad (2.31)$$

The number of coils per path per phase is

$$C_{pp} = \frac{N_s}{m \cdot a} \quad (2.32)$$

The number of turns per coil is

$$T_{pc} = \frac{T_{ph}}{C_{pp}} \quad (2.33)$$

The number of conductor per slot is

$$N_c = 2 \cdot T_{pc} \quad (2.34)$$

A current density, J_s , and a space factor, S_f , are assumed to calculate the slot area, A_s , and the slot depth, h_t . The conductor size is expressed as

$$A_{scs} = \frac{I_{pp}}{J_s} \quad (m.^2) \quad (2.35)$$

The area of the slot required is

$$A_s = \frac{A_{scs} \cdot N_c}{S_f} \quad (m.^2) \quad (2.36)$$

where a space factor, S_f , of between 0.4 to 0.5 was chosen.

The slot depth is expressed as

$$h_t = \frac{A_s}{W_o} \quad (m.) \quad (2.37)$$

where W_o is the slot width

If h_t is too big, either the current density J_s or the slot width W_o has to be increased. The current density J_s can be increased if it is within the current density limit. However, the I^2R loss of the winding is directly proportional to the square of the current density, therefore a small current density is recommended. If the slot width is increased, saturation may occur in the teeth. In the case when both current density and slot width cannot be changed, the stator bore diameter and the core length have to be increased.

2.5.1 Copper Loss In Stator

The mean length of a coil is estimated with the method suggested by Kuhlmann⁴. The shape of an armature coil for synchronous machine is shown in Fig 2.2. The length of the mean-turn is expressed as

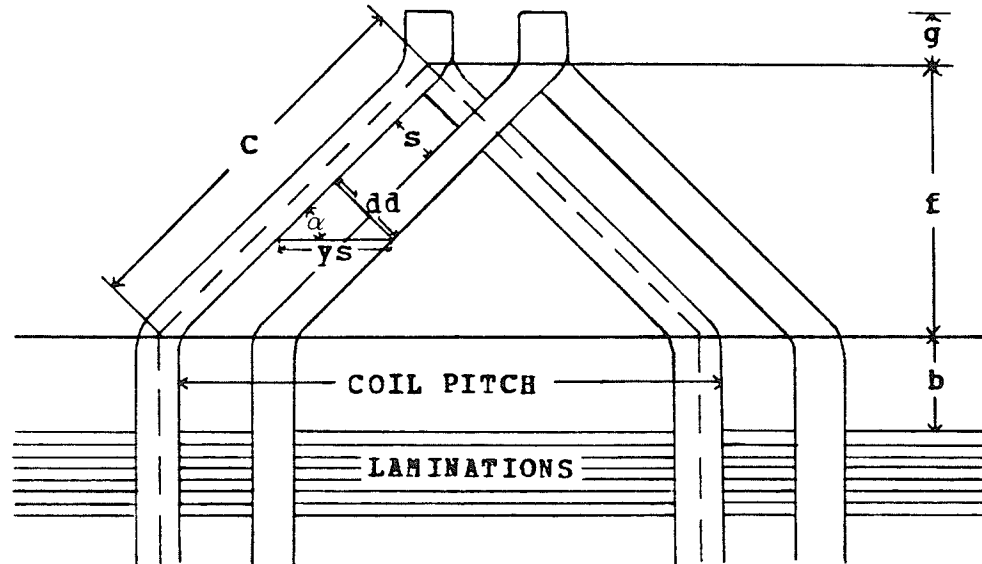


Figure 2.2: The Shape of Armature Coils

$$L_m = 2 \left\{ \frac{\pi \cdot (D_b + h_t) \cdot c_p}{P \cdot \cos \alpha} + 2b + h_t + L \right\} \quad (\text{m.}) \quad (2.38)$$

where $c_p = (\text{coil pitch}) / (\text{slot per pole})$

$$\alpha = \sin^{-1}(dd/ys)$$

$$dd = W_o + s$$

b is the coil extension,

s is the coil clearance,

L is the core length,

h_t is the slot depth.

Total length of coils per path is

$$L_p = L_m \cdot T_{pc} \cdot C_{pp} \quad (m.) \quad (2.39)$$

The resistance per path at $75^{\circ}C$ is

$$R_p = \frac{\rho \cdot L_p}{A_{scs}} \quad (Ohm) \quad (2.40)$$

where ρ is the resistivity of copper at $75^{\circ}C$.

The resistance per phase is written as

$$R_{ph} = \frac{R_p}{a} \quad (Ohm) \quad (2.41)$$

The I^2R losses at furling and threshold can be calculated with following expressions

$$C_{lf} = m \cdot I_{ff}^2 \cdot R_{ph} \quad (W) \quad (2.42)$$

$$C_{lt} = m \cdot I_{ft}^2 \cdot R_{ph} \quad (W) \quad (2.43)$$

2.6 Leakage Reactance

2.6.1 Slot Leakage Reactance

Fig 2.3 shows a slot with double-layer winding. The mmf of the slot currents will set up leakage flux in each of the five paths indicated in the diagram. These fluxes are

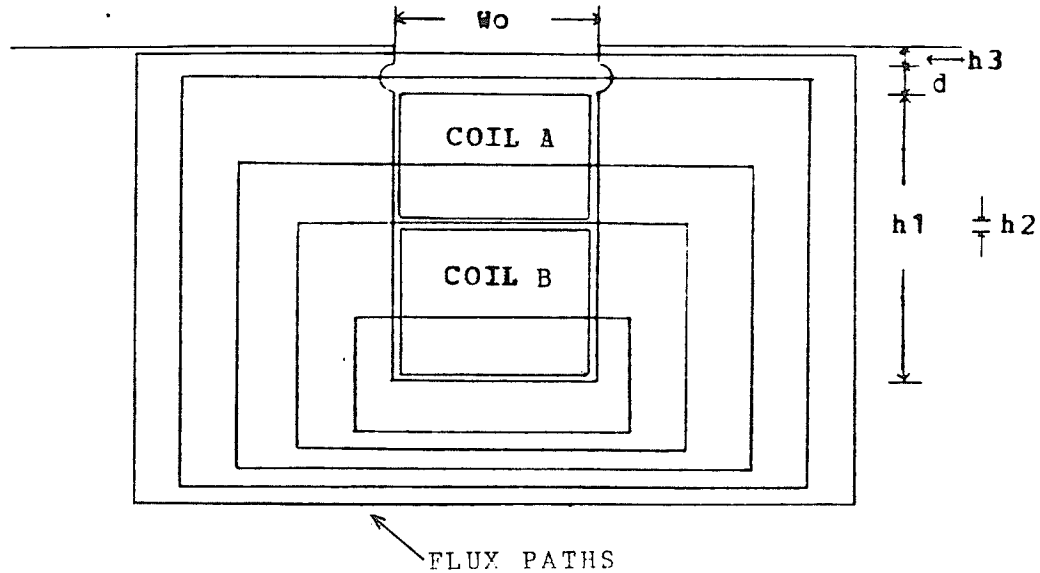


Figure 2.3: Slot Leakage Flux With Double-Layer Winding

computed with the assumption that the fluxes pass straight across the slots and the reluctance of the iron paths is negligible. For calculating the slot leakage flux, there are two cases to be considered:

(a) Full pitch coils--coil A and coil B are of the same phase.

(b) Short pitch coil--coil A and coil B are out of phase.

(a) Full pitch coil

Since coil A and coil B are coils of the same phase, the currents in the slot are also in phase. The derivation of the leakage flux per slot per length of core is similar to Alger⁶ and Landsdorf⁷. It is expressed as

$$\lambda_s = 4 \cdot T_{pc}^2 \cdot \mu_o \left\{ \frac{h_3}{W_o} + \frac{d}{W_o + d} + \frac{h_1}{3 \cdot W_o} - \frac{h_2}{12 \cdot W_o} \right\} \quad (2.44)$$

where μ_o is the permeability of air.

The leakage reactance for in phase coils is

$$X_s = 2 \cdot \pi \cdot F \cdot L \cdot \lambda_s \cdot S_{pi} \quad (\text{Ohm}) \quad (2.45)$$

where s_{pi} is the number of slots per phase.

(b) Short pitch coil

In this case, some slots has in phase coils so Equation 2.44 can be applied. For those slots with out of phase coils, assume the current in coil A leads the current in coil B by an angle θ ($2\pi/3$ for three-phase). The method suggested by Langdorf is used⁷. The self-inductance of coil A is proportional to the leakage flux λ_a . λ_a is expressed as

$$\lambda_a = T_{pc}^2 \cdot \mu_o \left\{ \frac{h_3}{W_o} + \frac{d}{W_o + d} + \frac{h_1 - h_2}{6 \cdot W_o} \right\} \quad (2.46)$$

The self inductance of coil B is proportional to the leakage flux λ_b . λ_b is expressed as

$$\lambda_b = T_{pc}^2 \cdot \mu_o \left\{ \frac{h_3}{W_o} + \frac{d}{W_o + d} + \frac{2 \cdot h_1 + h_2}{3 \cdot W_o} \right\} \quad (2.47)$$

The mutual inductance of coil A due to the unit current in coil B is proportional to the mutual flux leakage λ_{ab} . The mutual leakage flux is

$$\lambda_{ab} = T_{pc}^2 \cdot \mu_o \left\{ \frac{h_1 - h_2}{4 \cdot W_o} + \frac{h_3}{W_o} + \frac{d}{d + W_o} \right\} \quad (2.48)$$

The mutual leakage flux λ_{ab} of coil B due to the unit current in coil A is equal to the mutual leakage flux λ_{ab} . The leakage inductance of coil A and coil B are derived in Appendix I and they can be expressed as

$$L_a = (\lambda_a^2 + \lambda_{ab}^2 + 2 \cdot \lambda_a \cdot \lambda_{ab} \cdot \cos \theta)^{1/2} \quad (2.49)$$

$$L_b = (\lambda_b^2 + \lambda_{ba}^2 + 2 \cdot \lambda_b \cdot \lambda_{ba} \cdot \cos \theta)^{1/2} \quad (2.50)$$

The total leakage inductance per slot is

$$L_T = L_a + L_b \quad (2.51)$$

Therefore the leakage reactor per phase due to out of phase coils in a slot is

$$X_o = 2 \cdot F \cdot L \cdot L_T \cdot S_{po} \quad (2.52)$$

where S_{po} is slots per phase with out of phase coil,

F is the frequency at furling or threshold.

In general, some of the slots of fractional-pitch winding will be occupied by coil sides of the same phase. Thus, the total slot leakage reactance is the sum of Equation 2.45 and 2.52

$$X_{st} = X_o + X_s \quad (2.53)$$

2.6.2 Overhang Leakage Reactance

There are only empirical formulae for calculating overhang leakage reactance. The overhang leakage reactance is estimated with an empirical formula suggested by Alger⁶.

$$X_{oh} = \frac{38.4 \pi \cdot F \cdot \mu_o \cdot T_{pc}^2 \cdot D_b \cdot N_s \cdot (3p - 1)}{2 \cdot p} \quad (2.54)$$

where p is the coil pitch fraction.

The zig-zag leakage and the differential leakage are usually small enough to be ignored. Therefore, the total leakage considered is the sum of the slot leakage reactance and the overhang reactance. The total leakage reactance per phase is

$$X_T = X_{oh} + X_{st} \quad (2.55)$$

2.7 Magnetic Circuit

The total ampere turns per pole required is the sum of the ampere turns for each part. The flux per pole is expressed as

$$\Phi = Bt.\tau.L \quad (\text{Wb}) \quad (2.56)$$

where τ is the pole-pitch.

The fluxes in different parts are determined accordingly. Assume the average flux densities in the stator back core, frame, end-rings and poles as B_c , B_f , B_{er} , and B_p respectively. The estimated flux densities are dependent on the magnetic characteristic of the material. For an optimum use of the material, high flux density is desired; but due to magnetic saturation, a value below 1.8T is usually chosen.

The required cross-sectional area A of each component of the magnetic circuit can be calculated by the Equation

$$A = \frac{\Psi}{B} \quad (\text{m}^2) \quad (2.57)$$

where Ψ is the flux in that part of magnetic circuit,
 B is the flux density.

Hence the dimension of each part of the magnetic circuit is obtained.

2.7.1 Total Ampere Turns Per Phase

The magnetic characteristic of materials are obtained by experiment. The ampere turns per pole of each part of the magnetic path, except the main airgap, is the length of that part multiplied by the corresponding magnetic field intensity from the magnetic curves. The presence of the slots increases the gap reluctance so the effective airgap reluctance has to be determined. A method suggested by M.G. Say is to find an effective contracted slot pitch with the expression

$$y_s' = y_s - K_o W_o \quad (2.58)$$

where K_o is the Carter coefficient.

Carter coefficient K_o is obtained from the Carter's curve from the ratio of slot width to gap length. Hence the effective pole area becomes

$$A_p = y_s' \cdot L \cdot S_p \quad (2.59)$$

where S_p is slots per pole.

The effective airgap flux density is

$$B_g = \frac{\Phi}{A_p} \quad (2.60)$$

The ampere turns per pole at the main airgap is

$$AT_{mg} = \frac{L_g \cdot B_g}{\mu_0} \quad (2.61)$$

where L_g is the length of the air gap.

The sum of the total ampere turns in series is the total required ampere turns per pole for the magnetic circuit. The demagnetizing ampere turns per pole for armature reaction is

$$AT_{ar} = 1.35 K_w \cdot T_{ph} \cdot I_{ff} / P \quad (2.62)$$

The total A.T. per pole pair AT_{fd} for the field is equal twice the sum of the total A.T. of the magnetic circuit and the A.T. of armature reaction.

2.8 Field Winding Design

The rectified output voltage is used as the exciter voltage E_f . Since there are several rated output voltages, a number of parallel field circuits are required.

The cross-section area of the field winding is expressed as

$$A_{cf} = \frac{AT_{fd}}{S_f \cdot J_f} \quad (m.^2) \quad (2.63)$$

where S_f is the space factor (between 0.4 to 0.5),
 J_f is the current density.

A current density, J_f , is chosen to calculate A_{cf} . Allow sixty percent of the stator back core for placing the field winding and calculate the length of the frame.

The conductor size is expressed as

$$A_{sc} = \frac{ATfd \cdot \rho \cdot L_f}{af \cdot E_f} \quad (m.^2) \quad (2.64)$$

where ρ is the resistivity of copper at 75^0C ,
 af is the number of parallel paths,
 L_f is the mean turn.

The number of turns required for each path is

$$T_{pf} = \frac{ATfd}{af \cdot A_{sc} \cdot J_f} \quad (2.65)$$

The resistance per path is expressed as

$$R_f = \frac{\rho \cdot l_f \cdot T_{pf}}{A_{sc}} \quad (Ohm) \quad (2.66)$$

The total I^2R loss of the field is

$$P_{lf} = ATfd \cdot \rho \cdot L_f \cdot J_f \quad (W) \quad (2.67)$$

2.9 Iron Loss

The iron loss is calculated in the two separate parts: the teeth and the core. The weight of the teeth and the core are calculated. The iron loss is expressed as

$$P_e = \frac{1.65 B^2 \cdot F^2 \cdot t^2 \cdot wt}{\rho_s \cdot Dens} \quad (W) \quad (2.68)$$

where B is the average flux density,
 F is the frequency of the machine,
 t is the thickness of the lamination,
 wt is the weight,
 $Dens$ is the density of the laminations,
 ρ_s is the resistivity of the material.

Substitute the weight and the flux density of the teeth and core into Equation 2.68 accordingly. The total iron loss is the sum of the iron loss of the teeth and the stator core.

2.10 Eddy Loss

The Equation suggested by M.G.Say is used to calculate the eddy current loss in the conductors in slots. First, estimate the width of copper 'bb' occupied in the slot. Then find the number of layers of conductor 'c' in the slot. The

average eddy current loss ratio is expressed as

$$K_{ed} = (\sigma \cdot h)^4 (c^2/9) \quad (2.69)$$

where

$$\sigma = \left(\frac{\pi \cdot \mu_o \cdot F \cdot b b}{2 \cdot \rho \cdot W_o} \right)^{1/2}$$

The average eddy current loss is equal to K_{ed} multiplied by the $I^2 R$ loss of the conductors in the slots.

2.11 Temperature Rise

The power loss in the windings are dissipated as heat. The loss heat is transferred by a combination of conduction, radiation and convection. Assume the machine as a homogeneous body with surface area A , the power transferred by conduction across the interface between air and machine surface is

$$P_c = K_c (T_1 - T_2) \cdot A \quad (W) \quad (2.70)$$

where K_c is the coefficient of air (10 to 50),

T_1 is the final temperature inside the machine,

T_2 is the ambient temperature of the air.

The power transferred by radiation is

$$P_r = 5.7 \times 10^{-8} \epsilon_m (T_1^4 - T_2^4) \cdot A \quad (W) \quad (2.71)$$

where ϵ_m is the emissivity of the material.

The power transferred by convection is

$$P_v = 2 \cdot a_p^{1/2} (T_1 - T_2)^{5/4} \cdot A \quad (W) \quad (2.72)$$

where a_p is the number of atmosphere pressure

The final temperature T_1 is obtained by using an iteration method on Equations 2.70, 2.71 and 2.72.

2.12 Efficiency

The losses in various part of the machine are summed up. The efficiencies at furling and threshold is calculated from the Equation

$$\text{Eff} = 1 - \frac{\text{PL}}{\text{PL} + \text{W}} \quad (\%) \quad (2.73)$$

where PL is the total power loss,

W is the rated output power.

The above design procedures are applied for a sample design in the following chapter.

Chapter III

SAMPLE DESIGN

3.1 Specification For Design

A set of specifications has been chosen for the sample design to demonstrate the concept and the feasibility of the proposed design. The specifications are given in Table 3.1. There were some limitations on the design due to the constraint of the available material. The armature laminations and the frame are available, which fix the stator bore diameter, the slot number, the tooth width and the length of the frame. The design procedure discussed earlier has therefore to be modified. A computer program is written for the purpose of design and is given in Appendix II.

TABLE 3.1

Specifications of Design

	<u>Threshold</u>	<u>Furling</u>
Speed (r.p.m.)	: 87	174
Full load power (W)	: 20	160
Power factor	: 0.6	0.6
Phase voltage (V)	: 8,16,32	8,16,32
Number of phase	: 3	3

Details of available stator laminations :

Bore Diameter D_b - 0.3046 m.

Outside Diameter D_{os} - 0.4315 m.

Number of Slots - 72

Slot Pitch y_s - 0.016 m.

Slot Width W_o - 0.008 m.

Slot Depth h_t - 0.03 m.

Teeth - tapered

The length of the frame, L_f , is 0.11 m. and the thickness, T_f , is 0.011 m. The stator core length, L , is chosen at 0.02538 m. Twenty four poles are chosen to give an output frequency of 17.4 Hz at the threshold, and 34.8 Hz at furling. The peripheral speeds at furling and threshold are checked by Equations 2.20 and 2.21, and found to be 2.77 m/s and 1.38 m/s respectively. They satisfy the requirement that the peripheral speed be less than 15 m/s.

The design schedule is shown in Table 3.2.

3.2 Stator Winding

Since the number of poles chosen is 24, it gives one slot per pole per phase. The phase spread is 60^0 . Integral slot double-layer lap winding is used. Full pitch coils are used such that the distribution factor and coil span factor

TABLE 3.2

Design Schedule

RATING	8 W. OUTPUT		16 W. OUTPUT		32 W. OUTPUT	
	THRESHOLD	FOPLING	THRESHOLD	FOPLING	THRESHOLD	FOPLING
MAIN DIMENSIONS						
PULL LOAD (VA)	33.33333	266.66650	33.33333	266.66650	33.33333	266.66650
PULL LOAD POWER (W)	20.00000	160.00000	20.00000	160.00000	20.00000	160.00000
LINE VOLTAGE (V)	13.85640	13.85640	27.71280	27.71280	55.42560	55.42560
PHASE VOLTAGE (V)	8.00000	8.00000	16.00000	16.00000	32.00000	32.00000
CURRENT PER PHASE (A)	1.38889	11.11102	0.69444	5.55556	0.34722	2.77778
POWER FACTOR	0.60000	0.60000	0.60000	0.60000	0.60000	0.60000
FREQUENCY (Hz)	17.39999	34.79999	17.39999	34.79999	17.39999	34.79999
SPEED (RPM)	87.00000	174.00000	87.00000	174.00000	87.00000	174.00000
NUMBER OF POLES	24.00000	24.00000	24.00000	24.00000	24.00000	24.00000
MAIN DIMENSIONS						
MAGNETIC LOADING (T)	0.60000	0.30000	0.60000	0.30000	0.60000	0.30000
ELECTRIC LOADING (AC/E)	1487.115	11896.910	1487.115	11896.910	1487.115	11896.910
OUTPUT COEFFICIENT (KVA/RPS/8**3)	0.97652 01	0.39062 02	0.97652 01	0.39062 02	0.97652 01	0.39062 02
STATOR BORE DIAMETER (M)	0.30462 00	0.30462 00	0.30462 00	0.30462 00	0.30462 00	0.30462 00
STATOR OUTSIDE DIAMETER (M)	0.43002 00	0.43002 00	0.43002 00	0.43002 00	0.43002 00	0.43002 00
GROSS CORE LENGTH (M)	0.25382 01	0.25382 01	0.25382 01	0.25382 01	0.25382 01	0.25382 01
IRON LENGTH (M)	0.22842 01	0.22842 01	0.22842 01	0.22842 01	0.22842 01	0.22842 01
POLE PITCH (M)	0.39872 01	0.39872 01	0.39872 01	0.39872 01	0.39872 01	0.39872 01
FRAME OUTSIDE DIAMETER (M)	0.45202 00	0.45202 00	0.45202 00	0.45202 00	0.45202 00	0.45202 00
THICKNESS OF THE FRAME (M)	0.11002 01	0.11002 01	0.11002 01	0.11002 01	0.11002 01	0.11002 01
LENGTH OF THE FRAME (M)	0.11002 00	0.11002 00	0.11002 00	0.11002 00	0.11002 00	0.11002 00
END-RING OUTSIDE DIAMETER (M)	0.45202 00	0.45202 00	0.45202 00	0.45202 00	0.45202 00	0.45202 00
END-RING INSIDE DIAMETER (M)	0.30462 00	0.30462 00	0.30462 00	0.30462 00	0.30462 00	0.30462 00
THICKNESS OF THE END-RING (M)	0.11422 01	0.11422 01	0.11422 01	0.11422 01	0.11422 01	0.11422 01
STATOR						
WINDING						
NUMBER OF PARALLEL CIRCUIT	2.00000	2.00000	2.00000	2.00000	2.00000	2.00000
NUMBER OF SLOTS	72.00000	72.00000	72.00000	72.00000	72.00000	72.00000
SLOTS/POLE/PHASE	1.00000	1.00000	1.00000	1.00000	1.00000	1.00000
CONDUCTORS/SLOT	66.39871	66.39871	66.39871	66.39871	66.39871	66.39871
URNS/PARALLEL CIRCUIT	199.19610	199.19610	398.39200	398.39200	796.78400	796.78400
PITCH FACTOR	0.96600	0.96600	0.96600	0.96600	0.96600	0.96600
DISTRIBUTION FACTOR	0.96600	0.96600	0.96600	0.96600	0.96600	0.96600
WINDING FACTOR	0.99900	0.99900	0.99900	0.99900	0.99900	0.99900
CONDUCTOR SIZE (8**2)	0.13142 05	0.13142 05	0.13142 05	0.13142 05	0.13142 05	0.13142 05
CURRENT DENSITY (A/8**2)	0.21142 07	0.21142 07	0.21142 07	0.21142 07	0.21142 07	0.21142 07
SLOT PITCH (M)	0.13292 01	0.13292 01	0.13292 01	0.13292 01	0.13292 01	0.13292 01
SLOT WIDTH (M)	0.80002 02	0.80002 02	0.80002 02	0.80002 02	0.80002 02	0.80002 02
SLOT DEPTH (M)	0.30002 01	0.30002 01	0.30002 01	0.30002 01	0.30002 01	0.30002 01
TOOTH WIDTH (M)	0.53162 02	0.53162 02	0.53162 02	0.53162 02	0.53162 02	0.53162 02
RESISTANCE/PHASE (OHM)	0.26322 00	0.26322 00	0.10532 01	0.10532 01	0.42102 01	0.42102 01
I**2R LOSS (W)	1.52249	97.46497	1.52249	97.46497	1.52249	97.46497
EDDY CURRENT LOSS (W)	0.00058	0.14952	0.00058	0.14952	0.00058	0.14952
STRAY LOSS (W)	0.30469	19.52289	0.30469	19.52289	0.30469	19.52289
LEAKAGE REACTANCE (OHM)	0.29589	0.59178	0.42575	0.84510	0.68549	1.37046
ROTOR						
LUNDHILL TYPE						
POLE ARC (M)	0.27912 01	0.27912 01	0.27912 01	0.27912 01	0.27912 01	0.27912 01
THICKNESS OF THE POLE (M)	0.24472 01	0.24472 01	0.24472 01	0.24472 01	0.24472 01	0.24472 01
LENGTH OF POLE-SHOE (M)	0.67692 01	0.67692 01	0.67692 01	0.67692 01	0.67692 01	0.67692 01
FIELD TURNS	77.64662	77.64662	77.64662	77.64662	77.64662	77.64662
NUMBER OF PARALLEL CIRCUIT	2.00000	2.00000	2.00000	2.00000	2.00000	2.00000
CONDUCTOR SIZE (8**2)	0.17572 05	0.17572 05	0.17572 05	0.17572 05	0.17572 05	0.17572 05
CURRENT DENSITY (A/8**2)	40.06757	27.55853	20.03378	13.77927	10.01689	6.88963
CURRENT DENSITY (A/8**2)	0.57002 07	0.57002 07	0.57002 07	0.57002 07	0.57002 07	0.57002 07
RESISTANCE (OHM)	0.29949	0.29949	1.19798	1.19798	4.79190	4.79190
I**2R LOSS (W)	480.81030	227.45750	480.81030	227.45750	480.81030	227.45750
PERIPHERAL VELOCITY (M/S)	1.38736	2.77473	1.38736	2.77473	1.38736	2.77473
MAGNETISATION						
POLE/POLE (W)	0.54642 03	0.27322 03	0.54642 03	0.27322 03	0.54642 03	0.27322 03
CORE FLUX DENSITY (T)	0.18852 00	0.18852 00	0.18852 00	0.18852 00	0.18852 00	0.18852 00
TOOTH FLUX DENSITY (T)	0.66442 00	0.66442 00	0.66442 00	0.66442 00	0.66442 00	0.66442 00
FRAME FLUX DENSITY (T)	0.75002 00	0.75002 00	0.75002 00	0.75002 00	0.75002 00	0.75002 00
GAP LENGTH AT STATOR (M)	0.00100	0.00100	0.00100	0.00100	0.00100	0.00100
GAP LENGTH AT END-RING (M)	0.00100	0.00100	0.00100	0.00100	0.00100	0.00100
FIELD A.T./POLE	1555.55400	1069.91300	1555.55400	1069.91300	1555.55400	1069.91300
ARMATURE A.T./POLE	15.5466	124.3731	15.5466	124.3731	15.5466	124.3731
WEIGHT OF THE MACHINE						
WEIGHT OF STATOR WINDING	9.2429	9.2429	9.2429	9.2429	9.2429	9.2429
WEIGHT OF FIELD WINDING	6.2718	6.2718	6.2718	6.2718	6.2718	6.2718
WEIGHT OF THE STATOR CORE	12.7297	12.7297	12.7297	12.7297	12.7297	12.7297
WEIGHT OF THE FRAME	12.9084	12.9084	12.9084	12.9084	12.9084	12.9084
WEIGHT OF THE POLES	20.0000	20.0000	20.0000	20.0000	20.0000	20.0000
WEIGHT OF THE POLE SUPPORT	0.6611	0.6611	0.6611	0.6611	0.6611	0.6611
WEIGHT OF THE END RING	12.7715	12.7715	12.7715	12.7715	12.7715	12.7715
TOTAL WEIGHT	63.1288	63.1288	63.1288	63.1288	63.1288	63.1288
EFFICIENCY						
TEMPERATURE RISE (C)	20.0000	15.0000	20.0000	15.0000	20.0000	15.0000
TEMPERATURE INSIDE THE MACHINE (C)	45.0000	40.0000	45.0000	40.0000	45.0000	40.0000
IRON LOSS	0.2502	0.2502	0.2502	0.2502	0.2502	0.2502
STATOR I**2R LOSS (W)	1.5229	97.4650	1.5229	97.4650	1.5229	97.4650
EDDY CURRENT LOSS (W)	0.0006	0.1495	0.0006	0.1495	0.0006	0.1495
FIELD I**2R LOSS (W)	0.3047	19.5229	0.3047	19.5229	0.3047	19.5229
FIELD I**2R LOSS (W)	480.8103	227.4575	480.8103	227.4575	480.8103	227.4575
TOTAL LOSS (W)	482.8884	344.8447	482.8884	344.8447	482.8884	344.8447
EFFICIENCY (%)	3.9770	31.6929	3.9770	31.6929	3.9770	31.6929

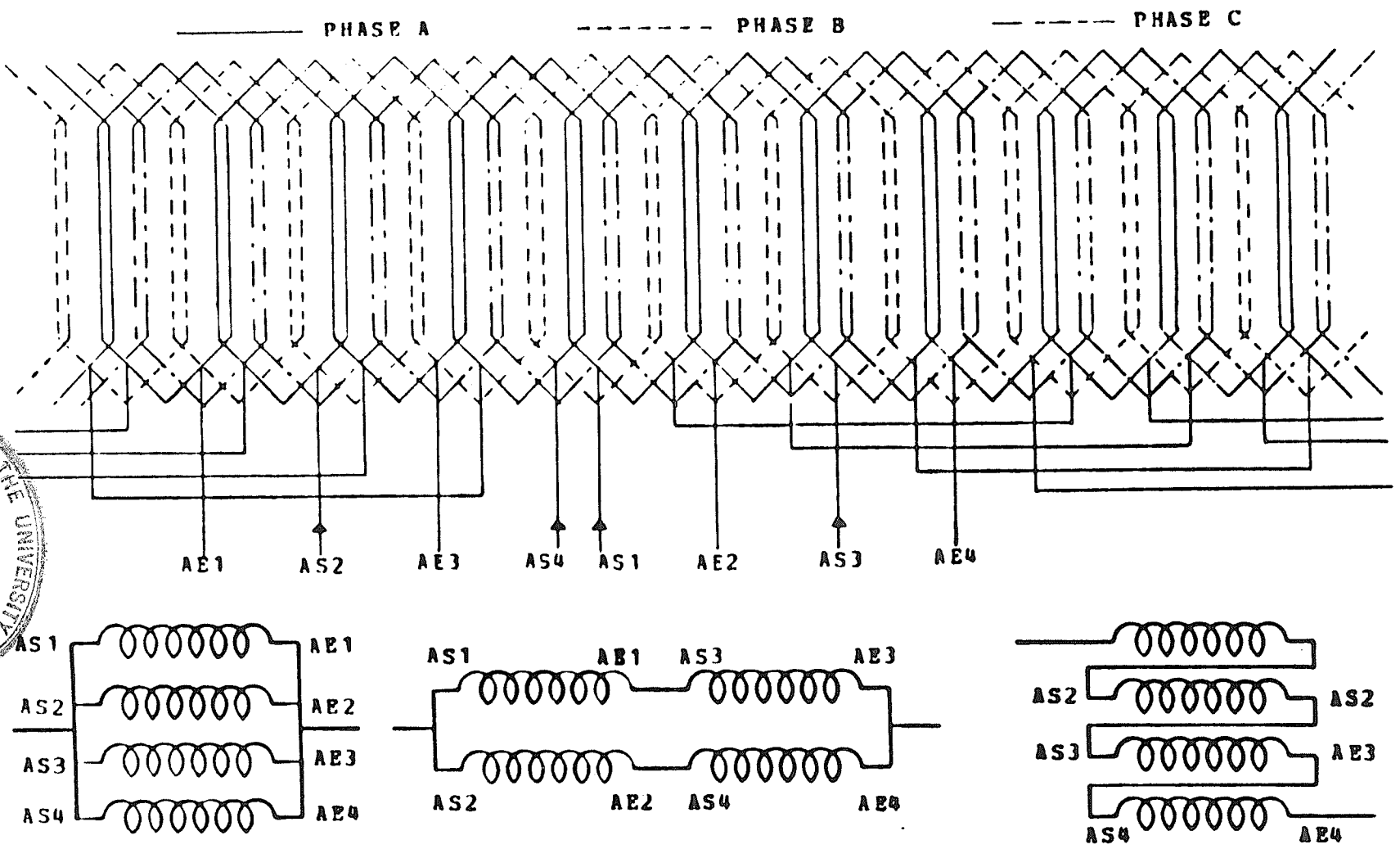
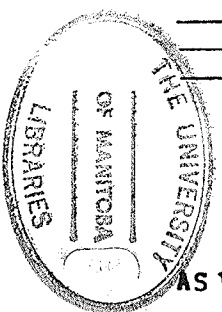
are equal to one. The stator laminations are skewed by one slot pitch. The skew factor obtained from Equation 2.26 is 0.99. Hence the winding factor is equal to 0.966.

There are three rated output voltages and the minimum number of parallel paths required is four. The winding diagram is shown in Fig. 3.1. The number of turns per phase is equal to 198. A space factor of 0.4 is used in calculating the conductor size. The conductor size is $0.1289 \times 10^{-6} \text{ m}$. The resistance and the I^2R loss of stator winding are calculated from Equations 2.40, 2.41, 2.42 and 2.43. The leakage reactance per phase is obtained from Equations 2.44 and 2.55 because all the coils are full pitch coils.

3.3 Magnetic Circuit

The average airgap flux density at threshold for the main airgap and the auxiliary airgaps are all equal to 0.6 T. The average flux density in the pole and in the end-ring are chosen to be 0.4 T and 0.675 T. The pole width is taken as 0.7 of the pole pitch. The average flux per pole is calculated from Equation 2.56. From Equation 2.57 the thickness of the pole and the end-rings are determined.

The ampere turns of each part are calculated. The armature reaction is determined by Equation 2.61. The total



-42-

8 V CONNECTION OF PHASE A 16 V CONNECTION OF PHASE A 32 V CONNECTION OF PHASE A
Figure 3.1: Stator Winding of The Machine

ampere turns per pole pair turns out to be 3500 A.T.

3.4 Field Winding

There are three exciter voltages, so four parallel circuits are required. Since the frame and the stator back core are fixed, the cross-section area of the field winding is also fixed.

A 0.4 space factor is used for calculation. A current density greater than $5.7 \times 10^6 \text{ A/m}^2$ is required to fit in the area provided. Since the field loss depends on the current density, JF, the minimum value of $5.7 \times 10^6 \text{ A/m}^2$ is used. From Equations 2.63 and 2.64 the conductor size and the number of turns per path are $0.21 \times 10^{-5} \text{ m}^2$ and 78. The I^2R loss of field winding is obtained from Equation 2.66.

3.5 Performance

The efficiency at furling and threshold are calculated to be 31.7% and 4.0% respectively. The weight of the machine is 63 Kg. The temperature rise inside the machine is 45°C at threshold and 40°C at furling. The performance of the machine is not satisfactory because of the limitations of the material.

A prototype machine of the sample design was built

despite the unsatisfactory performance. The main purpose of fabrication of the machine is to demonstrate the concept of the design, to test the design procedure and to verify the calculations.

3.6 Measurement of Material Properties

The magnetic characteristics of the material are not known. A specimen of the stator laminations and the frame were tested in the laboratory to obtain the magnetic characteristics of the material.

The experiment set up is shown in Fig. 3.2. The test specimen had two coils around it. The primary coil was connected to the power supply through the amplifier and a two-way switch. The secondary coil was connected to the integrator of the analog computer and then to a X-Y plotter. Since the integral of the secondary voltage with respect to time is equal to the flux linkage in the specimen, the output from the integrator would give the change in flux. A d.c. current was supplied to the primary side. By changing the current direction with the switch, a change in flux was recorded in the plotter. The field intensity was calculated by dividing the ampere turns of the primary coil by the mean length of the specimen. The corresponding flux density was derived from the amplitude of the curve, the number of turns

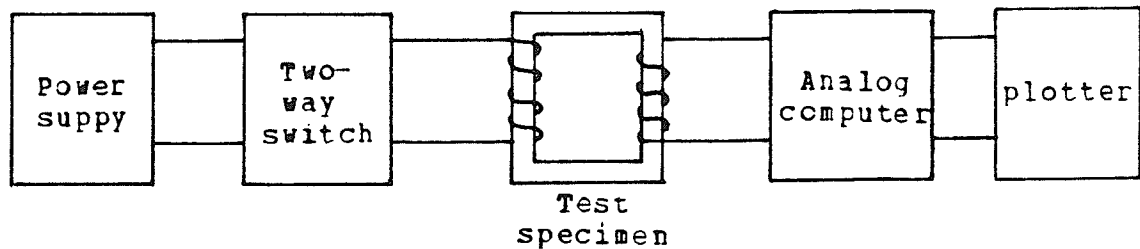


Figure 3.2: Experimental Set-Up of Material Properties
Measurement

in the secondary side and the cross-section area of the specimen. By using different input currents and calculating the corresponding field intensity and flux density, the magnetic characteristic curve of the material was plotted. Fig. 3.3 and Fig. 3.4 show the magnetic characteristics of the laminations and the frame respectively. These two curves were used in the preceeding design and the computer design program.

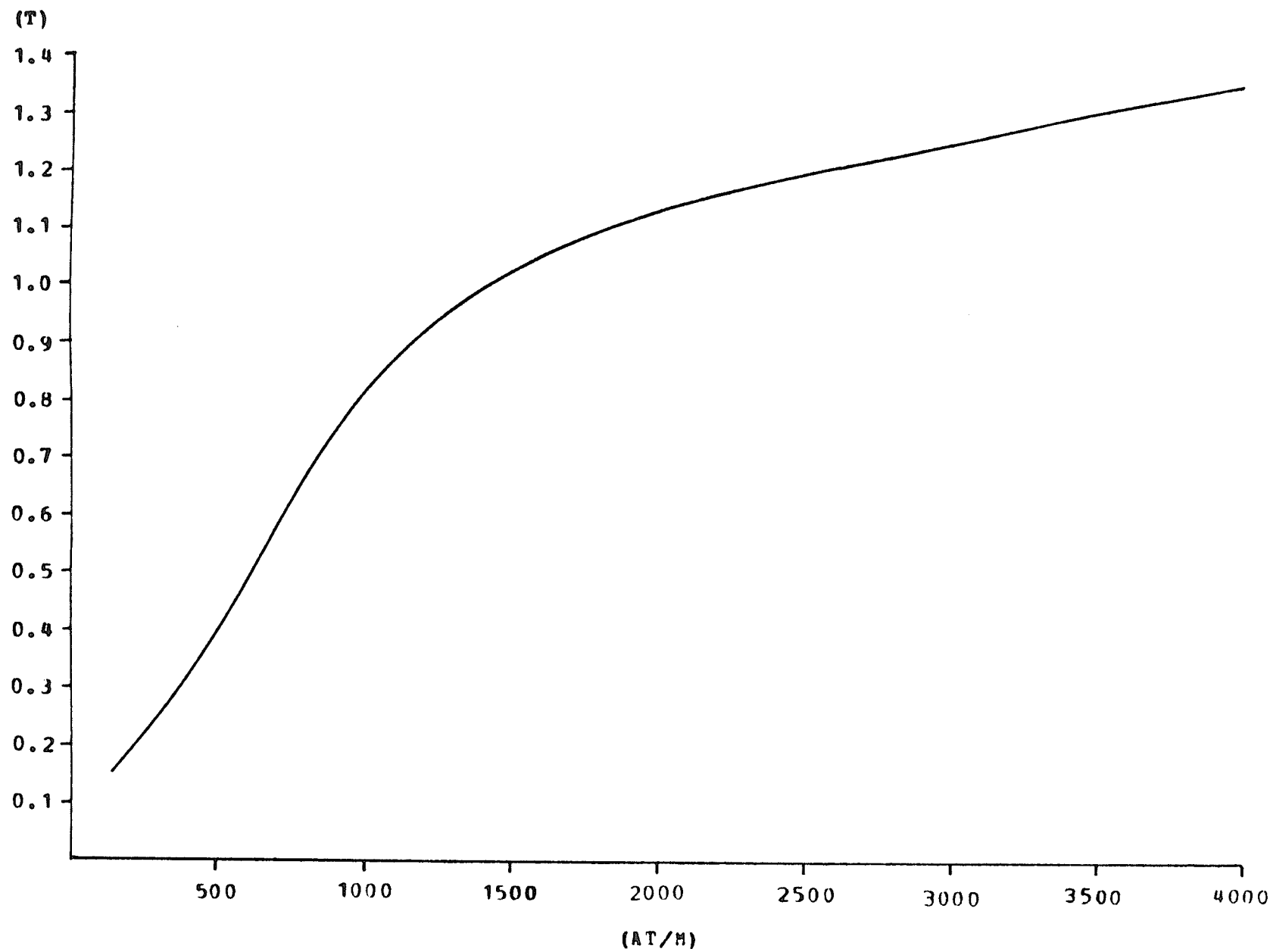


Figure 3.3: Magnetic Characteristic of The Stator Laminations

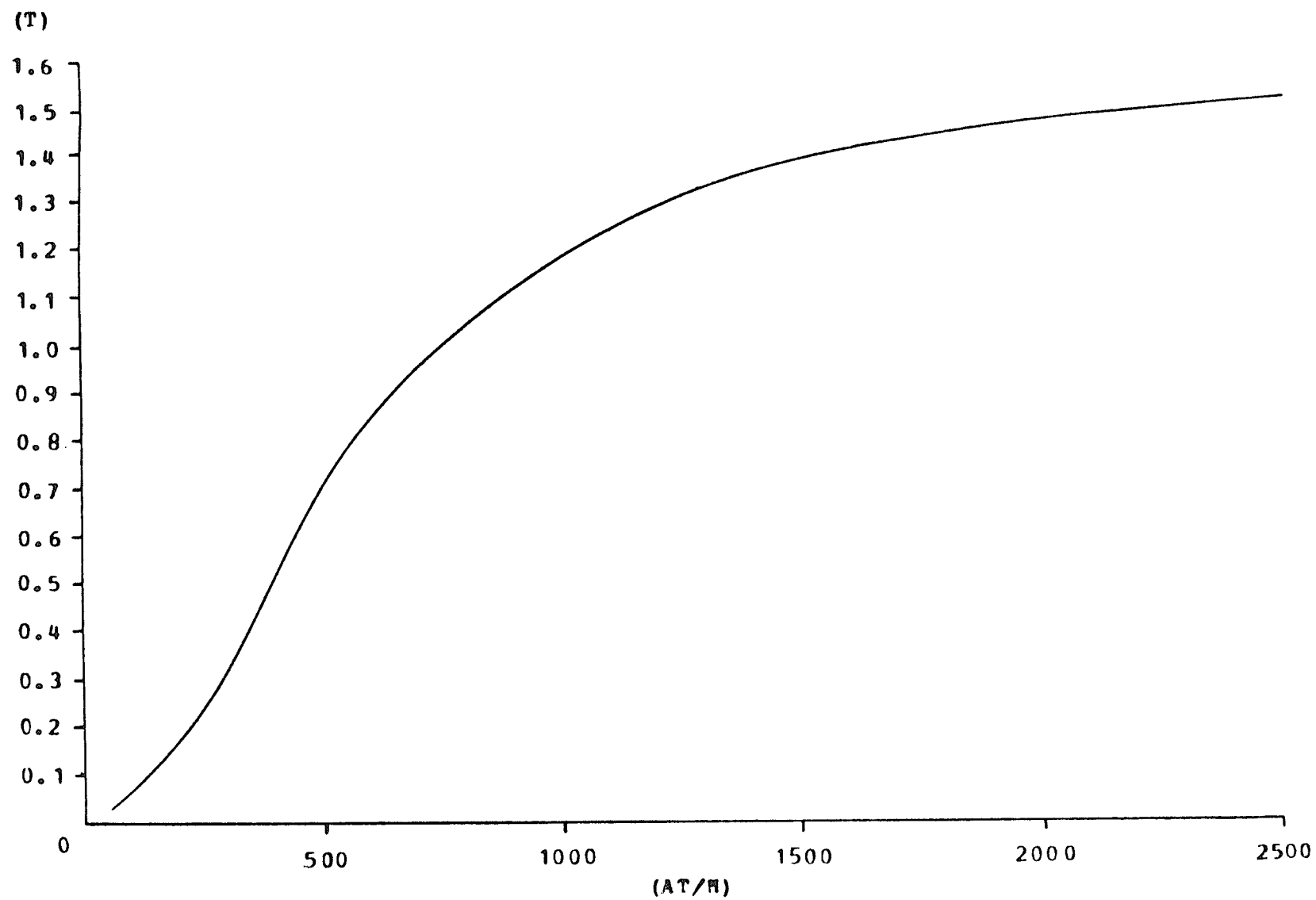


Figure 3.4: Magnetic Characteristic of The Frame

Chapter IV

TESTS ON THE PROTOTYPE MACHINE

4.1 Introduction

The prototype brushless machine was tested in the laboratory instead of testing it on the existing windmill, due to uncontrollable wind speed in the natural setting. A d.c. motor, with the Ward-Leonard speed control, was used as the prime mover. Three tests had been applied to the machine :

- (1) Open-Circuit Test,
- (2) Short-Circuit Test,
- (3) Zero Power Factor Test.

The test results were compared with the computer simulation results in order to demonstrate the accuracy of the computer program.

4.2 Open-Circuit Test

There are three different stator connections to provide three rated voltages of 8 V, 16 V and 32 V. The open-circuit tests were performed on each connection at constant threshold speed and constant furling speed separately. Fig. 4.1 to Fig. 4.3 show the open-circuit test results with 8 V, 16 V and 32 V connections respectively.

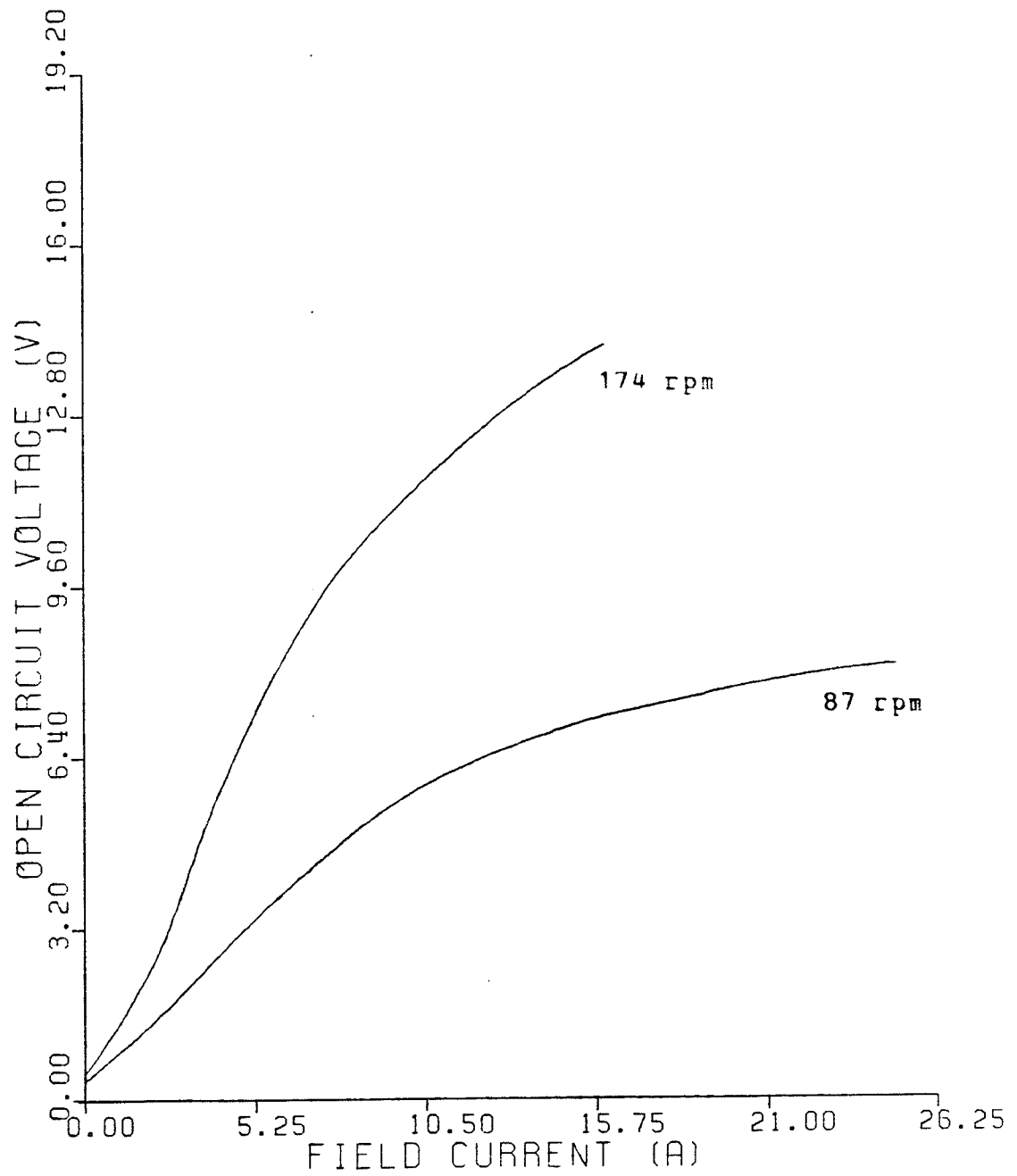


Figure 4.1: Open-Circuit Test With 8 V Connection

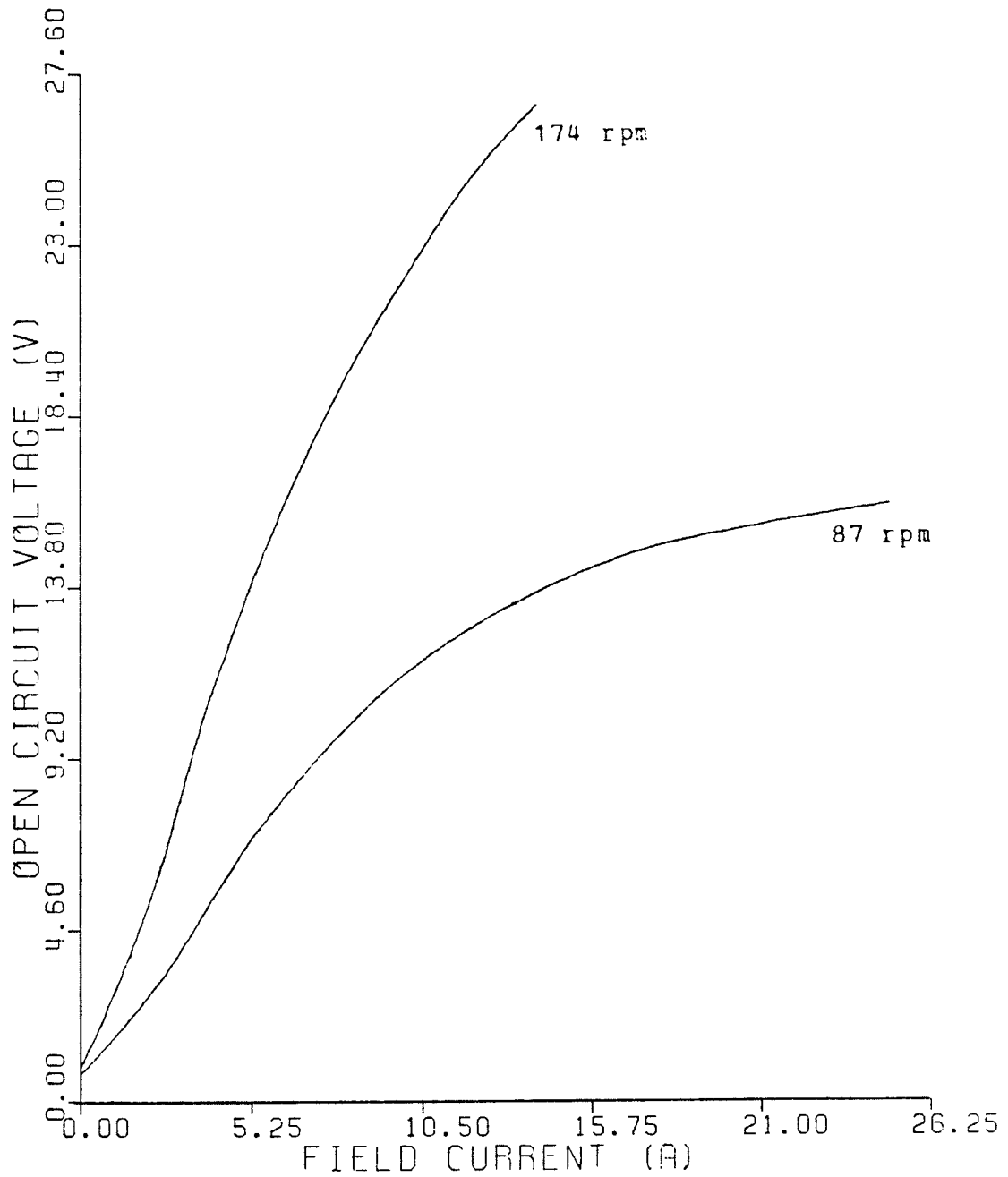


Figure 4.2: Open-Circuit Test With 16 V Connection

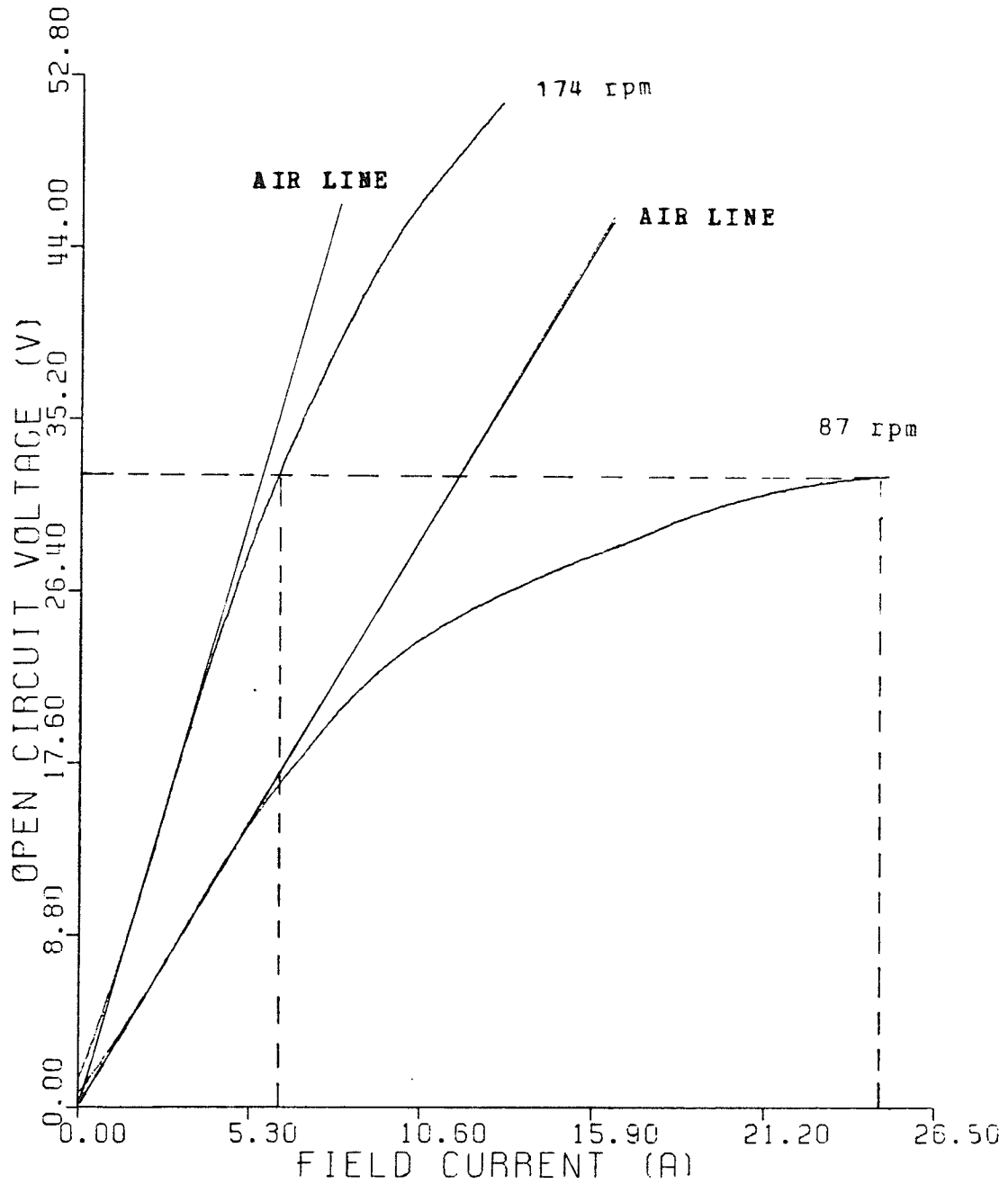


Figure 4.3: Open-Circuit Test With 32 V Connection

At furling speed, the open-circuit test results are close to the calculated value, while at threshold speed, the test results are not comparable to the expected values. Table 4.1 shows the discrepancies between the test results and the calculated results at rated voltage with the 32 V connection. It also shows the ampere-turns required for the airgaps from the airgap-line analysis. The average flux per pole in the machine at furling and threshold was slightly different from the calculated values. At low speed, the mmf required for the iron path was much higher than expected. It indicated that some parts of the iron path were heavily saturated during low speed operation.

TABLE 4.1

Discrepance Between Test And Calculated Results

	<u>Furling</u>	<u>Threshold</u>
Calculated field A.T.	: 1891	3080
Tested field A.T.	: 1903.2	7488
% difference in A.T.	: 0.65%	143%
A.T. from air line	: 1716	3588
A.T. for iron	: 187.2	3900
Flux per pole (wb)	: 2.51×10^{-4}	5.25×10^{-4}
Calculated flux per pole (wb)	: 2.732×10^{-4}	5.46×10^{-4}
% difference in flux/pole	: 8%	3.9%

The teeth of the stator were found to be saturated at low speed due to the change in pole arc dimension. In the original design, the pole arc was 70% of the pole pitch, but due to some changes made to ease the fabrication, the pole arc was reduced to 64% of the pole pitch. Apparently, instead of three teeth under each pole, there were only two teeth under each pole all the time. Most of the flux went directly to the teeth right under the pole arc, thus caused very high flux density in the teeth.

At furling speed, the average flux per pole was low, so there was no significant effect on the open-circuit characteristic. But at threshold speed, the average flux per pole was doubled, so the flux density in the teeth was doubled accordingly. The average flux density in the teeth at rated open-circuit voltage was 1.9 T. Because of the saturation in the teeth, a much higher mmf was required to obtain the rated open-circuit voltage.

4.3 Short-Circuit Test

Fig. 4.4 to Fig. 4.6 show the short-circuit test results with the 8V, 16V and 32V connections respectively. Higher field excitation than the calculated values were found in the short-circuit tests. At rated short-circuit current with the 32V connection, at furling speed, the field current was 17% higher than the calculated value of 3.42 A, and at

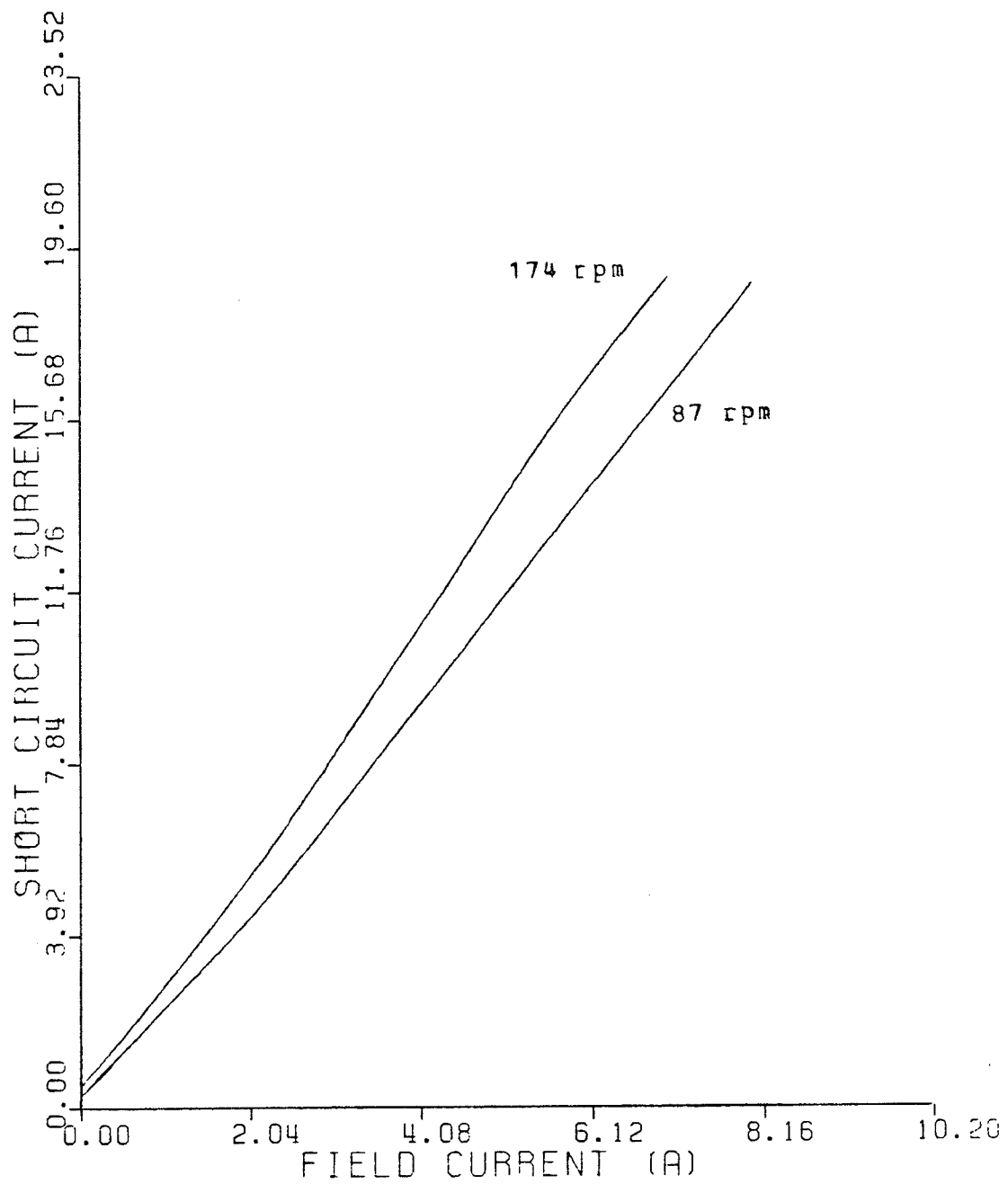


Figure 4.4: Short-Circuit Test With 8 V Connection

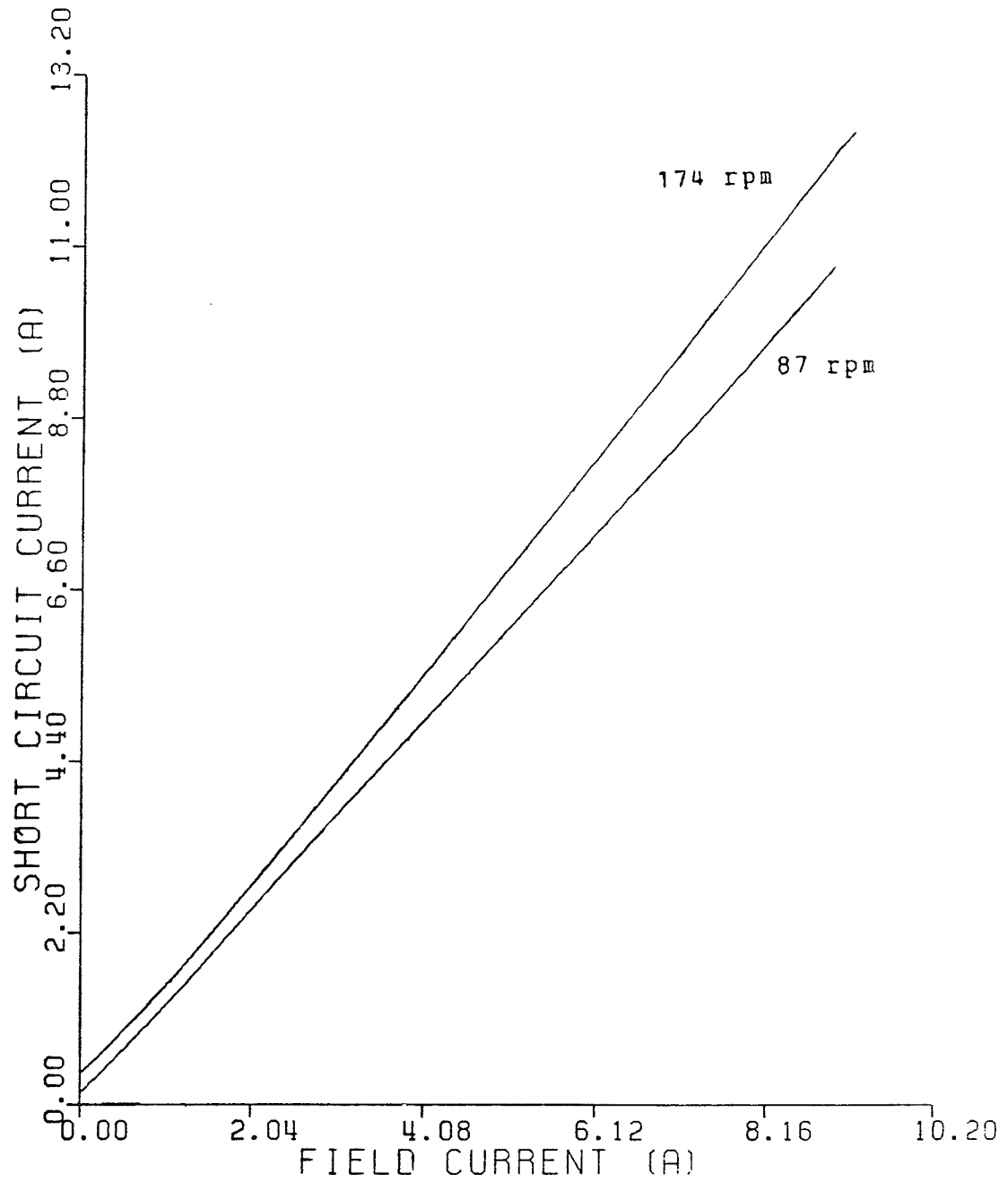


Figure 4.5: Short-Circuit Test With 16 V Connection

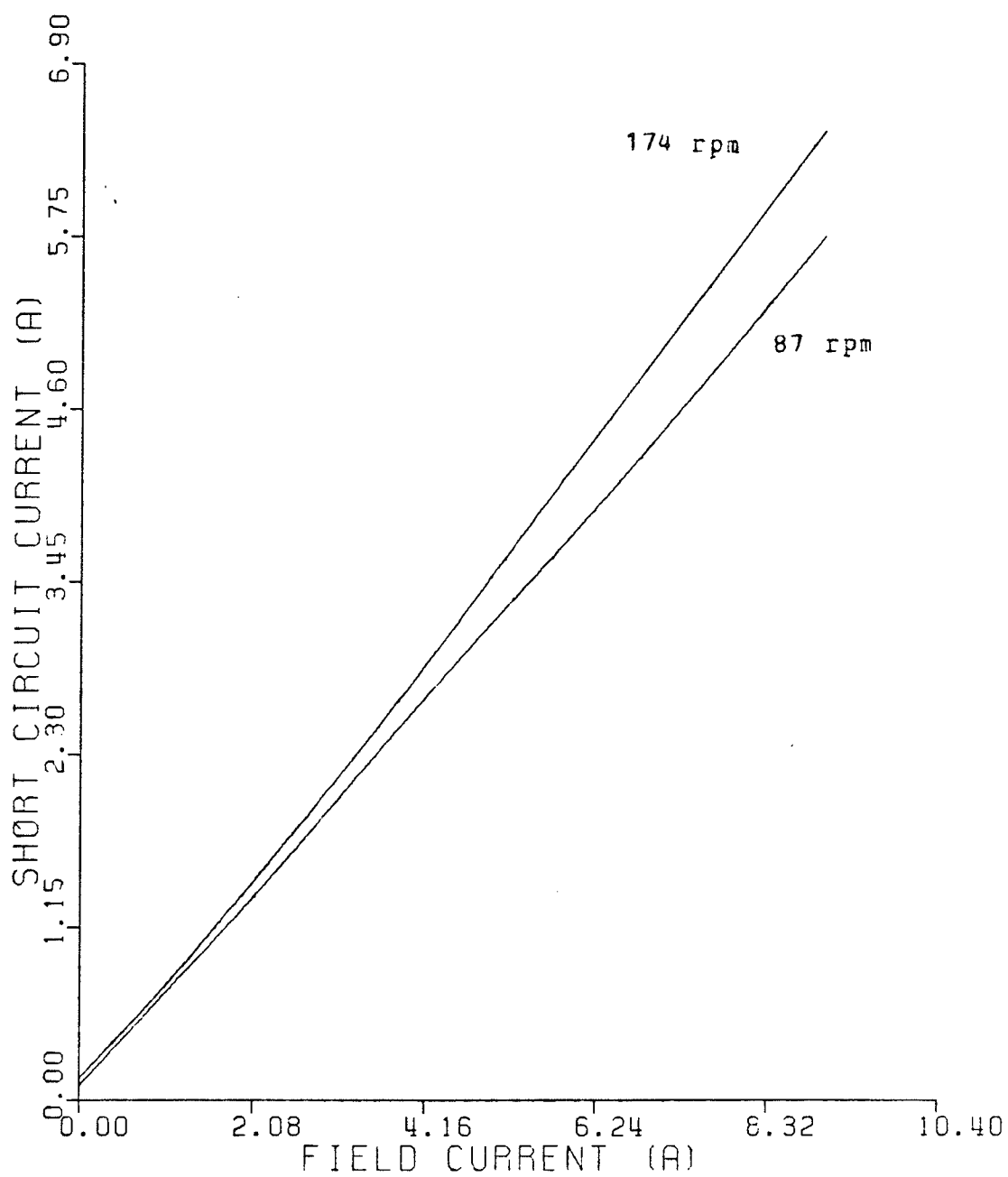


Figure 4.6: Short-Circuit Test With 32 V Connection

threshold speed, the field current was 6.3% higher than the calculated value of 0.5 A. The cause of higher field excitation needed was due to higher synchronous reactance of the machine. Since the synchronous reactance includes the effects of flux leakage and armature reaction, the cause of the discrepancy will be identified after obtaining the equivalent circuit of the machine.

4.4 Equivalent Circuit of The Machine

The equivalent circuit of the machine was obtained from the open-circuit test, short-circuit test and the zero power factor test. Fig. 4.7 shows the curves of the zero power factor load test and the open-circuit test at furling speed with 32V connection. A constant stator current of 54% the rated value was used in this test. The resistance, R_s , of the stator winding was measured by d.c. current at operating temperature. The synchronous reactance was calculated from the ratio of open-circuit voltage at rated value and the short-circuit current with the same field excitation. The synchronous reactance was further separated by the Potier triangle method into the leakage reactance, X_l , and the magnetising reactance, X_a , due to armature reaction. Fig. 4.8 shows the equivalent circuit of the machine at furling with 32V connection.

The resistance of the winding was 2.4% lower than the

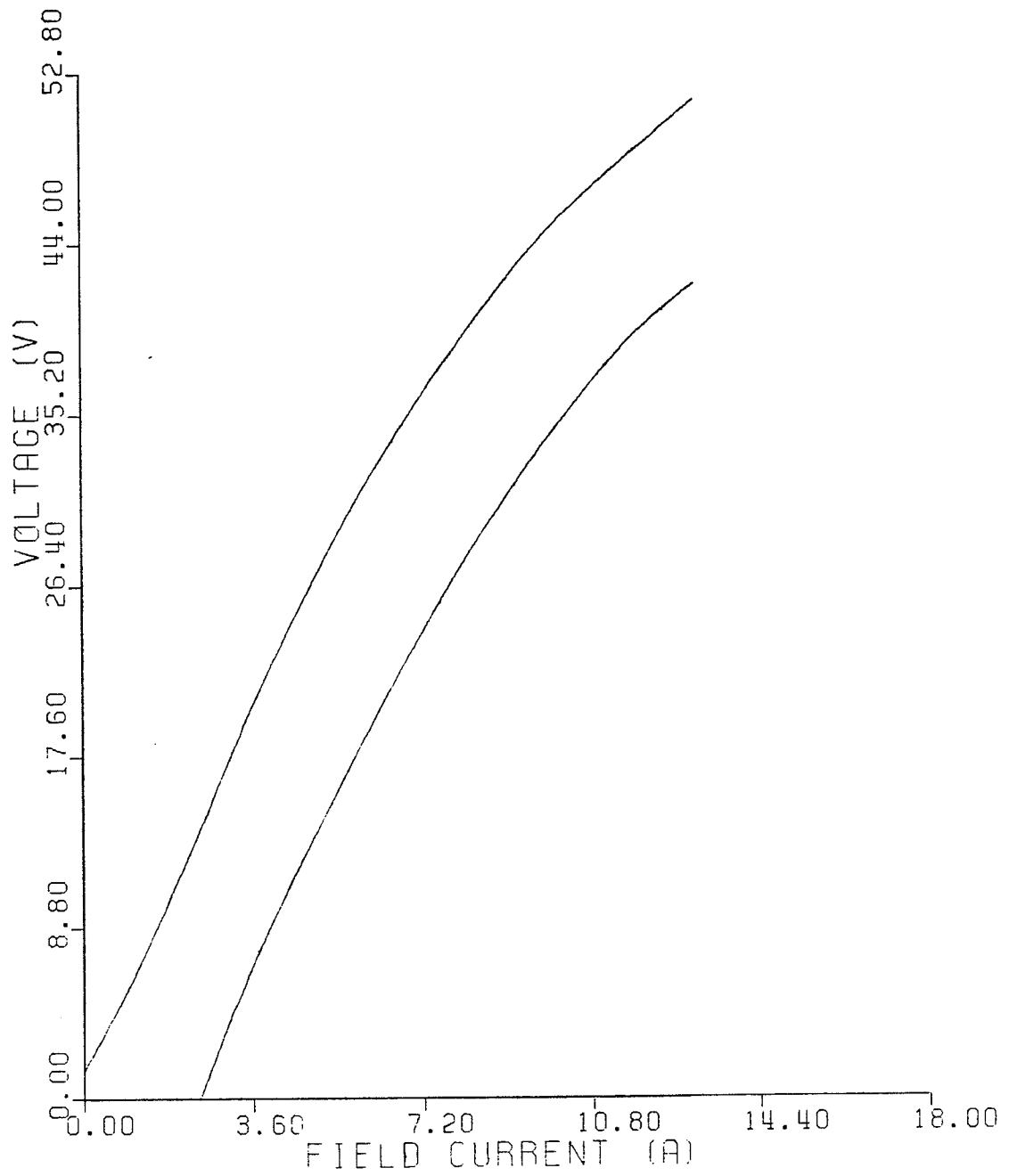


Figure 4.7: Inductive Load Test With 32 V Connection

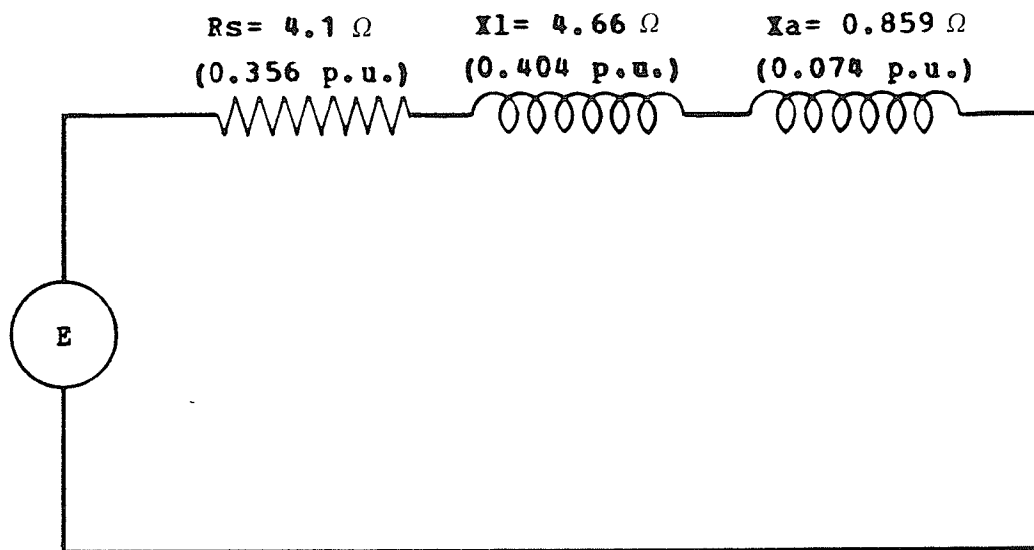


Figure 4.8: Equivalent Circuit of The Machine With 32 V
Connection

calculated value. Since the resistance was measured by d.c. current, the skin effect and the eddy current loss in the winding were not included in the measurement, therefore a lower resistance was obtained. The armature reaction was 5.7% lower than the expected value. The leakage reactance was 290% higher than the calculated value. The low calculated leakage reactance was due to the under estimation of the overhang leakage reactance, based on an empirical formula, and neglect of the zig-zag leakage and the differential leakage reactances. Therefore, a lower

calculated leakage reactance was obtained. Since a complete field analysis of the overhang, zig-zag and differential leakage flux is outside the scope of the thesis, the exact expression will not be derived. The empirical formula will continue be used in the design in later chapters but the overhang leakage reactance will be multiplied by a factor of three to include the zig-zag and differential leakage reactances.

Although the actual performance of the prototype machine did not meet the requirements of the original design, the computer results were reasonably accurate. Except for the overhang leakage reactance, the other parameters were within 6% accuracy. The tooth saturation was completely due to the difference between the design and actual dimensions of the machine.

Chapter V

OPTIMUM DESIGN OF BRUSHLESS ALTERNATORS

The design in the previous chapter, due to the limitation of the available materials, is not an efficient one. Improvement is made in this section to obtain an optimal design. The main objective is to improve the efficiency and reduce the weight of the machine. A suitable range of power output is suggested in this section.

There are some drawbacks in the previous design. The I^2R loss in the field winding is high because of the fixed stator outside diameter and the frame size. The full load I^2R loss of the stator winding is also high due to the fixed slot size. To improve the field and stator losses, a shorter mean turn and lower current density are desired.

The new design is based on the following improvements :

- (1) reduced mean turn length, and
- (2) reduced current densities of field and stator.

The frame length is made longer so that a larger conductor cross-section for the field can be accommodated. The stator bore and outside diameter are smaller so that the mean turn is shorter. The stator winding is designed again using fractional pitch winding. The mean turn is only around one core tooth. Fig. 5.1 shows the diagram of the

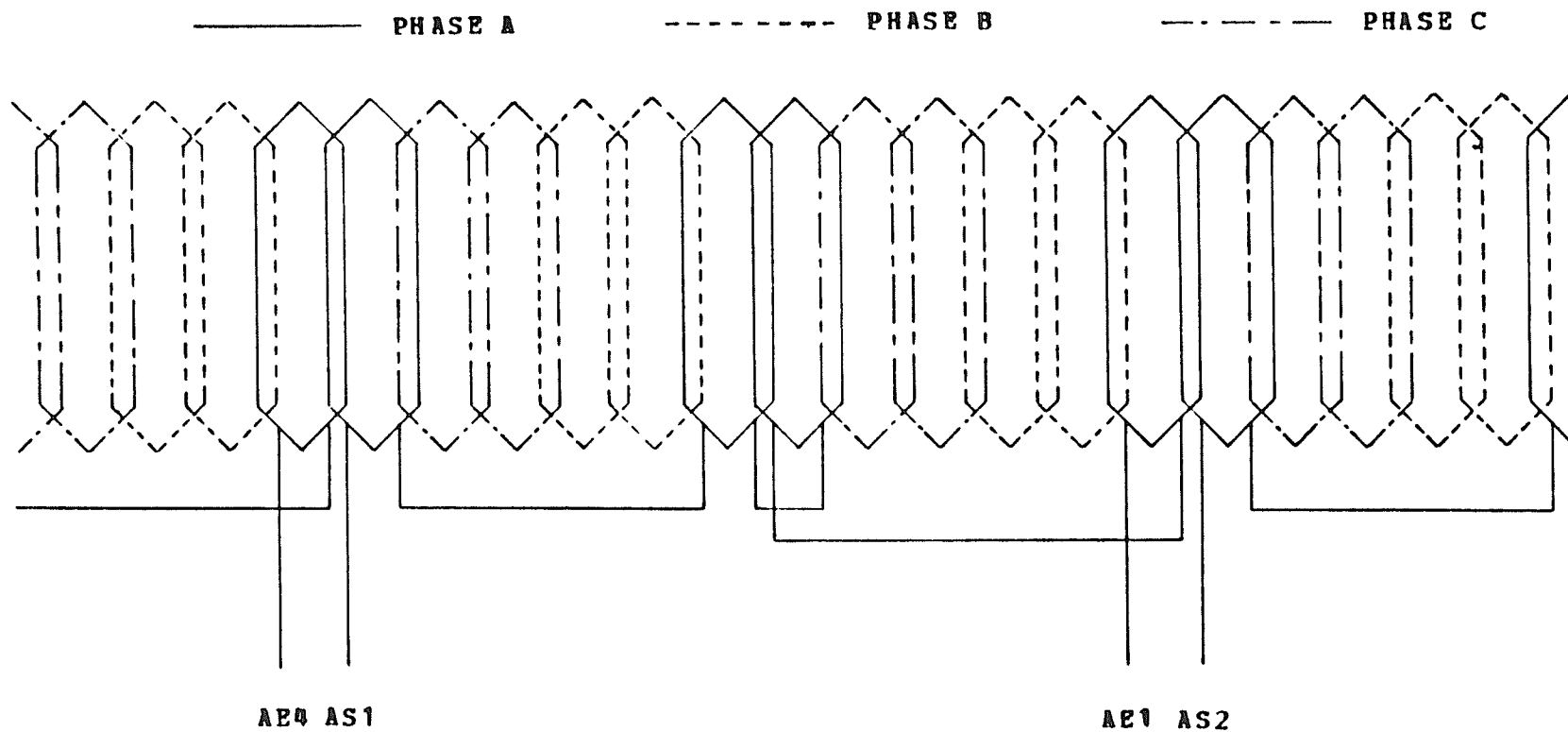


Figure 5.1: Stator Winding of New Design

TABLE 5.1

New Design Parameters

Full load power (W)	: 20-160
Core length (m)	: 0.3867
Stator bore diameter (m)	: 0.1969
Stator outside diameter (m)	: 0.3662
Number of slots	: 48
number of poles	: 40
Length of the frame (m)	: 1.178
Thickness of the frame (m)	: 0.00733
Stator current density (A/m^2)	: 1.5×10^6
Field current density (A/m^2)	: 0.75×10^6
Total weight (Kg)	: 243.3
Efficiency at furling (%)	: 70.63
Efficiency at threshold (%)	: 22.56

stator winding. The new design is shown in Table 5.1

This design has a better performance than the last design but the weight of the machine is heavier. The efficiencies at furling and threshold are higher, however they are still not within the feasible range of over 75% efficiency at all speeds. In order to obtain an optimal feasible design, this design is used as the starting original design in the optimisation program. Six independent parameters are chosen as the variables.

5.1 Effects of Some Parameters on Machine Performance

The performance of the machine depends on many parameters. Among all these factors, only six major parameters are considered :

- (a) Average airgap flux density,
- (b) Stator bore diameter,
- (c) Stator core length,
- (d) Current density of stator winding,
- (e) Current density of field winding, and
- (f) Stator core flux density.

To show the effects of the above parameters, each parameter is varied in steps in the original design program. Figure 5.2 to 5.7 show the performance of the machine with each parameter varying alone while the rest are fixed. It can be shown that for a particular range, the efficiency is higher and the weight is lighter. In order to improve the performance, all six parameters are varied. An optimisation technique is applied to obtain the feasible design.

5.2 Optimisation

The main purpose of optimisation is to minimize the cost or the weight of the machine while meeting the specifications. Different optimisation techniques have been used for different applications in the past. The least pth

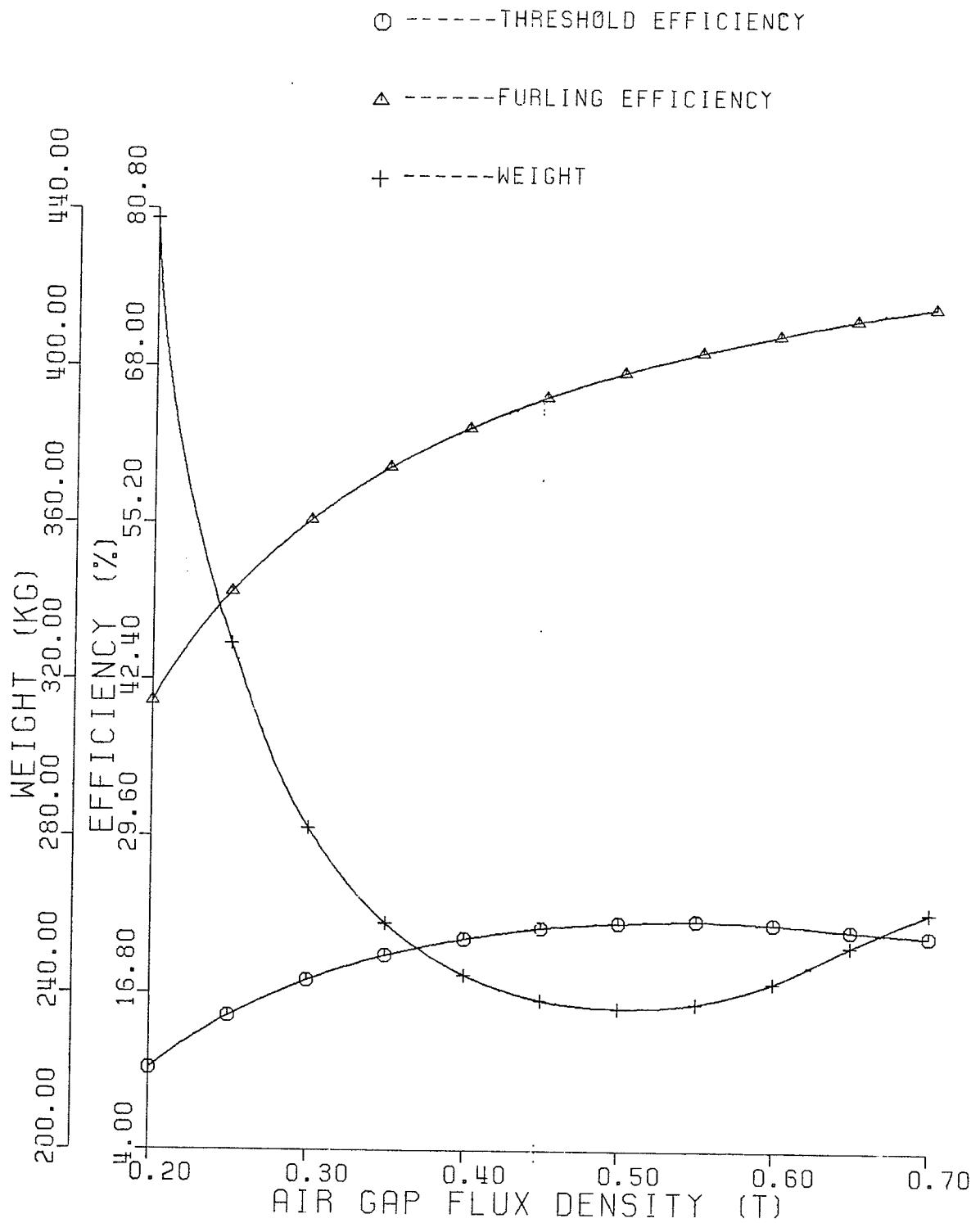


Figure 5.2: Air Gap Flux Vs. Efficiency And Weight

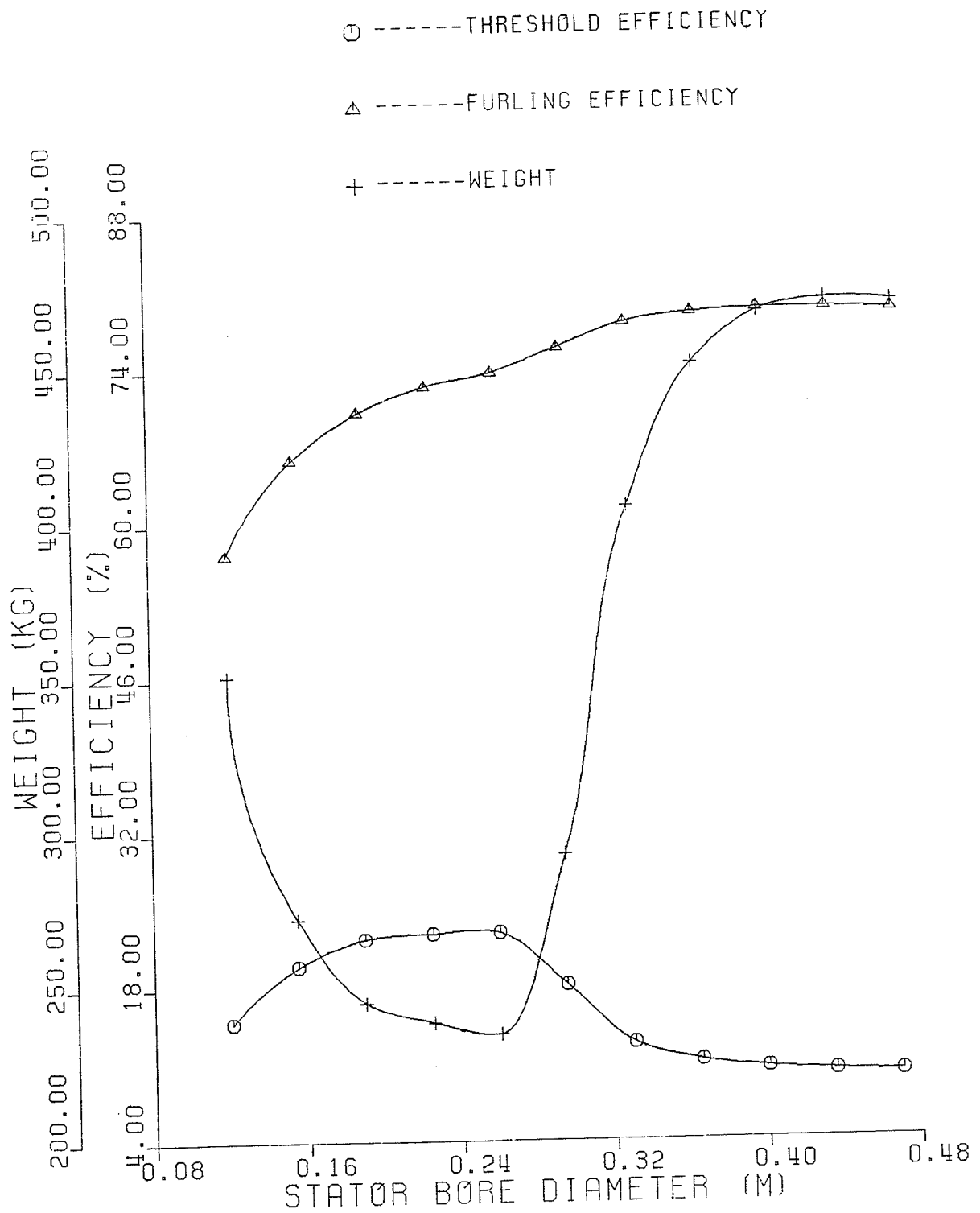


Figure 5.3: Stator Bore Diameter Vs. Efficiency And Weight

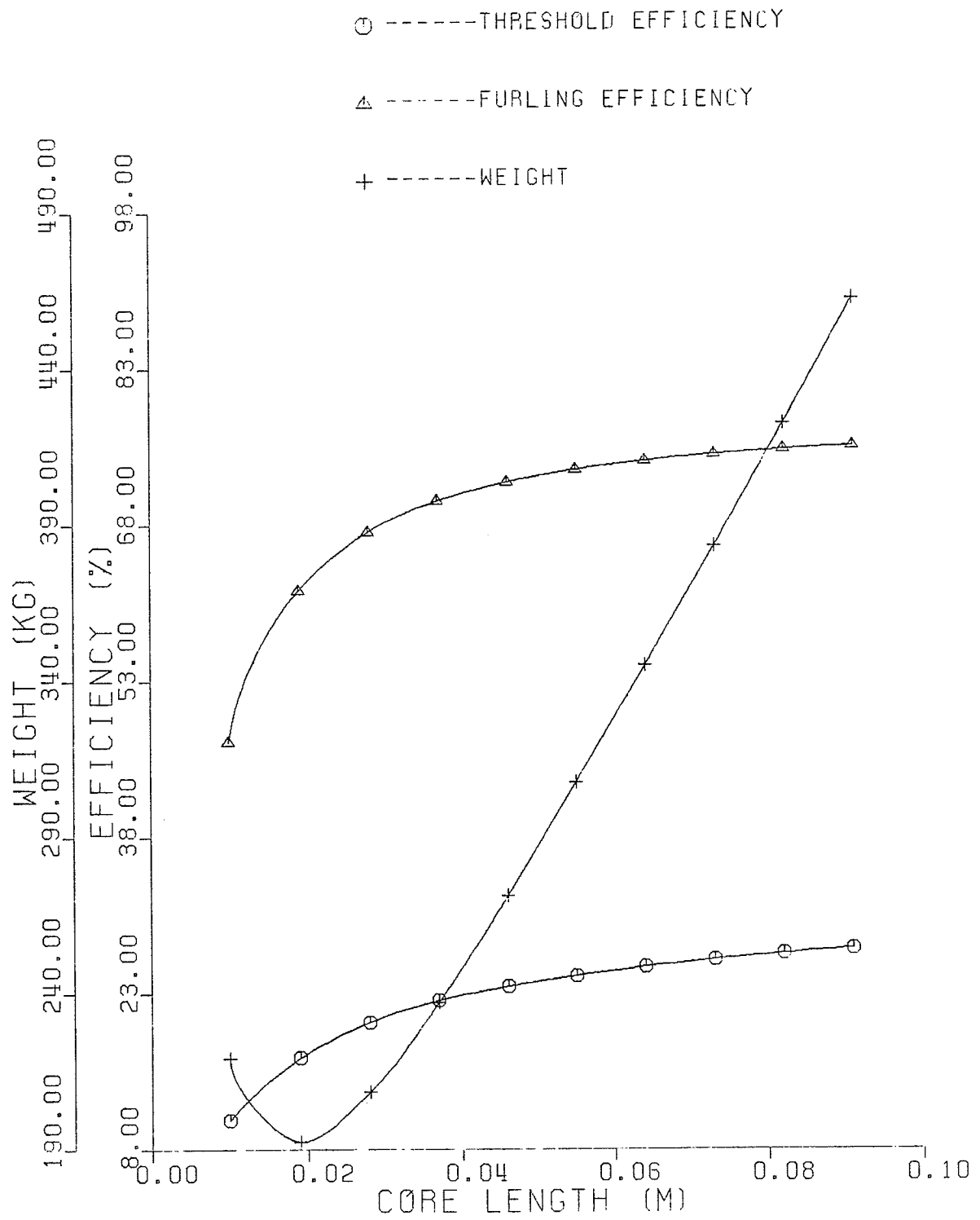


Figure 5.4: Stator Core Length Vs. Efficiency And Weight

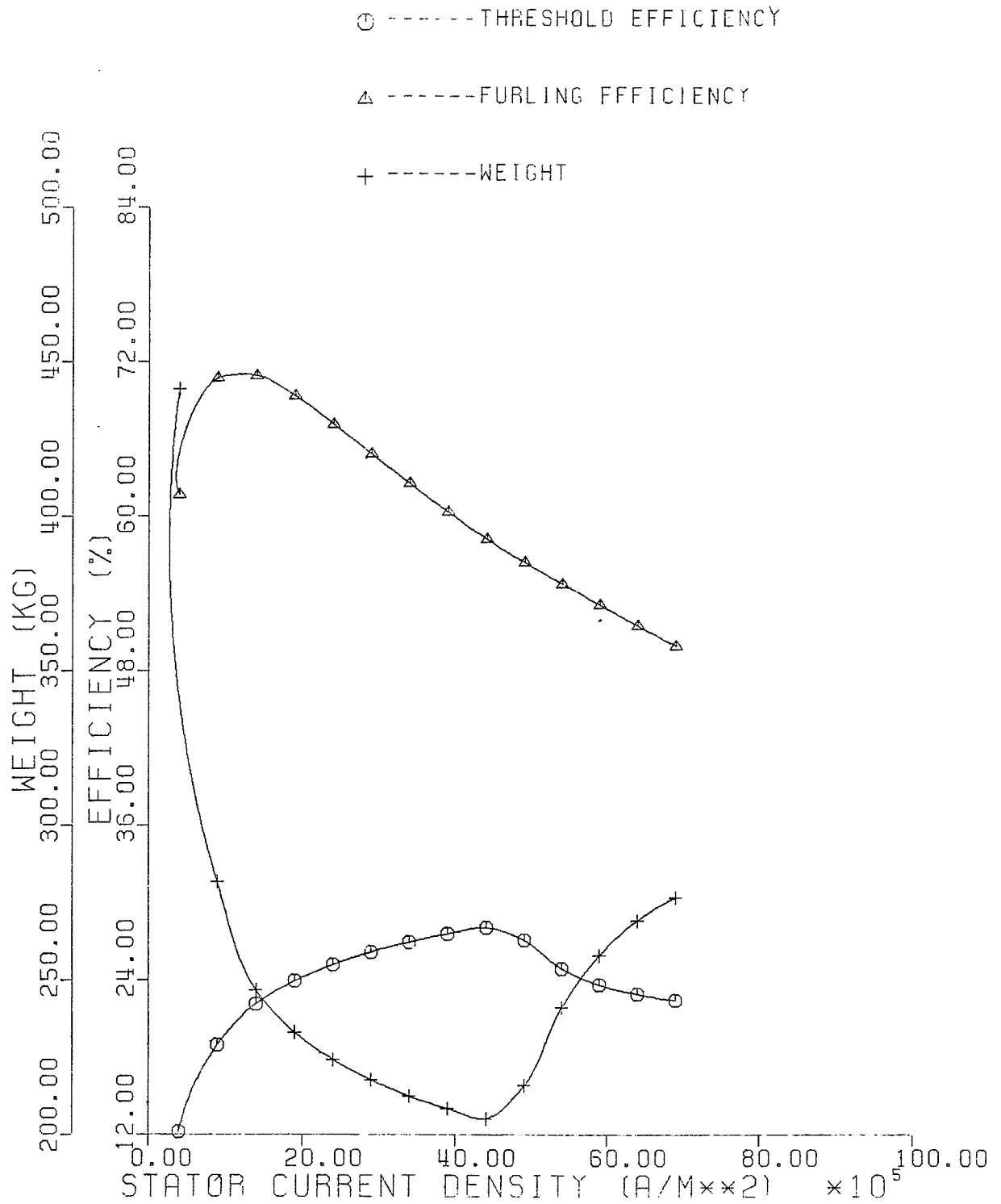


Figure 5.5: Stator Current Density Vs. Efficiency And Weight

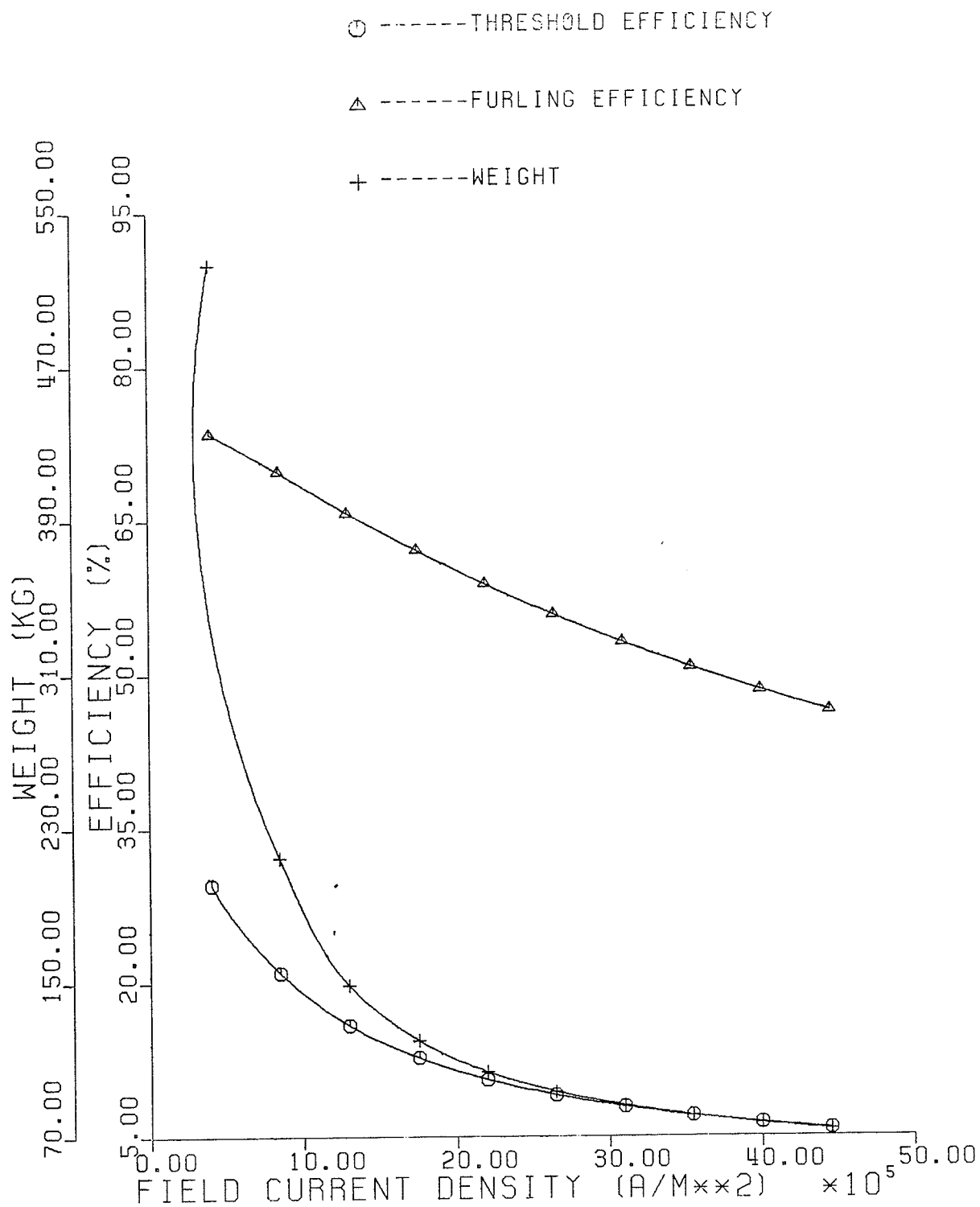


Figure 5.6: Field Current Density Vs. Efficiency And Weight

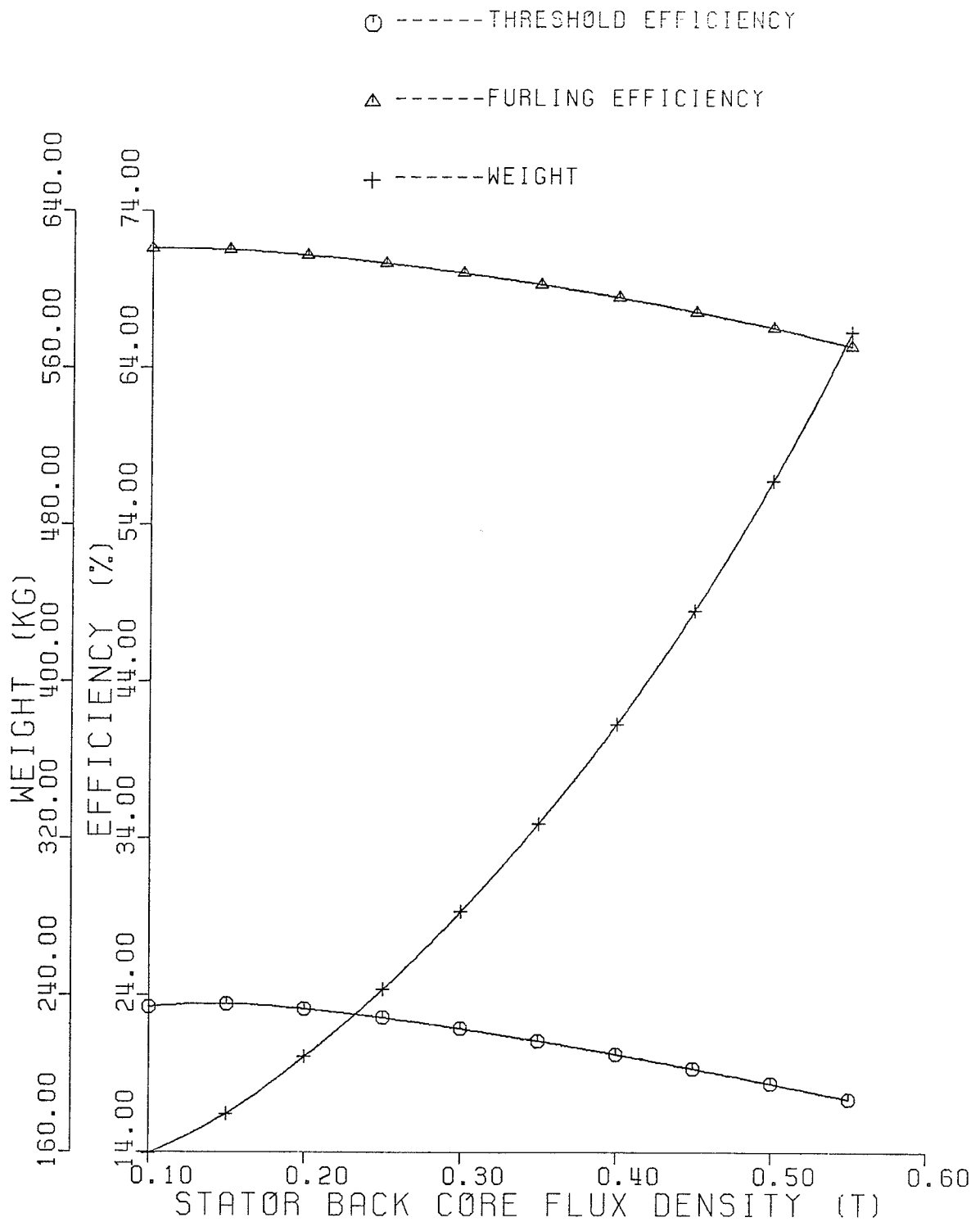


Figure 5.7: Stator Back Core Vs. Efficiency And Weight

approximation method⁸ with a direct search technique⁹ was used in this particular study.

A design which satisfies all the specifications is called a feasible design. Many other techniques require to start from a feasible design, but with this method it can also start from a nonfeasible design. This reduces the effort to obtain a feasible design from a synthesis program. The efficiency of the direct search method was found to be high for machine designing¹⁰.

5.2.1 Optimisation Problems

The basic mathematical optimisation problem is to minimize a scalar quantity which is the value of a function of n variables $x_1, x_2, x_3, \dots, x_n$, i.e.,

$$E = f(X) \quad (5.1)$$

where $X = (x_1, x_2, x_3, \dots, x_n)^T$

The function f is referred to as the function to be minimized and the vector X is a set of independent parameters. There are constraints attached to some of the parameters. A common constraint on the variable x_i is the upper and lower bound in the form

$$x_{li} \leq x_i \leq x_{ui} \quad (5.2)$$

where x_{li} and x_{ui} are the lower and upper bounds.

Most inequality constraints can be put into a constraint function of the form

$$g(x_1, x_2, \dots, x_n) \leq 0 \quad (5.3)$$

For the case of upper and lower limits, the expression (5.2) is replaced by two expressions:

$$x_i - x_{ui} \leq 0 \quad (5.4)$$

$$x_{li} - x_i \leq 0 \quad (5.5)$$

The region of search in which all the constraints are satisfied is the feasible region. The choice of independent parameters depends on individual design. In this particular design the six parameters mentioned in the last section were chosen.

5.2.2 Objective Function

The objective function reduces the constrained problem into an unconstrained problem. The best known sequential unconstrained minimization technique of Fiacco and McCormick¹¹ was shown not so efficient compared to least pth approximation method of Bandler and Charalambous¹⁰.

The least pth approximation method was used to formulate the objective function. In this method, the function to be

minimized is formed into a constraint function.

$$g(x) = F_s - F(x) \quad (5.6)$$

where F_s is the specified constrained value desired.

The objective function is defined as

$$P(X, F_s) = M(X) \left[\sum_{i \in K} \left(\frac{\alpha_i \cdot g_i}{M(X)} \right)^q \right] \frac{1}{q} \quad (5.7)$$

where $M(x) = \text{Max} \{ \alpha_i \cdot g_i(x) \}$

α_i is a position scaling factor for the
 i^{th} constraint function,

$$q = p \cdot \text{sign}(M), \quad p \geq 1$$

$g_i(x)$ is the constraint function,

$$K(x) = \{ i, g_i(x) > 0, i \in I \} \text{ for } M > 0,$$

$$K(x) = I \text{ for } M < 0,$$

I is the index set $1, 2, 3, \dots, m$.

There are two cases to be considered:

(I) $M > 0$, some constraints are violated, and

(II) $M < 0$, all constraints are satisfied.

Case I

When some of the constraints are violated, $M > 0$, the objective function is the p th root of the sum of only the violated constraints raised to the p th power. The index

set, $K(X)$, that controls the sample points, is dependent on X . The sample points are included if the corresponding constraints are violated, and excluded when the corresponding constraints are satisfied. The value of p determines the weight placed on the larger constraints. When the value of p is larger the maximum violated constraint would be emphasized. Since the value of p is positive the minimization method will attempt to minimize the largest constraint.

Case II

For the case when all the constraints are satisfied, $M < 0$, all the sample points are included in the objective function. This time, the value of q is negative so the least negative constraints will be emphasized. The minimization method will attempt to reduce the value of the constraints function exceeding the specification as much as possible. The design will move away from all the constraint boundaries and enter the centre of the feasible region.

The value of p used in the program varied from one to nine. With larger value of p , the design converged faster to the feasible region. But for values higher than ten, error may occur due to underflowing of computer when the constraint functions approached zero.

5.3 Specified Constraint Value And Scaling Factors

The specified constraints for this study were the weight of the machine and the efficiencies at furling and threshold. The specified weight was initially set at a low value. The specified efficiencies at furling and threshold were both set at 75% for the first run. The specified weight is adjusted accordingly after the minimum value of the objective function is reached. If the feasible region is reached, the specified weight is reduced, otherwise the weight will increase.

A method proposed by Morrison¹² for optimisation by least squares was used to select the value of the specified constraint. The constraint value is updated after each optimisation sequence by the formula:

$$Fs(i+1) = Fs(i) + P(x, Fs(i)) \quad (5.8)$$

Where $P(x, Fs(i))$ is the minimum value of the objective function from the i^{th} optimisation sequence.

In general, this method has yielded good results for a particular set of scaling factors. However, due to some of the constraint functions having too much weight placed on them, or due to uneven distribution of scaling factors, it happens that $P(x, Fs(i))$ has little effect on changing the

constraint value. Another weighting factor added to $P(x, F_s(i))$ is desirable in order to obtain better results.

There are no fixed rules for selecting the scaling factors. The scaling factors are selected arbitrarily to maintain a balance among all the constraint functions in the objective function.

5.4 Operation of The Optimisation Program

The optimisation program is added to the original design program. The optimisation consists of three subroutines namely, Pattern, Search and Function. Fig. 5.8 shows the flow diagram of the whole program.

The objective function and the constraint functions are in the Function subroutine. The Main subroutine is the original design program used in the previous design. The Search subroutine is used to determine the direction of the search. The Pattern subroutine determines the pattern of the search and controls the step size of the increment or decrement.

Initially, the Search subroutine finds the direction towards the minimum of the objective function at the first base point. If the search is successful, a pattern of searches is formed in the same direction. If the pattern

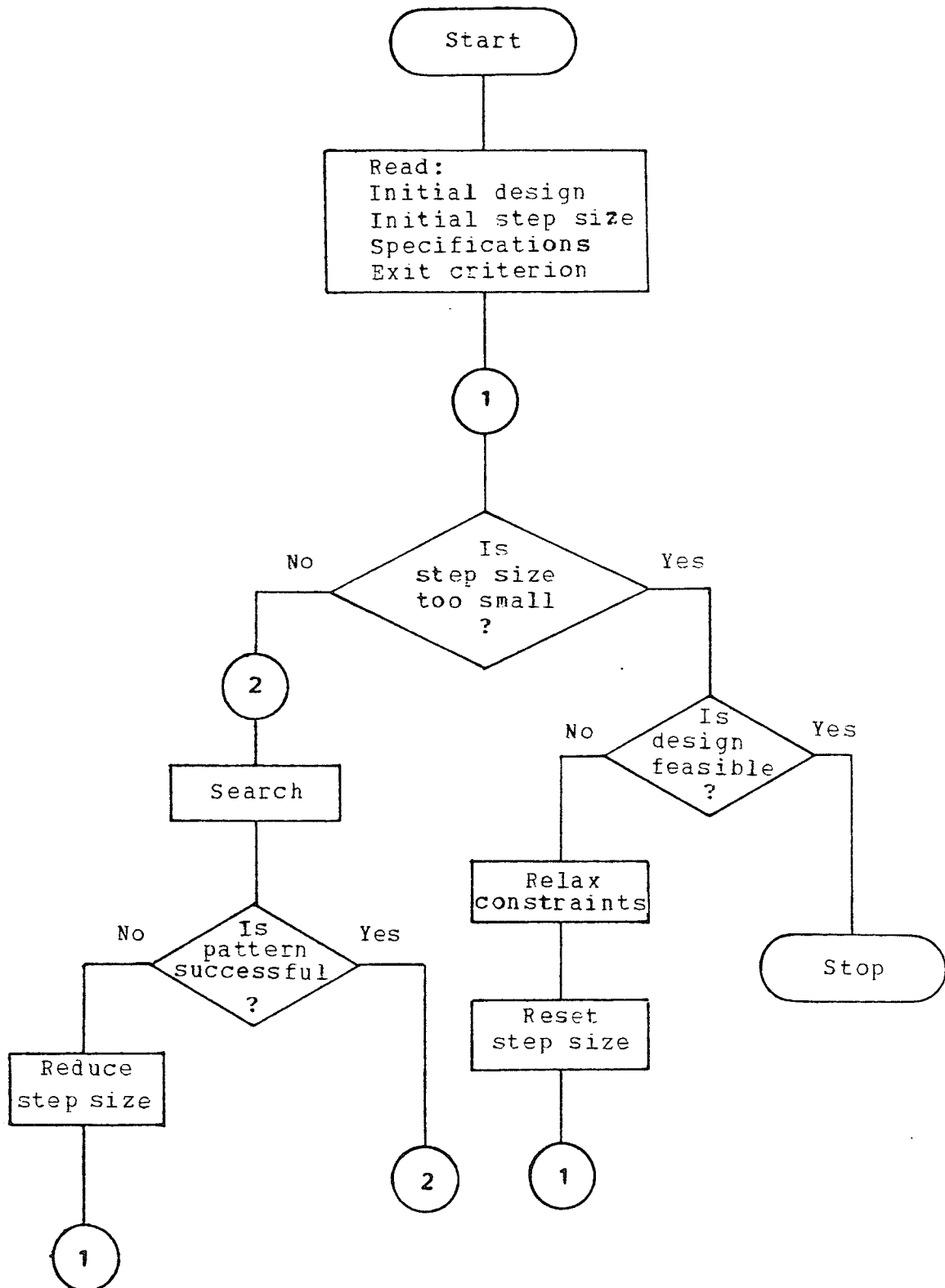


Figure 5.8: Flow diagram of the optimisation program

fails, a new direction has to be searched from the previous base point. If the search fails, the step size will be reduced and the search restarted. The process is repeated until the step size is reduced to the specified minimum value. If the specified minimum step size is reached but still some of the constraints are violated, the specification of the machine has to be changed.

5.5 Test Runs Results

The design in Table 5.1 was used as the start for the test runs. The first run is to obtain a feasible design with 75% efficiency at furling and threshold. In the second run, the specified efficiency is changed to compare with the first run. The third test run is to obtain a suitable range of rated output power for the machine.

Table 5.2 shows the results of optimal design of the first and second run. In order to obtain a feasible design with 75% efficiency, the minimum weight of the machine is increased to 1610 kg. For higher specified efficiency, the weight of the machine has also to increase. By reducing the specified efficiency to 60%, the weight is still very high. The field and stator current density have to keep very low to reduce the I^2R losses. The weight of the copper and the frame constitute a great part of the total weight. It is not economically to have a 1610 kg machine with 20 to 160W

TABLE 5.2

Results From The Test Runs

	<u>Original</u>	<u>First</u>	<u>Second</u>
	<u>design</u>	<u>run</u>	<u>run</u>
Core length (m)	: 0.3867	0.8853	0.0698
Stator bore diameter (m)	: 0.1969	0.211	0.2166
Stator outside diameter (m)	: 0.3662	0.6893	0.5028
Length of the frame (m)	: 1.178	1.477	0.8952
Thickness of the frame (m)	: 0.00733	0.00545	0.00493
Stator current density (A/m ²)	: 1.5X10 ⁶	1.69X10 ⁶	2.2X10 ⁶
Field current density (A/m ²)	: 7.5X10 ⁵	4.6X10 ⁴	1.26X10 ⁵
Threshold magnetic loading (T)	: 0.6	0.338	0.276
Total weight (Kg)	: 243.3	1607	460
Efficiency at furling (%)	: 70.63	75.4	65
Efficiency at threshold (%)	: 22.56	75	65.2

output. Thus, a suitable range of rated output power is sought.

Different specified rated power output of the machine were used in the third test run. Fig. 5.9 shows the minimum weight of the machine at different rated power output at 75% efficiency. It can be shown that the best range of operation is between 800W to 1500W rated output.

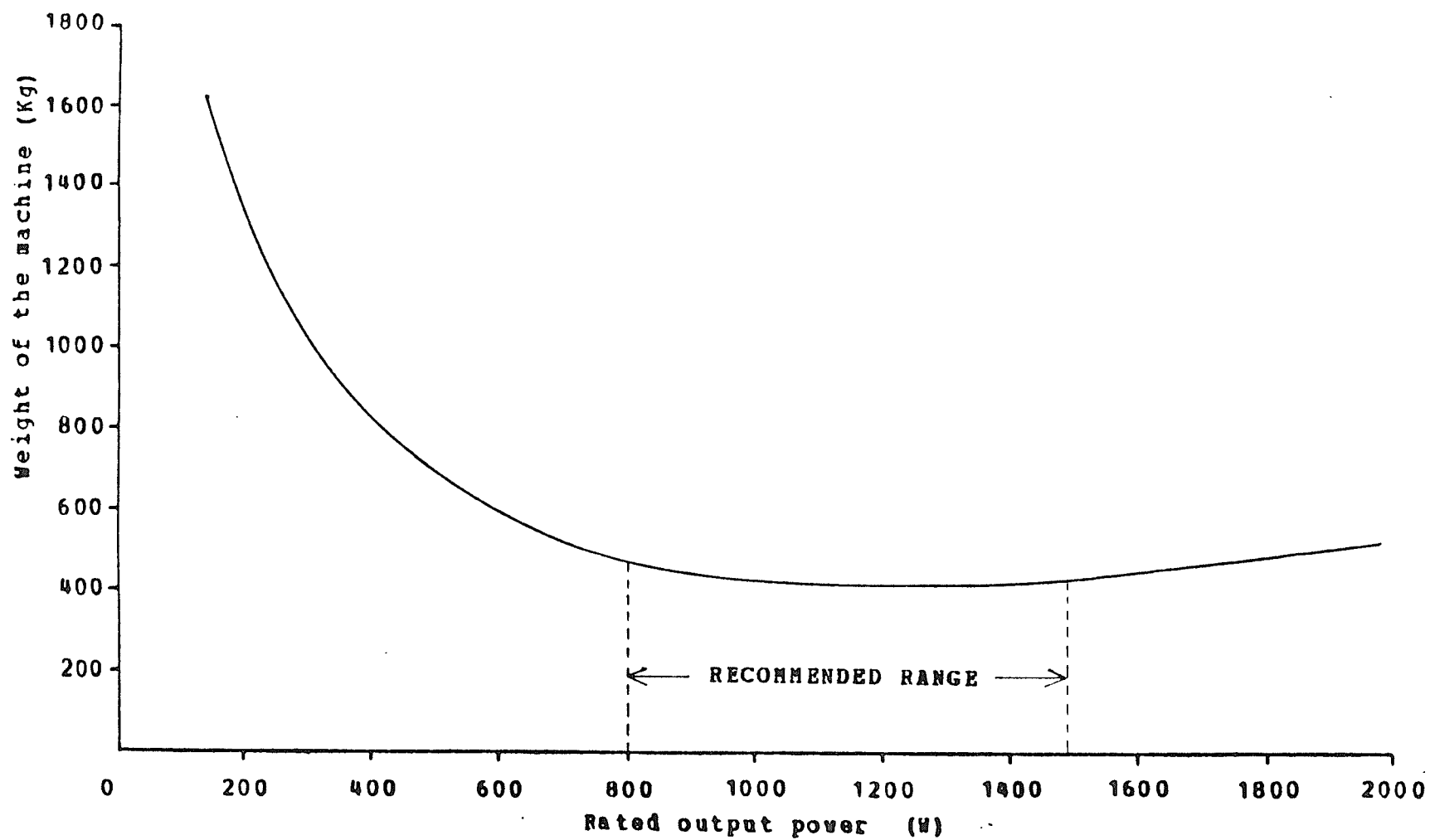


Figure 5.9: Weight of First Design Vs. Rated Power Outputs

Chapter VI

ALTERNATE DESIGNS

6.1 Introduction

In this section two alternate designs based on the same theory used in Chapter Two will be introduced. The two types of alternate designs are :

- (1) Field coils under poles type,
- (2) Inverted machine type.

These two types of design have two different field winding configurations. A theoretical sample design on Type 1 has been carried out, and since both designs are similar, Type 2 design will be discussed only briefly. The sensitivity of Type 1 is compared to the first design.

Type 1: Field coils under poles

The stator of this design is the same as that of first design, except that the field winding is placed inside the claw-poles. Fig. 6.1 shows the diagram of this design. The field coils are surrounding a stationary shaft. The stationary shaft is held at one end and supported by a bearing at the other end. The rotor is supported by three bearings such that it can rotate on the stationary shaft.

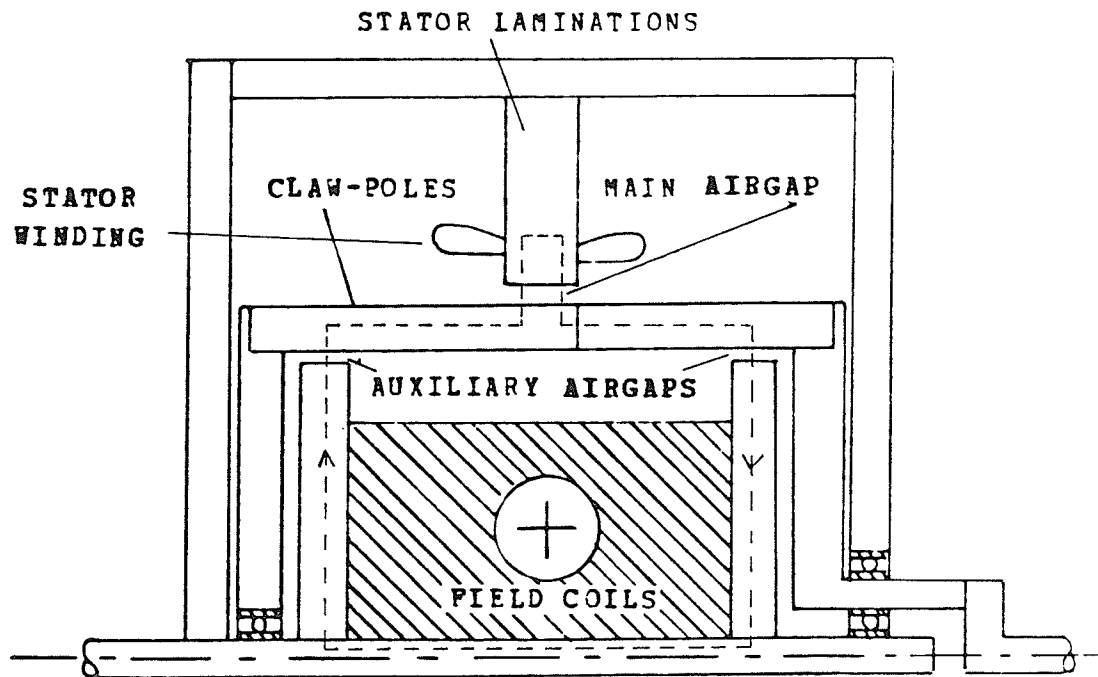


Figure 6.1: Type 1 Brushless Alternator

The broken line represent the magnetic path of this design. There are still four airgaps in the magnetic path as in the first design; however, the shorter mean turn of the field coil makes this type of design more efficient.

Type 2: Inverted Machine

This type is specially designed for the application of Darrius wind turbine. Fig. 6.2 shows the diagram of this design. The stator and the field windings are situated on the shaft which is stationary. The claw-poles ring is

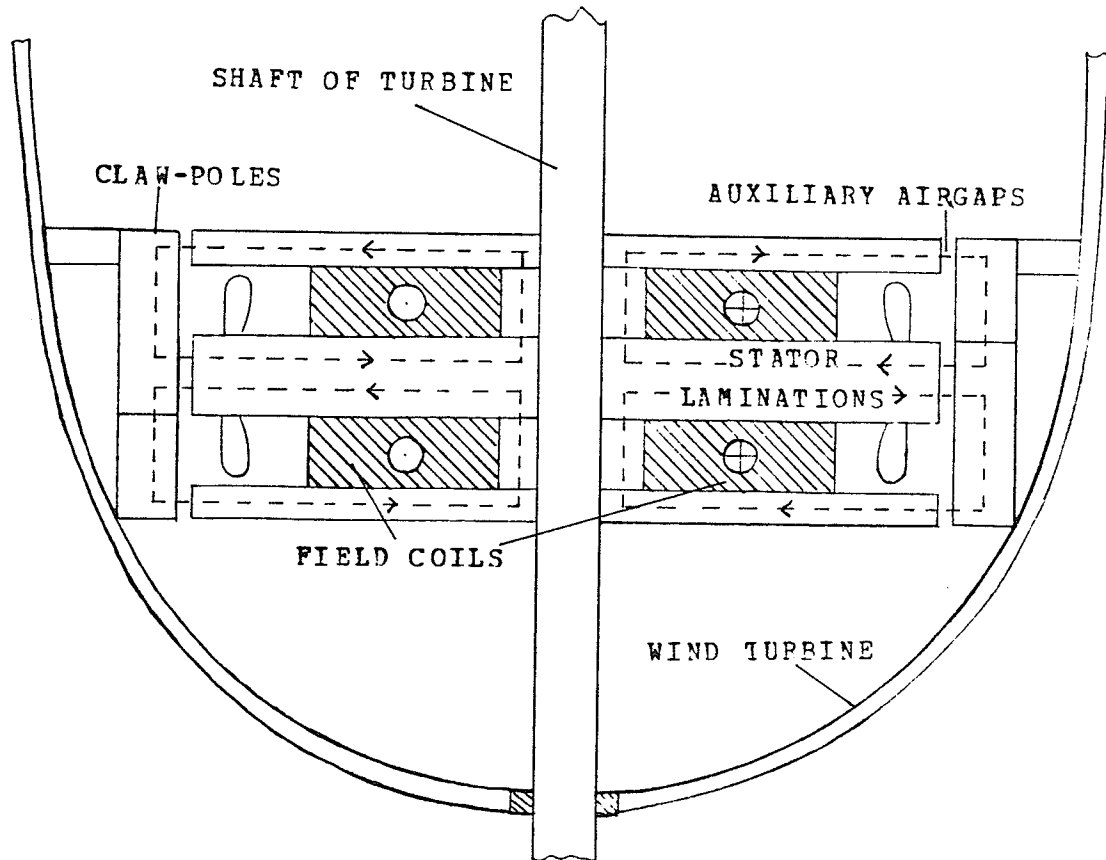


Figure 6.2: Type 2 Brushless Alternator

mounted on the blades of the turbine. When the blades are turning, only the claw-poles ring is moving. The field winding resided on both side of the stator core remains stationary. The broken lines show the magnetic paths of this machine. The main advantage of this design is the shorter field mean turn compared to the first design. In this design, no additional bearing is required other than that for the turbine. But the blades have to be rigid enough to support the poles ring and maintain the same airgap at all times. This is not easily achieved in practice and therefore may not be a practical alternative.

6.2 Sample Design On Type 1

Sample designs with the same specifications as the first design has been done with the simulation program. The optimal design of Type 1 is compared with the optimal design of the first design. A suitable range of operation is suggested.

Table 6.1 shows the comparison of two optimal designs with 75% specified efficiency. The weight of Type 1 design is lighter than the first design because the windings of Type 1 have shorter mean turn. The loss in the field is not as high as the first design, so a smaller conductor size can be used in the field to reduce the weight. The frame and the stator outside diameter are smaller than the first design because the field winding is situated under the pole instead of beside the stator back core.

Type 1 machine has a power output of 160W at furling but the weight is 120Kg, which is too high, only giving 1.3 W/Kg at furling. Fig. 6.3 shows the weight of the Type 1 machine with 75% efficiency varied as the rated output power at furling increased. In order to have a machine giving 3 W/Kg or more, the recommended range of operation is between 400W to 700W rated output power. For the rated power over 700W, the weight of the machine is increased faster, and the rated output current with 8V connection is too high. Therefore,

TABLE 6.1

<u>Comparison of Two Designs</u>		
	<u>First Design</u>	<u>Type 1</u>
Core length (m)	: 0.0885	0.03
Stator bore diameter (m)	: 0.211	0.273
Stator outside diameter (m)	: 0.689	0.477
Length of the frame (m)	: 1.477	0.189
Thickness of the frame (m)	: 0.00545	0.0127
Stator current density (A/m^2)	: 1.69×10^6	1.35×10^6
Field current density (A/m^2)	: 4.6×10^4	3.1×10^6
Threshold magnetic loading (T)	: 0.338	0.322
Total weight (Kg)	: 1607	120
Efficiency at furling (%)	: 75.4	75
Efficiency at threshold (%)	: 75	75.2

it is not practical to go for higher power output unless the rated voltage of the machine is increased as well.

Although Type 1 is more complicated to fabricate, the weight is much lighter and the efficiency is higher. For low power output and low r.p.m., Type 1 design can achieve better performance than the first design. For higher rated power outputs, both designs will provide a lighter machine. So it is recommended that both designs should be applied for machines of higher ratings.

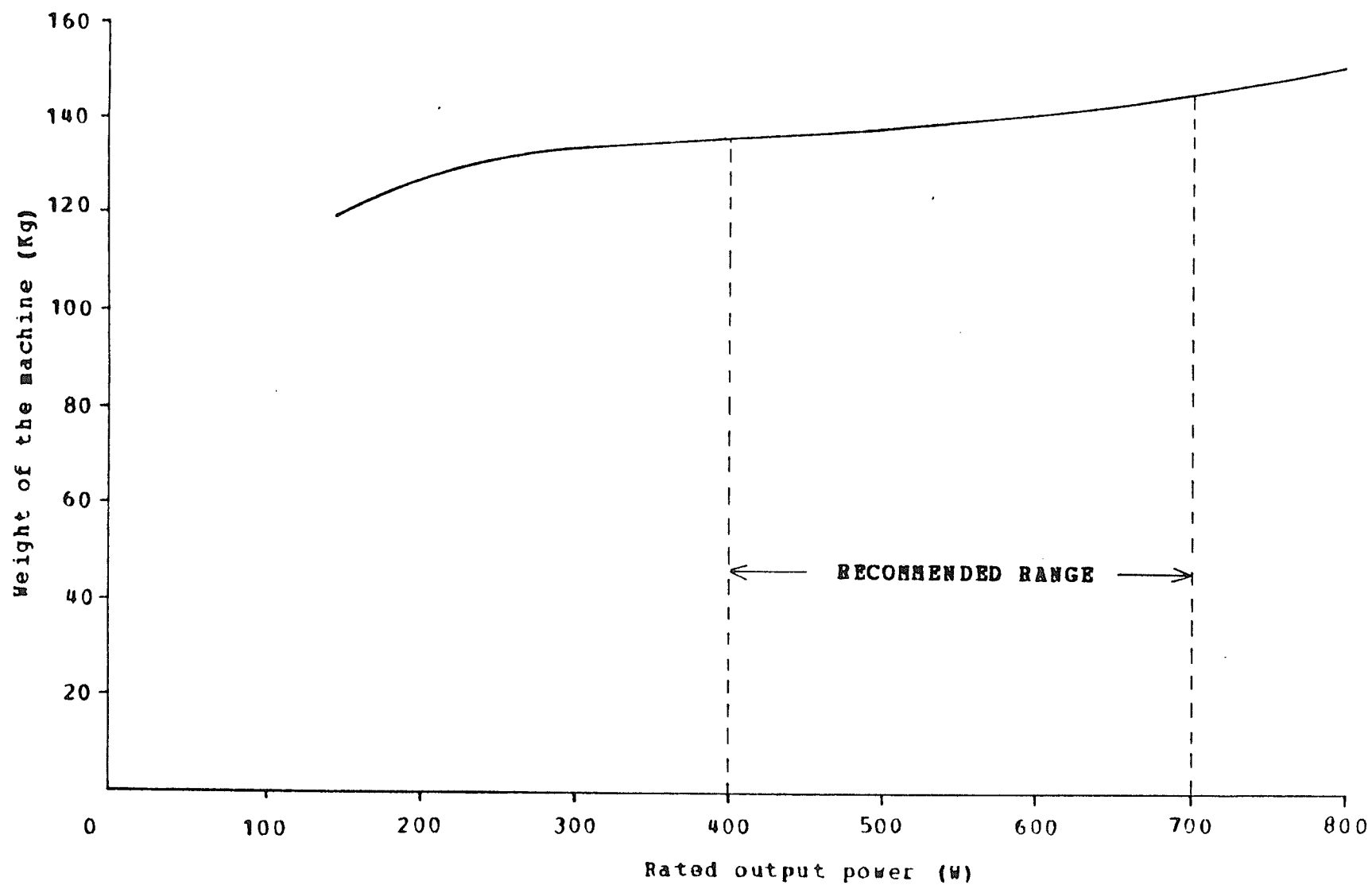


Figure 6.3: Weight of Type 1 Vs. Rated Power Outputs

Chapter VII

CONCLUSIONS

The following conclusions are drawn from the research work described in this thesis :

- (1) The design concept and procedures for the design of a brushless alternator are practicable.
- (2) The first design is not suitable for machines of low ratings.
- (3) Type 1 design has potential to be a viable candidate for wind power generation.
- (4) Both designs are suitable for operation at higher rated voltage and higher rated power.
- (5) The least pth approximation method with a direct search technique was successfully applied to the brushless alternator design.

Suggestions for future work are :

- (1) The first design has to be further developed to eliminate the high field loss.
- (2) The brushless Lundell alternator design concept can be extended to areas other than windpower.

REFERENCES

- (1) MENZIES, R.W., and MATHUR, R.M., " Development of a vertical axis wind power conversion system 1-10 KW range ", A proposal submitted to BRISTOL AEROSPACE LTD. Winnipeg, Manitoba, Feb., 1976.
- (2) HOFER, E., " Brushless claw-pole stationary-field generation for ships " Siemens Review, No. 4, April 1966, pp 253-256.
- (3) TILTINS, J., Canadian Patent No. 773,214.
- (4) KUHLMANN, J.H., " Design of Electrical Apparatus ", (Wiley 1950)
- (5) SAY, M.G., " Design of alternating current machines ", (PITMAN 1948)
- (6) ALGER, P.L., " Calculation of Armature Reactance of Synchronous Machines " AIEE Trans., 1928, 47, pp 493.
- (7) LANGSDORF, A.S., " Theory of alternating-current machinery " (McGRAW-HILL, 1955)
- (8) BANDLER, J.W., and CHARALAMBOUS, B., " Practical least pth optimisation of networks " IEEE Trans., 1972, MTT-20, pp 834-840.
- (9) HOOKE, R., and JEEVES, T.A., " Direct search solution of numerical and statistical problems ", J. ACM., 1961, 8, pp. 212-229.
- (10) MENZIES, R.W. and NEAL, G.W., " Optimization Program for Large Induction Motor Design ", Proc. IEE, Vol. 122, no. 6, pp. 643-646, June 1975.

- (11) FIACCO,A.V., and McCORMICK,G.P., " Nonlinear programming: sequential unconstrained minimization techniques " (Wiley, 1969)
- (12) MORRISON,D.D., " Optimisation by least squares ", SIAM J. Numer. Anal. Vol. 5, No.1, March 1978, pp 83-88.
- (13) GOLDING,E.W., " The gereration of electricity by wind power " (E. & F. N. SPON LTD., 1977)
- (14) SAY,M.G., " Alternating current machines ", (PITMAN 1977)
- (15) WARNE,D.F., And CALNAN,P.G., " Generation of electricity from the Wind " Proc. IEE, vol.124, No.11R, Nov. 1977, IEE Reviews, pp. 963-985.

Appendix I

Leakage Mutual Inductance of The Slot

The mutual inductance of the coil B due to the unit current in coil A is equal to the mutual inductance in coil A due to the unit current in coil B, i.e.

$$\lambda_{ab} = \lambda_{ba} \quad (1)$$

Since the currents in each coil are out of phase by an angle θ , assume the currents are given as

$$i_a = I_m \sin \omega t \quad (2)$$

$$i_b = I_m \sin(\omega t + \theta) \quad (3)$$

where I_m is the magnitude of the currents.

The total flux linkage in coil A and coil B are

$$\Psi_a = \lambda_a i_a + \lambda_{ab} i_b \quad (4)$$

$$\Psi_b = \lambda_{ba} i_a + \lambda_b i_b \quad (5)$$

Substitute Eqns. (2) and (3) into (4), the total flux leakage in coil A becomes,

$$\Psi_a = \lambda_a \cdot I_m \cdot \sin \omega t + \lambda_{ab} \cdot I_m \cdot \sin(\omega t + \theta) \quad (6)$$

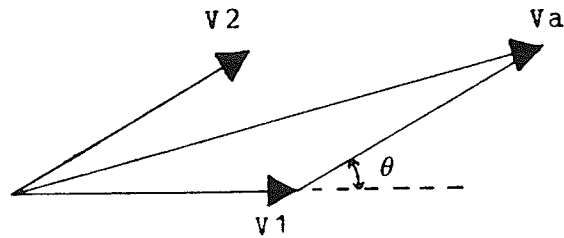
The voltage induced on coil A is

$$\begin{aligned} V_a &= \frac{d\Psi_a}{dt} \\ &= \omega \cdot I_m \cdot \lambda_a \cdot \cos \omega t + \omega \cdot I_m \cdot \lambda_{ab} \cdot \cos(\omega t + \theta) \\ &= V_1 \cdot \cos \omega t + V_2 \cdot \cos(\omega t + \theta) \end{aligned} \quad (7)$$

where $V_1 = \omega \cdot I_m \cdot \lambda_a$

$V_2 = \omega \cdot I_m \cdot \lambda_{ab}$

V_a can be represented by the following phasor diagram



The magnitude of V_a is

$$|V_a| = (V_1^2 + V_2^2 + 2 \cdot V_1 \cdot V_2 \cdot \cos \theta)^{1/2} \quad (8)$$

Since the inductance of the coil A is

$$\begin{aligned} L_a &= \frac{|V_a|}{I_m \cdot \omega} \\ &= (\lambda_a^2 + \lambda_{ab}^2 + 2 \cdot \lambda_a \cdot \lambda_{ab} \cdot \cos \theta)^{1/2} \end{aligned} \quad (9)$$

Similarly, the inductance of coil B is

$$L_b = (\lambda_b^2 + \lambda_{ab}^2 + 2 \cdot \lambda_{ab} \cdot \lambda_b \cdot \cos \theta)^{1/2} \quad (10)$$

APPENDIX II

Program Listing

```

$JOB  WATFIV CHEUNG,NOEXT
C
C  DESIGN PROGRAM OF BRUSHLESS ALTERNATOR
C
C
C  DESIGN=1 : FIRST DESIGN
C  DESIGN=2 : TYPE ONE DESIGN
C
1      REAL X(6)
2      READ,LA,DESIGN
3      READ,(X(K),K=1,LA)
4      CALL MAIN(EFFF,EPFT,TOTWT,X(1),X(2),X(3),X(4),X(5),X(6),1,
      @DESIGN)
5      STOP
6      END

C
C
C
C  MAIN

7      SUBROUTINE MAIN(EFFF,EPFT,TOTWT,BAVT,DB,LENG,JS,JF,BCA,KCON,
      @DESIGN)
8      REAL NT,NF,LAMDA
9      REAL IFB,IFC,ITB,ITC,IFFA,IFFB,IFFC,IRLT,IRLP
10     REAL LENGI,LENG,IFL,IPP,LF,KO,MSP,LGE,JF
11     REAL LM,LH,IP,JS,KP,KD,LR
12     REAL KW,KDT,KDF,LGS,LPS,ITH,NP,NPB,NPC,NS
13     REAL LSF,LST,LFLUX,IF,IT,IFF,IAF,IBF,ICF
14     BF=0.75
15     BB=0.03807
16     COPS=2
17     DENC=8900
18     DENS=7700
19     PF=0.4
20     FPA=4
21     FPB=2
22     FPC=1
23     H3=0.002
24     H2=0.003
25     KO=0.65
26     KW=0.999
27     KD=0.966
28     KP=0.966
29     LGE=LGS=0.001
30     NC=72
31     NP=4
32     NPB=2
33     NPC=1
34     NS=72
35     POWT=20
36     POWF=160
37     PHASE=3
38     PF=0.6
39     PI=3.14159
40     POLES=24
41     RHO=2.1E-8
42     RPMF=174
43     RPMT=87
44     SF=0.4
45     S=0.002538
46     TPP=3
47     UO=PI*4.E-7
48     VPHA=8
49     VPHB=16

```

```

50      VPHC=32
      C
      C*****
      C
      C CALCULATION OF ELECTRIC LOADING
      C
      C
51      VLINA=VPHA*(SQRT(3.0))
52      VLINB=VPHB*(SQRT(3.0))
53      VLINC=VPHC*(SQRT(3.0))
54      BAVF=BAVT/2
55      FT=POLES*RPMT/120
56      PF=POLES*RPMP/120
57      NF=RPMP/60
58      NT=RPMT/60
59      QF=POWF/PF
60      QT=POWI/PF
61      ACF=QF/(10.955*NF*BAVF*KW*LENGG*DB**2)
62      ACT=ACF/8
63      GT=10.955*ACT*BAVT*KW*1.0E-3
64      GF=10.955*ACF*BAVF*KW*1.0E-3
65      PST=PI*LB*NT
66      PSP=PI*CB*NF
67      LENGI=LENGG*0.9
68      PP=(PI*CB)/POLES
69      PHIP=BAVT*PP*LENGI
70      PHIPF=BAVF*PP*LENGI
71      PW=PP*0.7
      C
      C*****
      C
      C CALCULATION OF THE STATOR WINDING
      C
      C
      C
72      TPH=VPHA*1.05/(0.11624*RPMT*KW*EAVT*DB*LENGI)
73      TPHB=TPH*2
74      TPHC=TPH*4
75      IF=POWF/(3*PF*VPHA)
76      IT=POWT/(3*PF*VPHA)
77      IFB=POWF/(3*PF*VPHB)
78      ITB=POWT/(3*PF*VPHB)
79      IFC=POWF/(3*PF*VPHC)
80      ITC=POWT/(3*PF*VPHC)
      C
      C
      C
81      G=NC/PHASE
82      GPC=G/POLES
83      IPP=IF/NP
84      COPP=G/NP
85      TPC=TPH/COPP
86      CPS=TPC*COPS
87      AC=CPS*IPP
88      NSP=NS/POLES
      C
      C
89      YS=PI*CB/NS
90      TW=YS*2/5
91      WO=YS-TW
      C
92      ASCS=IPP/JS
93      AS=ASCS*CPS/SF
94      HT=AS/WO
95      D=WO+S

```

```

96      ALPHA=ARSIN (D/YS)
97      CP=PI*(CB+HT)/POLES
98      CC=CP/COS (ALPHA)
99      LH=CC+BB+HT+LENGG
100     LN=2*LH
101     LP=COFP*TPC*LN
102     RP=RHO*LP/ASCS
103     RPH=RHO*LP/(4*ASCS)
104     RPHB=RP
105     RPHC=RP*4.
106     LST=3*RPH*IT**2
107     LSF=3*RPH*IF**2
      C
108     CALL EDDY (WO,ASCS,CPS,PI,UO,RHO,KDT,PT)
109     CALL EDDY (WC,ASCS,CPS,PI,UO,RHO,KDF,FF)
110     EDT=KDT*LST
111     EDF=KDF*LSF
112     STLT=(EDT+LST)*0.2
113     STLF=(EDF+LSF)*0.2
      C
114     H1=HT-H2-H3
115     CALL LEAK (PT,H1,H2,H3,WO,UC,TPC,PI,LENGI,DB,NS,POLES,XT,XOT)
116     CALL LEAK (FF,H1,H2,H3,WO,UC,TPC,PI,LENGI,DB,NS,POLES,XF,XOF)
117     XAT=(XI+XOT)/16
118     XAF=(XF+XOF)/16
119     XBT=(XI+XOT)/4
120     XBF=(XF+XOF)/4
121     XCT=XI+XOT
122     XCF=XF+XOF
      C
      C
123     HC=PHIP/(2*LENGI*BCA)
124     DOS=DB+(HT+HC+LGS)*2
125     FFLUX=EAVT*PI*DB*LENGI/2
126     AF=FFLUX/BF
127     CALL THICK (TP,DOS,AF,PI)
128     DO=DOS+TF*2
      C
129     IF (DESIGN.EQ.1) THEN DO
      C
      C      CALCULATION OF FIRST DESIGN FIELD WINDING
      C
130     LF=0.0001
131     CALL F1 (ATFDP,ATFD,ATAR,ATART,YS,WO,NSP,LENGI,LENGG,PHIP,PHIPF,
      @LGS,LGE,POLES,DB,DO,DOS,TF,LF,PW,NS,HT,TPP,KW,TPH,IF,IT,UO,PI
      @,HC,BTA,BTAF,BCA,BCAF,TP,LPS,TE,1,BF1)
132     LL=1
133     WHILE (LL.LE.5) DO
134     CALL FRAME (LF,HC,LENGG,JF,ATFD)
135     CALL F1 (ATFDP,ATFD,ATAR,ATART,YS,WO,NSP,LENGI,LENGG,PHIP,PHIPF,
      @LGS,LGE,POLES,DB,DO,DOS,TF,LF,PW,NS,HT,TPP,KW,TPH,IF,IT,UO,PI
      @,HC,BTA,BTAF,BCA,BCAF,TP,LPS,TE,1,BF1)
136     LL=LL+1
137     END WHILE
      C
138     ELSE DO
      C
      C      CALCULATION OF TYPE 1 FIELD WINDING
      C
139     LR=LENGG
140     IN=1
141     WHILE (IN.LE.5) DO
142     CALL F2 (ATFDP,ATFD,LPS,TP,YS,WO,NSP,LENGI,LENGG,PHIP,PHIPF,
      @AGPP,LGS,LGE,PI,DB,PW,UO,HT,TPP,HC,POLES,IT,IF,TPH,KW,BTAF,
      @BTA,BCAF,BCA,LR,NS,DOS,DR,DS,ATAR,ATART,TR)
143     CALL LENG (LR,ATFD,JF,DR,DS,HFP,XH)

```

```

144      IN=IN+1
145      END WHILE
146      CALL F2(ATFDP,ATPD,LPS,TP,YS,WO,NSP,LENGI,LENGG,PHIP,PHIPF,
@AGPP,LGS,LGE,PI,DB,PW,UO,HT,TPP,HC,POLES,IT,IF,TPH,KW,BTAF,
@BTA,BCAF,BCA,LR,NS,DOS,DR,DS,ATAR,ATART,TR)
147      EC=0.01269
148      TF=0.01269
149      LF=LPS+0.02538
150      END IF
151      TWT=(( (DB+2*HT)/2)**2-(DB/2)**2)*PI-NS*WO*HT)*LENGI*DENS
152      CWT=((DOS**2)-(DB**2))*PI*LENGI*DENS/4-TWT
153      CALL IRON(BTAF,FF,TWT,PTF)
154      CALL IRON(BTA,FT,TWT,PTT)
155      CALL IRON(BCAF,FF,CWT,PCF)
156      CALL IRON(BCA,FT,CWT,PCT)
157      IRLT=PCI+PTT
158      IRLF=PCF+PTF

C
C
C
C
C*****
C
159      IF (DESIGN.EQ.1) THEN DO
160      CALL FW1(ASC,TPF,RF,IFF,PLF,ATFD,RHO,PI,JF,HC,DOS,DF)
161      CALL F1(ATFFP,ATFF,ATAR,ATART,YS,WO,NSP,LENGI,LENGG,PHIP,PHIPF,
@LGS,LGE,POLES,DB,DO,DOS,TF,LF,PW,NS,HT,TPP,KW,TPH,IF,IT,UO,PI,
@HC,BTA,BTAF,BCA,BCAF,TP,LPS,TE,2,BF2)
162      ICF=ATFF/(4.*TPF)
163      IAF=ICF*4.
164      IBF=ICF*2.
165      PLFF=4.*RF*ICF**2.
166      ELSE DO
167      CALL FW2(ASC,TPF,RF,IFF,PLF,ATFD,JF,LR,RHO,PI,DS,DF)
168      END IF
169      VOLP=(DO**2-DOS**2)*PI*LF/4
170      CALL STEEL(FRWT,VOLP)
171      STWT=TWT+CWT
172      VOLP=LPS*PW*TP*POLES
173      CALL STEEL(PPWT,VOLP)
174      VOLPS=((DB-2*(TP+LGS))**2)*PF*0.02538/4
175      CALL AL(PSWT,VOLPS)
176      SWT=12*LP*DENC*ASCS
177      FWT=4*TPF*PI*DF*DENC*ASC
178      IF (DESIGN.EQ.1) THEN DO
179      VOLER=(DOS**2)*PI*TE/4
180      CALL STEEL(ERWT,VOLER)
181      TOTWT=FRWT+PPWT+PSWT+FWT+SWT+ERWT+STWT
182      ELSE DO
183      VOLSD=(DR**2-DS**2)*PI*TR/2
184      CALL STEEL(SDWT,VOLSD)
185      VOLEC=(DO**2)*PI*0.02538/2
186      CALL AL(ECWT,VOLEC)
187      TOTWT=FRWT+PPWT+PSWT+FWT+SWT+SDWT+ECWT+STWT
188      END IF
189      RFA=RF/4
190      RFB=RF
191      RFC=RF*4
192      IFPA=IFF*4
193      IFPB=IFF*2
194      IFFC=IFF

```

```

C
C*****
C
C EFFICIENCY
C

```

```

195      C      TOLT=LST+EDT+STLT+PLF+IRIT
196      TOLF=LSF+EDF+STLF+PLFF+IRLF
197      EFFT=POWT*100./(POWT+TOLT)
198      EFFF=POWF*100./(POWF+TOLF)
199      OPF=(EFFF**30/TOTWT)*1.0E-60

200      C      IF (DESIGN.EQ.1) THEN DO
201      SFO=LF*DO*PI
202      SERO=((DO**2.)-(DB**2.))*PI/2.
203      DI=DOS-2*0.6*HC
204      SPI=LF*DI*PI
205      SERI=PI*((DI**2.)-(DB**2.))
206      STA=SFO+SERO+SPI+SERI
207      CALL TEMP1(PHIT,TT,TOLT,STA)
208      CALL TEMP1(PHIF,TTF,TOLF,STA)
209      ELSE DO
210      SFO=LF*DO*PI
211      SERO=(DO**2.)*PI/2
212      CALL TEMP2(PHIT,TT,TOLT,SFC,SERO)
213      CALL TEMP2(PHIF,TTF,TOLF,SFO,SERO)
214      END IF
215      C      IF (KCON.EQ.1) THEN DO

216      PRINT 100
217      PRINT 101
218      PRINT 102
219      PRINT 103
220      PRINT 10
221      PRINT 11
222      PRINT 12,QT,QF,QT,QF,QT,QF
223      PRINT 13,POWT,POWF,POWT,POWF,POWT,POWF
224      PRINT 14,VLINA,VLINA,VLINB,VLINB,VLINC,VLINC
225      PRINT 15,VPHA,VPHA,VPHB,VPHB,VPHC,VPHC
226      PRINT 104,IT,IF,ITB,IFB,ITC,IFC
227      PRINT 16,PF,PF,PF,PF,PF,PF
228      PRINT 17,FT,FF,FT,FF,FT,FF
229      PRINT 18,RPMT,RPMP,RPMT,RPMP,RPMT,RPMP
230      PRINT 19,POLES,POLES,POLES,PCLES,POLES,POLES
231      PRINT 20
232      PRINT 21
233      PRINT 22,BAVT,BAVF,BAVT,BAVF,BAVT,BAVF
234      PRINT 23,ACT,ACF,ACT,ACF,ACT,ACF
235      PRINT 24,GT,GF,GT,GF,GT,GF
236      PRINT 25,DB,DB,DB,DB,DB,DB
237      PRINT 26,DOS,DOS,DOS,DOS,DOS,DOS
238      PRINT 27,LENGG,LENGG,LENGG,LENGG,LENGG,LENGG
239      PRINT 28,LENGI,LENGI,LENGI,LENGI,LENGI,LENGI
240      PRINT 29,PP,PP,PP,PP,PP,PP
241      PRINT 30,DO,DC,DO,DO,DO,DO
242      PRINT 31,TF,TF,TF,TF,TF,TF
243      PRINT 32,LF,LF,LF,LF,LF,LF
244      PRINT 33,DO,DO,DO,DO,DO,DO
245      PRINT 34,CB,DB,CB,DB,DB,DB
246      IF (DESIGN.EQ.1) THEN DO
247      PRINT 35,TE,TE,TE,TE,TE,TE
248      ELSE DO
249      PRINT 123,TR,TR,TR,TR,TR,TR
250      PRINT 124,EC,EC,EC,EC,EC,EC
251      END IF
252      PRINT 36
253      PRINT 37
254      PRINT 38
255      PRINT 39,NP,NP,NPE,NPB,NPC,NPC
256      PRINT 40,NS,NS,NS,NS,NS,NS
257      PRINT 41,GPC,GPC,GEC,GPC,GPC,GPC

```

```
258 PRINT 42,CPS,CPS,CPS,CPS,CPS,CPS
259 PRINT 43,TPH,TPH,TPHB,TPHB,TPHC,TPHC
260 PRINT 44,KP,KP,KP,KP,KP,KP
261 PRINT 45,KD,KD,KD,KD,KD,KD
262 PRINT 46,KW,KW,KW,KW,KW,KW
263 PRINT 47,ASCS,ASCS,ASCS,ASCS,ASCS,ASCS
264 PRINT 48,JS,JS,JS,JS,JS,JS
265 PRINT 49,YS,YS,YS,YS,YS,YS
266 PRINT 50,WO,WO,WO,WO,WO,WO
267 PRINT 51,HT,HT,HT,HT,HT,HT
268 PRINT 52,TW,TW,TW,TW,TW,TW
269 PRINT 53,RPH,RPH,RPHB,RPHB,RPHC,RPHC
270 PRINT 54,LST,LSP,LST,LSP,LST,LSP
271 PRINT 55,EDT,EDF,EDT,EDF,EDT,EDF
272 PRINT 56,STLT,STLF,STLT,STLF,STLT,STLF
273 PRINT 57,XAT,XAP,XBT,XBP,XCT,XCF
274 PRINT 58
275 PRINT 59
276 PRINT 60
277 PRINT 61,PW,PW,PW,PW,PW,PW
278 PRINT 62,TP,TP,TP,TP,TP,TP
279 PRINT 63,LPS,LPS,LPS,LPS,LPS,LPS
280 PRINT 64,TPF,TPF,TPF,TPF,TPF,TPF
281 PRINT 65,FPA,FPA,FEB,FPB,FEC,FPC
282 PRINT 66,ASC,ASC,ASC,ASC,ASC,ASC
283 PRINT 67,IFFA,IAF,IFPB,IBF,IFFC,ICF
284 PRINT 68,JF,JF,JF,JF,JF,JF
285 PRINT 69,RFA,RFA,RFB,RFB,RFC,RFC
286 PRINT 70,PLF,PLFF,PLF,PLFF,PLF,PLFF
287 PRINT 71,PST,PSP,PST,PSF,PST,PSF
288 PRINT 72
289 PRINT 73
290 PRINT 74,PHIP,PHIPF,PHIP,PHIPF,PHIP,PHIPF
291 PRINT 75,BCA,BCAF,BCA,BCAF,BCA,BCAF
292 PRINT 76,BTA,BTAF,BTA,BTAF,BTA,BTAF
293 PRINT 77,BF1,BF2,BF1,BF2,BF1,BF2
294 PRINT 78,LGS,LGS,LGS,LGS,LGS,LGS
295 PRINT 79,LGE,LGE,LGE,LGE,LGE,LGE
296 PRINT 80,ATFDP,ATFFP,ATFDP,ATFFP,ATFDP,ATFFP
297 PRINT 81,ATART,ATAR,ATART,ATAR,ATART,ATAR
298 PRINT 111
299 PRINT 112
300 PRINT 113,SWT,SWT,SWT,SWT,SWT,SWT
301 PRINT 114,FWT,FWT,FWT,FWT,FWT,FWT
302 PRINT 122,STWT,STWT,STWT,STWT,STWT,STWT
303 PRINT 115,FRWT,FRWT,FRWT,FRWT,FRWT,FRWT
304 PRINT 116,POWT,POWT,POWT,POWT,POWT,POWT
305 PRINT 117,PSWT,PSWT,PSWT,PSWT,PSWT,PSWT
306 IF (DESIGN.EQ. 1) THEN DO
307 PRINT 118,ERWT,ERWT,ERWT,ERWT,ERWT,ERWT
308 ELSE DO
309 PRINT 119,SDWT,SDWT,SDWT,SDWT,SDWT,SDWT
310 PRINT 120,ECWT,ECWT,ECWT,ECWT,ECWT,ECWT
311 END IF
312 PRINT 121,TOTWT,TOTWT,TOTWT,TOTWT,TOTWT,TOTWT
313 PRINT 82
314 PRINT 83
315 PRINT 444,PHIT,PHIF,PHIT,PHIF,PHIT,PHIF
316 PRINT 445,TT,TF,TT,TF,TT,TF
317 PRINT 84,IRLT,IRLF,IRLT,IRLF,IRLT,IRLF
318 PRINT 85,LST,LSP,LST,LSP,LST,LSP
319 PRINT 86,EDT,EDF,EDT,EDF,EDT,EDF
320 PRINT 87,STLT,STLF,STLT,STLF,STLT,STLF
321 PRINT 88,PLF,PLFF,PLF,PLFF,PLF,PLFF
322 PRINT 89,TOLT,TOLF,TOLT,TOLF,TOLT,TOLF
323 PRINT 90,EFFT,EFFF,EFFT,EFFF,EFFT,EFFF
```

```

324 100 FORMAT('1',47X,'8 V. OUTPUT',21X,'16 V. OUTPUT',21X,'32 V. OUTPUT
325 101 FORMAT(' ',47X,'-----',21X,'-----',21X,'-----
    @,/)
326 102 FORMAT('0',40X,' THRESHOLD ',5X,'FURLING',10X,' THRESHOLD ',5X,
    @'FURLING',10X,' THRESHOLD ',5X,'FURLING')
327 103 FORMAT(' ',40X,'-----',5X,'-----',10X,'-----',5X,
    @'-----',10X,'-----',5X,'-----')
328 10 FORMAT(' ', 'RATING')
329 11 FORMAT(' ', '-----',///)
330 12 FORMAT(' ', 'FULL LOAD (VA) : ',F10.5,4X,
    @F10.5,4X,' ',4X,F10.5,4X,F10.5,4X,' ',4X,F10.5,4X,F10.5)
331 13 FORMAT(' ', 'FULL LOAD POWER (W) : ',F10.5,4X,
    @F10.5,4X,' ',4X,F10.5,4X,F10.5,4X,' ',4X,F10.5,4X,F10.5)
332 14 FORMAT(' ', 'LINE VOLTAGE (V) : ',F10.5,4X,
    @F10.5,4X,' ',4X,F10.5,4X,F10.5,4X,' ',4X,F10.5,4X,F10.5)
333 15 FORMAT(' ', 'PHASE VOLTAGE (V) : ',F10.5,4X,
    @F10.5,4X,' ',4X,F10.5,4X,F10.5,4X,' ',4X,F10.5,4X,F10.5)
334 104 FORMAT(' ', 'CURRENT PER PHASE (A) : ',F10.5,4X,
    @F10.5,4X,' ',4X,F10.5,4X,F10.5,4X,' ',4X,F10.5,4X,F10.5)
335 16 FORMAT(' ', 'POWER FACTOR : ',F10.5,4X,
    @F10.5,4X,' ',4X,F10.5,4X,F10.5,4X,' ',4X,F10.5,4X,F10.5)
336 17 FORMAT(' ', 'FREQUENCY (HZ) : ',F10.5,4X,
    @F10.5,4X,' ',4X,F10.5,4X,F10.5,4X,' ',4X,F10.5,4X,F10.5)
337 18 FORMAT(' ', 'SPEED (RPM) : ',F10.5,4X,
    @F10.5,4X,' ',4X,F10.5,4X,F10.5,4X,' ',4X,F10.5,4X,F10.5)
338 19 FORMAT(' ', 'NUMBER OF POLES : ',F10.5,4X,
    @F10.5,4X,' ',4X,F10.5,4X,F10.5,4X,' ',4X,F10.5,4X,F10.5)
339 20 FORMAT('0', 'MAIN DIMENSIONS')
340 21 FORMAT(' ', '-----',///)
341 22 FORMAT(' ', 'MAGNETIC LOADING (T) : ',F10.5,4X,
    @F10.5,4X,' ',4X,F10.5,4X,F10.5,4X,' ',4X,F10.5,4X,F10.5)
342 23 FORMAT(' ', 'ELECTRIC LOADING (AC/M) : ',F10.3,4X,
    @F10.3,4X,' ',4X,F10.3,4X,F10.3,4X,' ',4X,F10.3,4X,F10.3)
343 24 FORMAT(' ', 'OUTPUT COEFFICIENT (KVA/RPS/M**3) : ',E10.4,4X,
    @E10.4,4X,' ',4X,E10.4,4X,E10.4,4X,' ',4X,E10.4,4X,E10.4)
344 25 FORMAT(' ', 'STATOR BORE DIAMETER (M) : ',E10.4,4X,
    @E10.4,4X,' ',4X,E10.4,4X,E10.4,4X,' ',4X,E10.4,4X,E10.4)
345 26 FORMAT(' ', 'STATOR OUTSIDE DIAMETER (M) : ',E10.4,4X,
    @E10.4,4X,' ',4X,E10.4,4X,E10.4,4X,' ',4X,E10.4,4X,E10.4)
346 27 FORMAT(' ', 'GROSS CORE LENGTH (M) : ',E10.4,4X,
    @E10.4,4X,' ',4X,E10.4,4X,E10.4,4X,' ',4X,E10.4,4X,E10.4)
347 28 FORMAT(' ', 'IRON LENGTH (M) : ',E10.4,4X,
    @E10.4,4X,' ',4X,E10.4,4X,E10.4,4X,' ',4X,E10.4,4X,E10.4)
348 29 FORMAT(' ', 'POLE PITCH (M) : ',E10.4,4X,
    @E10.4,4X,' ',4X,E10.4,4X,E10.4,4X,' ',4X,E10.4,4X,E10.4)
349 30 FORMAT(' ', 'FRAME OUTSIDE DIAMETER (M) : ',E10.4,4X,
    @E10.4,4X,' ',4X,E10.4,4X,E10.4,4X,' ',4X,E10.4,4X,E10.4)
350 31 FORMAT(' ', 'THICKNESS OF THE FRAME (M) : ',E10.4,4X,
    @E10.4,4X,' ',4X,E10.4,4X,E10.4,4X,' ',4X,E10.4,4X,E10.4)
351 32 FORMAT(' ', 'LENGTH OF THE FRAME (M) : ',E10.4,4X,
    @E10.4,4X,' ',4X,E10.4,4X,E10.4,4X,' ',4X,E10.4,4X,E10.4)
352 33 FORMAT(' ', 'END-RING OUTSIDE DIAMETER (M) : ',E10.4,4X,
    @E10.4,4X,' ',4X,E10.4,4X,E10.4,4X,' ',4X,E10.4,4X,E10.4)
353 34 FORMAT(' ', 'END-RING INSIDE DIAMETER (M) : ',E10.4,4X,
    @E10.4,4X,' ',4X,E10.4,4X,E10.4,4X,' ',4X,E10.4,4X,E10.4)
354 35 FORMAT(' ', 'THICKNESS OF THE END-RING (M) : ',E10.4,4X,
    @E10.4,4X,' ',4X,E10.4,4X,E10.4,4X,' ',4X,E10.4,4X,E10.4)
355 123 FORMAT(' ', 'THICKNESS OF THE SHAFT DISC (M) : ',E10.4,4X,
    @E10.4,4X,' ',4X,E10.4,4X,E10.4,4X,' ',4X,E10.4,4X,E10.4)
356 124 FORMAT(' ', 'THICKNESS OF THE END CAP (M) : ',E10.4,4X,
    @E10.4,4X,' ',4X,E10.4,4X,E10.4,4X,' ',4X,E10.4,4X,E10.4)
357 36 FORMAT('0', 'STATOR')
358 37 FORMAT(' ', '-----',///)
359 38 FORMAT(' ', 'WINDING : TWO LAYERS P
    @ SLOT ')

```



```

360 39 FORMAT(' ', 'NUMBER OF PARALLEL CIRCUIT : ', F10.5, 4X,
    @F10.5, 4X, ' ', 4X, F10.5, 4X, F10.5, 4X, ' ', 4X, F10.5, 4X, F10.5)
361 40 FORMAT(' ', 'NUMBER OF SLOTS : ', F10.5, 4X,
    @F10.5, 4X, ' ', 4X, F10.5, 4X, F10.5, 4X, ' ', 4X, F10.5, 4X, F10.5)
362 41 FORMAT(' ', 'SLOTS/POLE/PHASE : ', F10.5, 4X,
    @F10.5, 4X, ' ', 4X, F10.5, 4X, F10.5, 4X, ' ', 4X, F10.5, 4X, F10.5)
363 42 FORMAT(' ', 'CONDUCTORS/SLOT : ', F10.5, 4X,
    @F10.5, 4X, ' ', 4X, F10.5, 4X, F10.5, 4X, ' ', 4X, F10.5, 4X, F10.5)
364 43 FORMAT(' ', 'TURNS/PARALLEL CIRCUIT : ', F10.5, 4X,
    @F10.5, 4X, ' ', 4X, F10.5, 4X, F10.5, 4X, ' ', 4X, F10.5, 4X, F10.5)
365 44 FORMAT(' ', 'PITCH FACTOR : ', F10.5, 4X,
    @F10.5, 4X, ' ', 4X, F10.5, 4X, F10.5, 4X, ' ', 4X, F10.5, 4X, F10.5)
366 45 FORMAT(' ', 'DISTRIBUTION FACTOR : ', F10.5, 4X,
    @F10.5, 4X, ' ', 4X, F10.5, 4X, F10.5, 4X, ' ', 4X, F10.5, 4X, F10.5)
C
367 46 FORMAT(' ', 'WINDING FACTOR : ', F10.5, 4X,
    @F10.5, 4X, ' ', 4X, F10.5, 4X, F10.5, 4X, ' ', 4X, F10.5, 4X, F10.5)
368 47 FORMAT(' ', 'CONDUCTOR SIZE (M**2) : ', E10.4, 4X,
    @E10.4, 4X, ' ', 4X, E10.4, 4X, E10.4, 4X, ' ', 4X, E10.4, 4X, E10.4)
369 48 FORMAT(' ', 'CURRENT DENSITY (A/M**2) : ', E10.4, 4X,
    @E10.4, 4X, ' ', 4X, E10.4, 4X, E10.4, 4X, ' ', 4X, E10.4, 4X, E10.4)
370 49 FORMAT(' ', 'SLOT PITCH (M) : ', E10.4, 4X,
    @E10.4, 4X, ' ', 4X, E10.4, 4X, E10.4, 4X, ' ', 4X, E10.4, 4X, E10.4)
371 50 FORMAT(' ', 'SLOT WIDTH (M) : ', E10.4, 4X,
    @E10.4, 4X, ' ', 4X, E10.4, 4X, E10.4, 4X, ' ', 4X, E10.4, 4X, E10.4)
372 51 FORMAT(' ', 'SLOT DEPTH (M) : ', E10.4, 4X,
    @E10.4, 4X, ' ', 4X, E10.4, 4X, E10.4, 4X, ' ', 4X, E10.4, 4X, E10.4)
373 52 FORMAT(' ', 'TOOTH WIDTH (M) : ', E10.4, 4X,
    @E10.4, 4X, ' ', 4X, E10.4, 4X, E10.4, 4X, ' ', 4X, E10.4, 4X, E10.4)
374 53 FORMAT(' ', 'RESISTANCE/PHASE (OHM) : ', E10.4, 4X,
    @E10.4, 4X, ' ', 4X, E10.4, 4X, E10.4, 4X, ' ', 4X, E10.4, 4X, E10.4)
375 54 FORMAT(' ', 'I**2R LOSS (W) : ', F10.5, 4X,
    @F10.5, 4X, ' ', 4X, F10.5, 4X, F10.5, 4X, ' ', 4X, F10.5, 4X, F10.5)
376 55 FORMAT(' ', 'EDDY CURRENT LOSS (W) : ', F10.5, 4X,
    @F10.5, 4X, ' ', 4X, F10.5, 4X, F10.5, 4X, ' ', 4X, F10.5, 4X, F10.5)
377 56 FORMAT(' ', 'STRAY LOSS (W) : ', F10.5, 4X,
    @F10.5, 4X, ' ', 4X, F10.5, 4X, F10.5, 4X, ' ', 4X, F10.5, 4X, F10.5)
378 57 FORMAT(' ', 'LEAKAGE REACTANCE (OHM) : ', F10.5, 4X,
    @F10.5, 4X, ' ', 4X, F10.5, 4X, F10.5, 4X, ' ', 4X, F10.5, 4X, F10.5)
379 58 FORMAT('0', 'ROTOR')
380 59 FORMAT(' ', '-----', '///)
381 60 FORMAT(' ', 'TYPE : LUNDELL TYPE')
382 61 FORMAT(' ', 'POLE ARC (M) : ', E10.4, 4X,
    @E10.4, 4X, ' ', 4X, E10.4, 4X, E10.4, 4X, ' ', 4X, E10.4, 4X, E10.4)
383 62 FORMAT(' ', 'THICKNESS OF THE POLE (M) : ', E10.4, 4X,
    @E10.4, 4X, ' ', 4X, E10.4, 4X, E10.4, 4X, ' ', 4X, E10.4, 4X, E10.4)
384 63 FORMAT(' ', 'LENGTH OF POLE-SHOE (M) : ', E10.4, 4X,
    @E10.4, 4X, ' ', 4X, E10.4, 4X, E10.4, 4X, ' ', 4X, E10.4, 4X, E10.4)
385 64 FORMAT(' ', 'FIELD TURNS : ', F10.5, 4X,
    @F10.5, 4X, ' ', 4X, F10.5, 4X, F10.5, 4X, ' ', 4X, F10.5, 4X, F10.5)
386 65 FORMAT(' ', 'NUMBER OF PARALLEL CIRCUIT : ', F10.5, 4X,
    @F10.5, 4X, ' ', 4X, F10.5, 4X, F10.5, 4X, ' ', 4X, F10.5, 4X, F10.5)
387 66 FORMAT(' ', 'CONDUCTOR SIZE (M**2) : ', E10.4, 4X,
    @E10.4, 4X, ' ', 4X, E10.4, 4X, E10.4, 4X, ' ', 4X, E10.4, 4X, E10.4)
388 67 FORMAT(' ', 'FIELD CURRENT (A) : ', F10.5, 4X,
    @F10.5, 4X, ' ', 4X, F10.5, 4X, F10.5, 4X, ' ', 4X, F10.5, 4X, F10.5)
389 68 FORMAT(' ', 'CURRENT DENSITY (A/M**2) : ', E10.4, 4X,
    @E10.4, 4X, ' ', 4X, E10.4, 4X, E10.4, 4X, ' ', 4X, E10.4, 4X, E10.4)
390 69 FORMAT(' ', 'RESISTANCE (OHM) : ', F10.5, 4X,
    @F10.5, 4X, ' ', 4X, F10.5, 4X, F10.5, 4X, ' ', 4X, F10.5, 4X, F10.5)
391 70 FORMAT(' ', 'I**2R LOSS (W) : ', F10.5, 4X,
    @F10.5, 4X, ' ', 4X, F10.5, 4X, F10.5, 4X, ' ', 4X, F10.5, 4X, F10.5)
392 71 FORMAT(' ', 'PERIPHERAL VELOCITY (M/S) : ', F10.5, 4X,
    @F10.5, 4X, ' ', 4X, F10.5, 4X, F10.5, 4X, ' ', 4X, F10.5, 4X, F10.5)
393 72 FORMAT('0', 'MAGNETIZATION')
394 73 FORMAT(' ', '-----', '///)

```

```

395 74 FORMAT(' ', 'FLUX/POLE (WB) : ', E10.4, 4X,
@E10.4, 4X, ' ', 4X, E10.4, 4X, E10.4, 4X, ' ', 4X, E10.4, 4X, E10.4)
396 75 FORMAT(' ', 'CORE FLUX DENSITY (T) : ', E10.4, 4X,
@E10.4, 4X, ' ', 4X, E10.4, 4X, E10.4, 4X, ' ', 4X, E10.4, 4X, E10.4)
397 76 FORMAT(' ', 'TOOTH FLUX DENSITY (T) : ', E10.4, 4X,
@E10.4, 4X, ' ', 4X, E10.4, 4X, E10.4, 4X, ' ', 4X, E10.4, 4X, E10.4)
398 77 FORMAT(' ', 'FRAME FLUX DENSITY (T) : ', E10.4, 4X,
@E10.4, 4X, ' ', 4X, E10.4, 4X, E10.4, 4X, ' ', 4X, E10.4, 4X, E10.4)
399 78 FORMAT(' ', 'GAP LENGTH AT STATOR (M) : ', F10.5, 4X,
@F10.5, 4X, ' ', 4X, F10.5, 4X, F10.5, 4X, ' ', 4X, F10.5, 4X, F10.5)
400 79 FORMAT(' ', 'GAP LENGTH AT END-RING (M) : ', F10.5, 4X,
@F10.5, 4X, ' ', 4X, F10.5, 4X, F10.5, 4X, ' ', 4X, F10.5, 4X, F10.5)
401 80 FORMAT(' ', 'FIELD A.T./POLE : ', F10.4, 4X,
@F10.4, 4X, ' ', 4X, F10.4, 4X, F10.4, 4X, ' ', 4X, F10.4, 4X, F10.4)
402 81 FORMAT(' ', 'ARMATURE A.T./POLE : ', F10.4, 4X,
@F10.4, 4X, ' ', 4X, F10.4, 4X, F10.4, 4X, ' ', 4X, F10.4, 4X, F10.4)
403 111 FORMAT('0', 'WEIGHT OF THE MACHINE')
404 112 FORMAT(' ', '-----', '///')
405 113 FORMAT(' ', 'WEIGHT OF STATOR WINDING : ', F10.4, 4X,
@F10.4, 4X, ' ', 4X, F10.4, 4X, F10.4, 4X, ' ', 4X, F10.4, 4X, F10.4)
406 114 FORMAT(' ', 'WEIGHT OF FIELD WINDING : ', F10.4, 4X,
@F10.4, 4X, ' ', 4X, F10.4, 4X, F10.4, 4X, ' ', 4X, F10.4, 4X, F10.4)
407 122 FORMAT(' ', 'WEIGHT OF THE STATOR CORE : ', F10.4, 4X,
@F10.4, 4X, ' ', 4X, F10.4, 4X, F10.4, 4X, ' ', 4X, F10.4, 4X, F10.4)
408 115 FORMAT(' ', 'WEIGHT OF THE FRAME : ', F10.4, 4X,
@F10.4, 4X, ' ', 4X, F10.4, 4X, F10.4, 4X, ' ', 4X, F10.4, 4X, F10.4)
409 116 FORMAT(' ', 'WEIGHT OF THE PCLES : ', F10.4, 4X,
@F10.4, 4X, ' ', 4X, F10.4, 4X, F10.4, 4X, ' ', 4X, F10.4, 4X, F10.4)
410 117 FORMAT(' ', 'WEIGHT OF THE PCLE SUPPORT : ', F10.4, 4X,
@F10.4, 4X, ' ', 4X, F10.4, 4X, F10.4, 4X, ' ', 4X, F10.4, 4X, F10.4)
411 118 FORMAT(' ', 'WEIGHT OF THE END RING : ', F10.4, 4X,
@F10.4, 4X, ' ', 4X, F10.4, 4X, F10.4, 4X, ' ', 4X, F10.4, 4X, F10.4)
412 119 FORMAT(' ', 'WEIGHT OF THE SHAFT DISC : ', F10.4, 4X,
@F10.4, 4X, ' ', 4X, F10.4, 4X, F10.4, 4X, ' ', 4X, F10.4, 4X, F10.4)
413 120 FORMAT(' ', 'WEIGHT OF THE END CAP : ', F10.4, 4X,
@F10.4, 4X, ' ', 4X, F10.4, 4X, F10.4, 4X, ' ', 4X, F10.4, 4X, F10.4)
414 121 FORMAT(' ', 'TOTAL WEIGHT : ', F10.4, 4X,
@F10.4, 4X, ' ', 4X, F10.4, 4X, F10.4, 4X, ' ', 4X, F10.4, 4X, F10.4)
415 82 FORMAT('0', 'EFFICIENCY')
416 83 FORMAT(' ', '-----', '///')
417 84 FORMAT(' ', 'IRON LOSS : ', F10.4, 4X,
@F10.4, 4X, ' ', 4X, F10.4, 4X, F10.4, 4X, ' ', 4X, F10.4, 4X, F10.4)
418 85 FORMAT(' ', 'STATOR I**2R LOSS (W) : ', F10.4, 4X,
@F10.4, 4X, ' ', 4X, F10.4, 4X, F10.4, 4X, ' ', 4X, F10.4, 4X, F10.4)
419 86 FORMAT(' ', 'EDDY CURRENT LOSS (W) : ', F10.4, 4X,
@F10.4, 4X, ' ', 4X, F10.4, 4X, F10.4, 4X, ' ', 4X, F10.4, 4X, F10.4)
420 87 FORMAT(' ', 'STRAY LOSS (W) : ', F10.4, 4X,
@F10.4, 4X, ' ', 4X, F10.4, 4X, F10.4, 4X, ' ', 4X, F10.4, 4X, F10.4)
421 88 FORMAT(' ', 'FIELD I**2R LOSS (W) : ', F10.4, 4X,
@F10.4, 4X, ' ', 4X, F10.4, 4X, F10.4, 4X, ' ', 4X, F10.4, 4X, F10.4)
422 89 FORMAT(' ', 'TOTAL LOSS (W) : ', F10.4, 4X,
@F10.4, 4X, ' ', 4X, F10.4, 4X, F10.4, 4X, ' ', 4X, F10.4, 4X, F10.4)
423 90 FORMAT(' ', 'EFFICIENCY (%) : ', F10.4, 4X,
@F10.4, 4X, ' ', 4X, F10.4, 4X, F10.4, 4X, ' ', 4X, F10.4, 4X, F10.4)
424 PRINT 200
425 444 FORMAT(' ', 'TEMPERATURE RISE (C) : ', F10.4, 4X,
@F10.4, 4X, ' ', 4X, F10.4, 4X, F10.4, 4X, ' ', 4X, F10.4, 4X, F10.4)
426 445 FORMAT(' ', 'TEMPERATURE INSIDE THE MACHINE (C) : ', F10.4, 4X,
@F10.4, 4X, ' ', 4X, F10.4, 4X, F10.4, 4X, ' ', 4X, F10.4, 4X, F10.4)
427 200 FORMAT(' ')
C
428 END IF
C
429 RETURN
430 END
C

```

```

C
C
C
C
431      SUBROUTINE CURVE1(BX,HX)
C
C      MAGNETIC CURVE OF THE FRAME
C
432      DIMENSION BS(16),HS(16)
433      DATA (BS(II),II=1,16,1)/.01,0.1,0.2,0.3,0.4,0.5,0.6,0.7,0.8,0.9,1
@,1.1,1.2,1.3,1.4,1.5/
434      DATA (HS(MH),MH=1,16,1)/0.,160.,170.,200.,220.,245.,275.,320.,350.
@,405.,475.,590.,720.,890.,1150.,1500./
435      L=1
436      WHILE (L.LE.16) DO
437          IF (BX.LE.BS(L)) THEN DO
438              HX=HS(L-1) + (BX-BS(L-1)) * (HS(L) -HS(L-1)) / (BS(L) -BS(L-1))
439              L=17
440          ELSE DO
441              L=L+1
442          END IF
443      END WHILE
444      RETURN
445      END

C
C
C

446      SUBROUTINE CURVE2(BY,HY)
C
C      MAGNETIC CURVE OF THE LAMINATIONS
C
447      DIMENSION BB(28),HH(28)
448      DATA (BB(K),K=1,28,1)/.01,0.15,0.2,0.25,0.3,0.35,0.4,0.45,0.5,0.6,
@,0.65,0.7,0.75,0.8,0.85,0.9,0.95,1.0,1.05,1.1,1.15,1.2,1.25,
@1.3,1.35,1.4,1.5/
449      DATA (HH(KK),KK=1,28,1)/0.,100.,240.,300.,380.,440.,500.,550.,60
@,650.,700.,750.,800.,850.,950.,1040.,1130.,1250.,1375.,1520.,
@1780.,2100.,2500.,2865.,3370.,3800.,4150.,4700./
450      L=1
451      WHILE (L.LE.28) DO
452          IF (BY.LE.BB(L)) THEN DO
453              HY=HH(L-1) + (BY-BB(L-1)) * (HH(L) -HH(L-1)) / (BB(L) -BB(L-1))
454              L=30
455          ELSE DO
456              L=L+1
457          END IF
458      END WHILE
459      RETURN
460      END

C
C
C

461      SUBROUTINE THICK(X,DOS,AF,PI)
C
C      CALCULATION OF THE THICKNESS OF THE FRAME
C
462      A=1
463      B=DOS
464      C=-AF/PI
465      TEST=B**2-4*A*C
466      IF (TEST.LT.0) THEN DO
467          PRINT,'***** ERROR *****'
468      ELSE DO

```

```

469      X=(-B+SQRT(B**2-4*A*C))/2*A
470      END IF
471      RETURN
472      END
      C
      C
      C

473      SUBROUTINE FRAME(LF,HC,LENGG,JF,ATP)
      C
      C      ESTIMATION OF THE FRAME SIZE
      C
474      REAL L,LF,LENGG,JF
475      SF=0.4
476      AF=ATP/(SF*JF)
477      HF=0.6*HC
478      L=AF/HF
479      LF=L+LENGG
480      RETURN
481      END
      C
      C
      C

482      SUBROUTINE IRON(B,F,WT,P)
      C
      C      CALCULATION OF IRON LOSS
      C
483      REAL L,KE
484      KE=2.1335E-4
485      RHOS=2.2E-7
486      D=3.807E-4
487      L=(KE*(B*F*D)**2)/RHOS
488      P=WT*L
489      RETURN
490      END
      C
      C

491      SUBROUTINE LEAK(F,H1,H2,H3,WO,UO,TPC,PI,LENGI,DB,NS,POLES,X,XO)
      C
      C      CALCULATION OF LEAKAGE REACTANCE
      C
492      REAL LAMS,LAM1,LAM2,LAM12,L1,L2,LT,LENGI,NS
493      LAMS=(H3/WO+H2/(WO+H2)+H1/(3*WO))*4*UO*TPC**2
494      LAM1=(H3/WO+H2/(WO+H2)+H1/(6*WO))*UO*TPC**2
495      LAM2=(H3/WO+H2/(WO+H2)+2*H1/(3*WO))*UO*TPC**2
496      LAM12=(H3/WO+H2/(WO+H2)+H1/(4*WO))*UO*TPC**2
497      L1=SQRT(LAM1**2+LAM12**2+LAM1*LAM12)
498      L2=SQRT(LAM2**2+LAM12**2+LAM2*LAM12)
499      LT=L1+L2
500      XS=LAMS*48*PI*F*LENGI
501      XH=LT*16*PI*F*LENGI
      C
      C      CALCULATION OF OVERHANG REACTANCE
      C
502      P=5./6.
503      XO=38.4*PI*F*UO*DB*NS*(TPC**2)*(3.0*P-1.0)/(POLES**2)
504      X=XS
505      RETURN
506      END
      C
      C
      C
      C

```

```

507      SUBROUTINE EDDY (WO,ASCS,CPS,PI,UO,RHO,KD,F)
      C
      C      EDDY CURRENT LCSS
      C
508      REAL N,M,KD
509      B=0.7*WO
510      D=SQRT(4.0*ASCS/PI)
511      N=B/D
512      M=CPS/N
513      A=SQRT(PI*F*UO*B/(RHO*WO))
514      KD=(M**2)*((A*D)**4)/9.0
515      RETURN
516      END
      C
      C

517      SUBROUTINE F1(ATFDP,ATPD,ATAR,ATART,YS,WO,NSP,LENGI,LENGG,PHIPT
      @,PHIPF,LGS,LGE,POLES,DB,DO,DOS,TF,LF,PW,NS,HT,TPP,KW,TPH,IF,IT,UC
      @PI,HC,BTA,BTAF,BCA,BCAF,TP,LPS,TE,L,BF)
      C
      C      FIRST DESIGN : MAGNETIC CIRCUIT
      C
518      REAL LENGI,LENGG,LGS,LF,KW,IF,IT,NS,KO,NSP,LGE,LPS
519      REAL PHIP(2),BCAX(2),BTAX(2)
520      PHIP(1)=PHIPT
521      PHIP(2)=PHIPF
      C
522      KO=0.65
523      BEI=0.6
524      BP=0.8
525      BPA=BP/2
      C
      C
      C      AMPERE-TURN FOR THE AIR GAP
      C
      C
526      YSE=YS-KO*WO
527      AGPP=YSE*NSP*LENGI
528      BGS=PHIP(L)/AGPP
529      HGS=BGS/UO
530      ATSGP=HGS*LGS
      C
      C      A.T. FOR THE END RING
      C
      C
      C
531      TE=PHIP(1)*POLES/(BEI*PI*DB*2)
532      BEO=PHIP(L)*POLES/(PI*2*TE*(DO-TF))
533      BEAV=(BEO+BEI)/2
534      CALL CURVE1(BEAV,HE)
535      ATER=HE*(DO-DB-TF)/2
      C
      C      A.T. FOR ROTOR POLE
      C
      C
536      CALL CURVE1(BPA,HPA)
537      CALL CURVE1(BP,HP)
538      LPS=(LF+LENGG)/2
539      TP=PHIP(1)/(2*BPA*PW)
540      ATRP=HPA*TE+LENGG*HPA+(LF-LENGG)*HP/2
      C
      C      A.T. FOR THE GAP AT END-RING
541      BGE=BEI
542      ATGE=LGE*BGE/UO
      C
      C      A.T. FOR THE FRAME

```

```

C
C
543      BF=PHIP(L)*POLES/(2*PI*(DO-TF)*TF)
544      CALL CURVE1(BF,HFA)
545      ATF=HFA*LF/2
C
C      A.T. FOR THE TEETH
C
C
546      BT=PI*(2*HT/3+2*LGS+DB)/NS-WO
547      BT=0.006
548      BTAX(L)=PHIP(L)/(TPP*BT*LENGI)
549      BTAX(2)=PHIP(2)/(TPP*BT*LENGI)
550      CALL CURVE2(BTAX(L),HTA)
C
551      BTA=BTAX(1)
552      BTAF=BTAX(2)
C
553      ATT=HT*HTA
C
C      A.T. FOR THE CORE
C
C
554      DCM=(DOS-HC)
555      BCAX(L)=PHIP(L)/(HC*LENGI*2)
556      BCAX(2)=PHIP(2)/(HC*LENGI*2)
557      CALL CURVE2(BCAX(L),HCA)
558      ATC=PI*DCM*HCA/(POLES*2)
C
559      BCA=BCAX(1)
560      BCAF=BCAX(2)
C
C
C      A.T. FOR ARMATURE REACTION
C
C
561      ATAR=1.35*KW*TPH*IF/POLES
562      ATART=1.35*KW*TFH*IT/POLES
C
C      TOTAL FIELD A.T.
C
C
563      ATFDP=ATSGP+ATER+ATRP+ATGE+ATF+ATT+ATC+ATAR
564      ATFD=ATFDP*2
565      RETURN
566      END
C
C*****
C
C
567      SUBROUTINE F2(ATFDP,ATFD,LPS,TP,YS,WO,NSP,LENGI,LENGG,PHIP
        @,PHIPP,AGPP,LGS,LGE,PI,DB,PW,UO,HT,TPP,HC,POLES,IT,IF,TPH,
        @KW,BTAF,BTA,BCAF,BCA,LR,NS,DOS,DR,DS,ATAR,ATART,TR)
C
C      TYPE 1 : MAGNETIC CIRCUIT
C
568      REAL LPS,NSP,LENGI,LENGG,LGS,LGE,IF,IT,LR,KO,KW,NS
569      BP=0.8
570      BS=1.4
571      BPA=BP/2
572      BRI=1.2
573      KO=0.65

```

```

C
C   AMPERE-TURN FOR THE AIR GAP
C
C
574       YSE=YS-KO*WO
575       AGPP=YSE*NSP*LENGI
576       BGS=PHIP/AGPP
577       HGS=BGS/UO
578       ATSGP=HGS*LGS
C
C   A.T. FOR THE SHAFT
C
579       DS=SQRT(2*PHIP*POLES/(PI*BS))
580       CALL CURVE1(BS,HS)
581       ATS=LR*HS/2
C
C   A.T. FOR THE SHAFT DISC
C
C
582       CALL CURVE1(BPA,HPA)
583       CALL CURVE1(BP,HP)
584       TP=PHIP/(2*BPA*PW)
585       DR=CB-(TP*LGE+LGS)*2
586       TR=PHIP*POLES/(2*PI*DS*BRI)
587       BRO=PHIP*POLES/(2*PI*DR*TR)
588       BRAV=(BRI+BRO)/2
589       CALL CURVE1(BRAV,HR)
590       ATR=HR*(DR-DS)/2
C
C
C
C   A.T. FOR THE ROTOR POLE
C
591       LPS=TR+0.02538*(LR+LENGG)/2
592       ATRP=HPA*TR+LENGG*HPA*(LR-LENGG)*HP/2
C
C
C   A.T. FOR THE GAP AT END-RING
593       BGE=BRO
594       ATGE=LGE*BGE/UO
C
C   A.T. FOR THE TEETH
C
C
595       BT=PI*(2*HT/3+2*LGS+DB)/MS-WO
596       BTA=PHIP/(TPP*BT*LENGI)
597       BTAF=PHIP/(TPP*BT*LENGI)
598       CALL CURVE2(BTA,HTA)
599       ATT=HT*HTA
C
C
C   A.T. FOR THE CORE
C
C
C
600       DCM=(DOS-HC)
601       BCA=PHIP/(HC*LENGI*2)
602       BCAF=PHIP/(HC*LENGI*2)
603       CALL CURVE2(BCA,HCA)
604       ATC=PI*DCM*HCA/(POLES*2)
C
C
C   A.T. FOR ARMATURE REACTION
C
C

```

```

605      ATAR=1.35*KW*TPH*IF/POLES
606      ATART=1.35*KW*TPH*IT/POLES
      C
      C
      C      TOTAL FIELD A.T.
      C
      C
607      ATFD=ATSGP+ATR+ATRP+ATGE+ATS+ATT+ATC+ATAR
608      ATFD=ATFD*2
609      RETURN
610      END
      C
      C

611      SUBROUTINE FW2(ASC,TPF,RF,IPF,PLF,ATFD,JF,LR,RHO,PI,DS,DF)
      C
      C      TYPE 1 : FIELD WINDING CALCULATION
      C
612      REAL IPF,LR,JF
      C
613      SF=0.4
614      PERCEN=0.6
615      EF=12
616      CACF=ATFD/(SF*JF)
617      HRF=CACF/LR
618      DF=HRF+DS
619      ASC=(ATFD*RHO*PI*DF)/(4*EF)
620      TPF=ATFD/(4*ASC*JF)
621      RF=RHO*PI*DF*TPF/ASC
622      IPF=EF/RF
623      PLF=RHO*PI*LF*ATFD*JF
624      RETURN
625      END
      C

626      SUBROUTINE FW1(ASC,TPF,RF,IPF,PLF,ATFD,RHO,PI,JF,HC,DOS,DF)
      C
      C      FIRST DESIGN : FIELD WINDING CALCULATION
      C
627      REAL IPF,JF
628      SF=0.4
629      PERCEN=0.6
630      EF=12
631      HF=PERCEN*HC
632      DF=DOS-HF
633      ASC=(ATFD*RHO*PI*DF)/(4*EF)
634      TPF=ATFD/(4*ASC*JF)
635      RF=RHO*PI*DF*TPF/ASC
636      IPF=EF/RF
637      PLF=RHO*PI*DF*ATFD*JF
638      RETURN
639      END
      C
      C

640      SUBROUTINE LENG(LR,ATFD,JF,DR,DS,HRF,XH)
      C
      C      CALCULATION OF FRAME LENGTH
      C
641      REAL LR,JF
642      SF=0.4
643      CACF=ATFD/(SF*JF)
644      XH=(DR-DS)*0.8/2
645      HRF=XH
646      LR=CACF/XH

```



```

647      RETURN
648      END
      C

649      SUBROUTINE STEEL(WT,VOL)
      C
      C  WEIGHT OF IRON
      C
650      DENS=7700
651      WT=VOL*DENS
652      RETURN
653      END
      C
      C

654      SUBROUTINE AL(WT,VOL)
      C
      C  WEIGHT OF ALUMINUM
      C
655      DENAL=2700
656      WT=VOL*DENAL
657      RETURN
658      END
      C

659      SUBROUTINE TEMP1(PHI,TT,PL,STA)
      C
      C  FIRST DESIGN : CALCULATION OF TEMPERATURE
      C
660      I=1
661      WHILE(I.LE.150) DO
662      T=I+298
663      PHI=T-298
664      PC=30.*PHI
665      PV=2*PHI**(5./4.)
666      PR=(3.135E-8)*((T**4.)-(298.**4.))
667      PD=(PP+PV+PC)*STA
668      S=PD-PL
669      I=I+1
670      IF(S.GE.0) THEN DO
671      I=200
672      END IF
673      END WHILE
674      TT=T-273
675      RETURN
676      END
      C
      C

677      SUBROUTINE TEMP2(PHI,TT,PL,SFO,SERO)
      C
      C  TYPE 1 : CALCULATION OF TEMPERATURE
      C
678      I=1
679      WHILE(I.LE.100) DO
680      T=I+298
681      PHI=T-298
682      PC=30.*PHI
683      PV=2*PHI**(5./4.)
684      PR=(3.135E-8)*((T**4.)-(298.**4.))
685      P1=(PV+PC+PR)*SFO
686      PRA=(5.7E-8)*0.1*((T**4.)-(298.**4.))
687      PVA=2*PHI**(5./4.)
688      P2=(PRA+PC+PVA)*SERO
689      S=P1+P2-PL
690      I=I+1

```

```
691      IF(S.GE.0) THEN DO
692          I=200
693      END IF
694      END WHILE
695      TT=T-273
696      RETURN
697      END
```

C

\$ENTRY